

Articles

Potent, Plasmodium-Selective Farnesyltransferase Inhibitors That Arrest the Growth of Malaria Parasites: Structure–Activity Relationships of Ethylenediamine-Analogue Scaffolds and Homology Model Validation

Steven Fletcher,[†] Christopher G. Cummings,[†] Kasey Rivas,[‡] William P. Katt,[†] Carrie Hornéy,[‡] Frederick S. Buckner,[‡] Debopam Chakrabarti,[#] Saïd M. Sebti,^{||} Michael H. Gelb,[§] Wesley C. Van Voorhis,[‡] and Andrew D. Hamilton^{*†}

Department of Chemistry, Yale University, 225 Prospect Street, New Haven, Connecticut 06511, Department of Medicine and Department of Chemistry and Biochemistry, University of Washington, Seattle, Washington 98195, Department of Molecular Biology and Microbiology, University of Central Florida, Orlando, Florida 32826, and Department of Oncology and Department of Biochemistry and Molecular Biology, H. Lee Moffitt Cancer Center and Research Institute, University of South Florida, Tampa, Florida 33612

Received February 3, 2008

New chemotherapeutics are urgently needed to combat malaria. We previously reported on a novel series of antimalarial, ethylenediamine-based inhibitors of protein farnesyltransferase (PFT). In the current study, we designed and synthesized a series of second generation inhibitors, wherein the core ethylenediamine scaffold was varied in order to examine both the homology model of *Plasmodium falciparum* PFT (*Pf*PFT) and our predicted inhibitor binding mode. We identified several *Pf*PFT inhibitors (*Pf*PFTIs) that are selective for *Pf*PFT versus the mammalian isoform of the enzyme (up to 136-fold selectivity), that inhibit the malarial enzyme with IC₅₀ values down to 1 nM, and that block the growth of *P. falciparum* in infected whole cells (erythrocytes) with ED₅₀ values down to 55 nM. The structure–activity data for these second generation, ethylenediamine-inspired PFT inhibitors were rationalized by consideration of the X-ray crystal structure of mammalian PFT and the homology model of the malarial enzyme.

Introduction

Malaria is an infectious disease, prevalent primarily in the tropics and subtropics. With as many as 300–500 million cases reported each year, malaria causes between 1 and 3 million deaths annually, approximately 90% of which occur in Africa.^{1,2} Unfortunately, malaria mortality is increasing, especially in the highest risk group, African children.³ There are a number of likely reasons for this increase, the most important of which is increased resistance of malaria parasites to existing drugs.^{4–6} There is now a general consensus that new antimalarials are urgently needed.⁷

Transmitted by mosquitoes of the genus *Anopheles*, four species of the protozoal parasite *Plasmodium* are known to cause malaria in humans, namely *falciparum*, *vivax*, *malariae*, and *ovale*. Of these, *P. falciparum*^a is the most virulent, and malaria mortality is almost exclusively attributable to infection by this species.^{1,7} Chloroquine, which is believed to disrupt heme polymerization, is one of the cheapest and most widespread drugs for malaria chemotherapy. However, *P. falciparum* has developed considerable resistance to chloroquine and to other

antimalarial drugs, such as mefloquine and sulfadoxime/pyrimethamine,^{6,7} and in those countries that are affected most seriously, existing alternative chemotherapeutics are virtually unaffordable. Of significant concern is the identification of multidrug resistant strains of *P. falciparum*.⁵ The development of drug resistance is not the only cause of the increasing spread of malaria. Other factors also contribute to this worsening scenario, such as the resistance of the *Anopheles* mosquito to the pesticide DDT, the migration of refugee populations, and an ever-warming climate.⁸ The associated increase in malaria mortality has accelerated research into new antimalarial drugs, to disrupt not only conventional targets, such as heme polymerization, but also more novel targets, such as the biochemical pathways of fatty acid biosynthesis and mevalonate-independent isoprenoid biosynthesis.⁵ We believe that exploitation of these alternative targets will fast become essential, owing to the existence of multidrug resistant strains of *P. falciparum* coupled with the observation that the parasite readily mutates to develop resistance to new drugs (designed for conventional targets).⁵ Since the economic reality of the effective treatment of malaria is beyond the means of Third World countries, where this disease is most prevalent, this raises the need for inexpensive chemotherapeutics. Subsequently, while it is acknowledged that the majority of the cost of a new therapeutic lies in its clinical trials, to minimize the cost at the drug development stage and to expedite access to new antimalarials, there has been considerable research into the possible antimalarial activity of drugs designed for other diseases in a so-called “piggy-back” approach.^{9–14}

Mammalian protein farnesyltransferase (PFT) is a key target for the antagonism of oncogenic Ras activity that is found in around 30% of human cancers,¹⁵ and a number of protein

* To whom correspondence should be addressed. Phone: (203) 432-5570. Fax: (203) 432-3221. E-mail: andrew.hamilton@yale.edu.

[†] Yale University.

[‡] Department of Medicine, University of Washington.

[#] Department of Molecular Biology and Microbiology, University of Central Florida.

^{||} University of South Florida.

[§] Department of Chemistry and Biochemistry, University of Washington.

^a Abbreviations: PFT, protein farnesyltransferase; *P. falciparum*, *Plasmodium falciparum*; *Pf*PFT, *P. falciparum* protein farnesyltransferase; FPP, farnesyl pyrophosphate; ED₅₀, effective dose that inhibits 50% of *P. falciparum* proliferation; IC₅₀, inhibitor concentration that inhibits 50% of PFT enzyme activity; rt, room temperature.

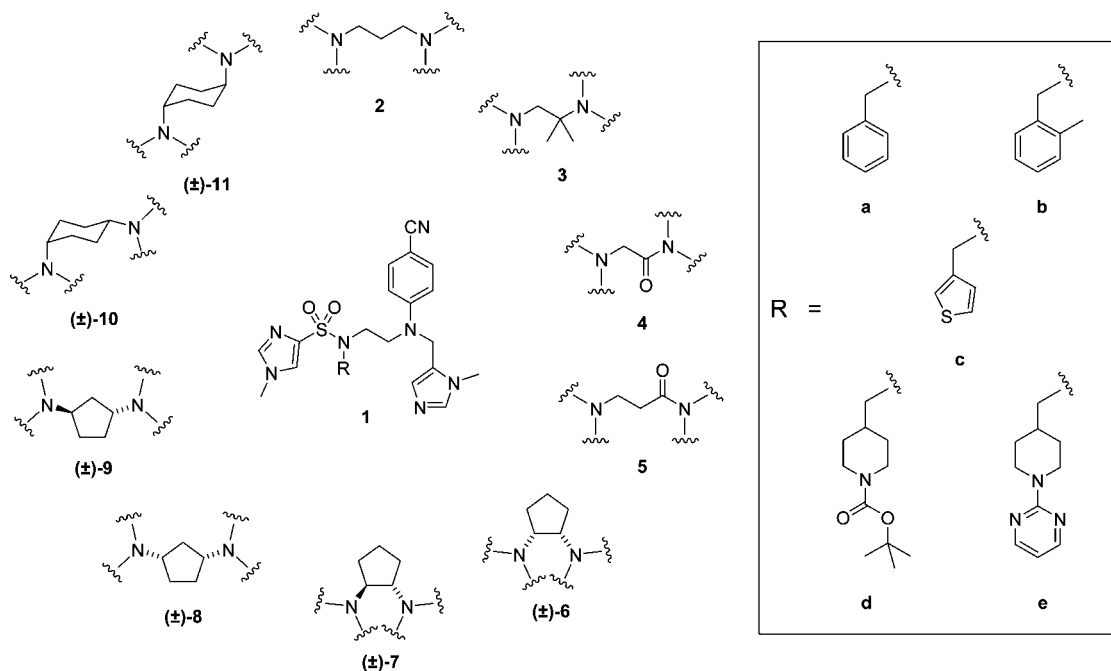


Figure 1. The various scaffolds used in this study as alternatives to the ethylenediamine scaffold in **1**.

farnesyltransferase inhibitors (PFTIs) have shown antitumor activity, having progressed to phase II/III in clinical trials.¹⁶ PFT, a member of the prenyltransferase family, is one of three closely related heterodimeric zinc metalloenzymes (the others being the protein geranylgeranyltransferases I and II, PGGT-I and PGGT-II, respectively) that are important post-translational modification enzymes, catalyzing protein prenylation and subsequent membrane association.¹⁷ PFT catalyzes the transfer of a C15 isoprenoid (farnesyl) unit from farnesylpyrophosphate (FPP) to the free thiol of a cysteine residue within a specific CaaX tetrapeptide sequence, located at the C-terminus of the substrate protein (e.g., RasGTPase), where a = an aliphatic amino acid and X (which contributes to substrate specificity) = M, S, A, or Q. Chakrabarti et al. have identified prenylated proteins and associated prenyltransferase activity in *P. falciparum* and confirmed the viability of *P. falciparum* protein farnesyltransferase (*PfPFT*) as a new antimalarial target.^{9,18} Upon administration of mammalian-designed anticancer PFTIs to *P. falciparum*-infected erythrocytes, a reduction in the cellular levels of farnesylated proteins was observed coupled with lysis of the parasites.^{13,18} More recently, Van Voorhis and co-workers have identified two *P. falciparum* mutants, each with single amino acid substitutions (Y837C¹⁹ and G612A²⁰) in *PfPFT* that map to the predicted inhibitor binding site, which show resistance to tetrahydroquinoline (THQ)-based *PfPFT* inhibitors both in vitro and in whole cells, further supporting *PfPFT* as the target for antimalarial activity.^{19,20} We^{10,21–23} and others¹⁴ have successfully adopted this “piggy-back” approach with several series of anticancer PFTIs and observed antimalarial activity in every case.^{10,21–23} Notably, in animal studies we have cured rats infected with malaria via oral dosing of our PFT-targeted THQ-based inhibitors,²⁴ while Schlitzer et al. have cured mice infected with malaria by intraperitoneal injection of their benzophenone-based PFTIs.¹⁴ The now-complete genome of *P. falciparum* indicates an apparent lack of PGGT-I,²⁵ suggesting that no alternative protein prenylation can occur upon *PfPFT* inhibition, which may explain the observation that PFTIs have been found to be significantly more toxic to plasmodial cells than to mammalian cells.¹³ Indeed, if PFTIs are to be effective antimalarials, plasmodium selectivity may be required,

since the antiproliferative nature of PFTIs may preclude or at least restrict their use in children and pregnant women, the main target groups in malaria therapy.

Using the sequence alignment of *PfPFT* on the template crystal structure of rat PFT complexed with the nonsubstrate tetrapeptide inhibitor CVFM and the cosubstrate FPP, we have developed a homology model of the active site of *PfPFT*.^{19,26} This model reveals a large ($\sim 20 \times 20 \times 20 \text{ \AA}^3$), open, and predominantly hydrophobic cavity, with FPP extending across the cavity base, itself forming part of the binding surface for the enzyme substrate. Further inspection of the active site homology model indicates that there are four subpockets. In the first, the Zn(II) ion is chelated by three residues (Cys661, Asp659, His838), with a water molecule hydrogen-bonded between the terminal phosphate of FPP and Asp659, defining the limit of the Zn binding domain. Second and third are two well-defined, predominantly hydrophobic subpockets (Lys149, Asn317, Ser150, Phe151, where Asn317 and Ser150 form a hydrophilic domain at the deepest point; and Trp456, Trp452, Tyr837). The fourth subpocket is a larger hydrophilic domain formed by Arg564 and three water molecules participating in a hydrogen-bonded network between Ser449 and Gln152. We have previously reported on a series of ethylenediamine-based inhibitors that were predicted to allow simultaneous access to the four subpockets within the *PfPFT* active site.^{26,27} Lead inhibitors displayed excellent activity in vitro ($\text{IC}_{50} < 1 \text{ nM}$) and toxicity toward cultured parasites in whole cells ($\text{ED}_{50} < 100 \text{ nM}$). Furthermore, these PFTIs represent the first antimalarials to exhibit selectivity for plasmodial over mammalian PFT (up to 145-fold selectivity). With such potent data and plasmodium PFT-isoform selectivity already achieved, the main aim of the present research was to investigate the validity of the *PfPFT* active site homology model, as well as the initial docking studies reported in our previous work,^{26,27} by introducing alternative scaffolds with different rigidities/flexibilities and with different nitrogen–nitrogen distances into our ethylenediamine-based inhibitors. In turn, we hoped that our findings would assist in future, potent *PfPFT* inhibitor design.

First, we illustrate the scaffold modifications that we chose to investigate and then comment on their abilities to dock in

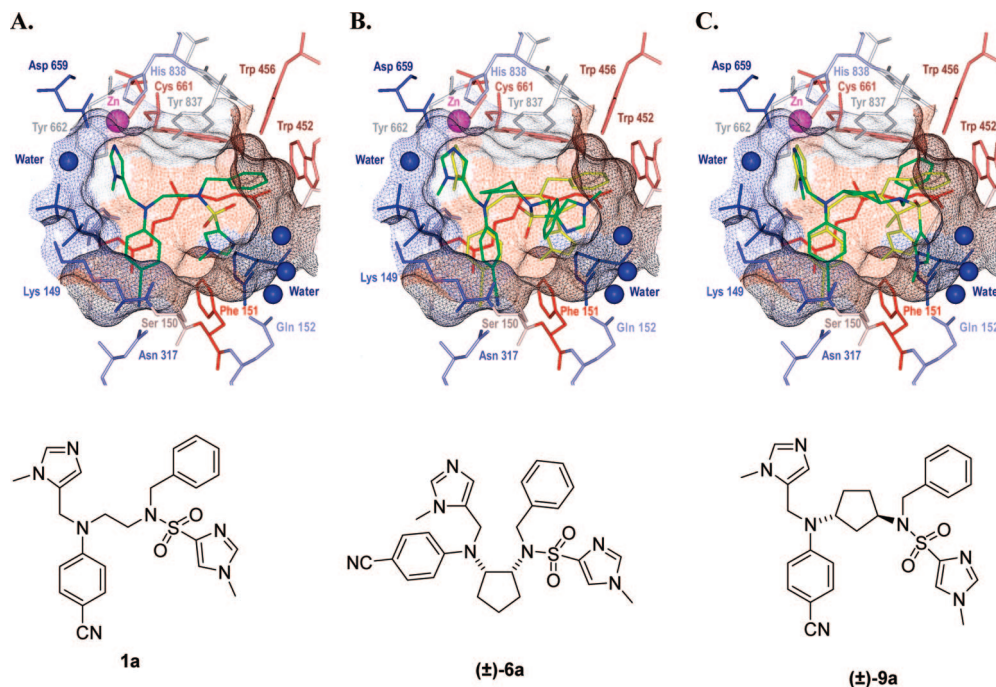


Figure 2. Low energy docked conformations (GOLD²⁸) of inhibitors loosely constrained to the predicted binding mode of **1a**.^{26,27} Docked inhibitors are colored by atom type and are overlaid by the predicted docking pose of **1a** in yellow. Farnesylpyrophosphate (FPP) is shown in red. Hydrophobic surface residues are colored red, hydrophilic residues and structural waters are blue, and the Zn²⁺ ion is pink: (A) **1a** docked alone; (B) (±)-**6a** overlaid with **1a**; (C) (±)-**9a** overlaid with **1a**.

the *PfPFT* active site homology model using the computer modeling program GOLD.²⁸ We describe the syntheses of these novel inhibitors and then present in vitro *PfPFT* inhibition data, as well as two sets of whole cell data of erythrocytes infected with either the 3D7 (chloroquine-sensitive) or the K1 (chloroquine-resistant, pyrimethamine-resistant) strain of *P. falciparum*. To conclude the manuscript, we utilize our computational and experimental data to present quantitative structure–activity relationship (QSAR) models of *PfPFT* and discuss their implications.

Design

Previous research identified that our most potent ethylenediamine-based inhibitors were functionalized as in **1** and where varying the R group proved critical to inhibitor potency. As reference compounds, we selected five derivatives of **1** with the following R groups: **a**, R = benzyl; **b**, R = 2-methylbenzyl; **c**, R = thiophen-3-ylmethyl; **d**, R = *N*-Boc-piperidin-4-ylmethyl; **e** = *N*-(2-pyrimidinyl)-piperidin-4-ylmethyl. The ethylenediamine-alternative scaffolds selected to test both our predicted inhibitor binding mode and the *PfPFT* active site homology model are illustrated in Figure 1. These fall into three categories with respect to their rigidities/flexibilities relative to the ethylenediamine scaffold (**1**). The first category possesses only 1,3-diaminopropane (**2**), which is acyclic and, with the additional methylene group, more flexible than ethylenediamine. The second category includes *gem*-dimethylethylenediamine (**3**), 2-aminoethanamide (**4**), and 3-aminopropanamide (**5**), which are acyclic and more rigid than ethylenediamine. The third category incorporates (±)-*cis*-1,2-diaminocyclopentane (**6**) and (±)-*trans*-1,2-diaminocyclopentane (**7**), (±)-*cis*-1,3-diaminocyclopentane (**8**) and (±)-*trans*-1,3-diaminocyclopentane (**9**), and (±)-*cis*-1,4-diaminocyclohexane (**10**) and (±)-*trans*-1,4-diaminocyclohexane (**11**), all of which are cyclic and more rigid than ethylenediamine and exhibit gradually increasing distances between the scaffold nitrogens. The corresponding rigid (±)-

cis- and (±)-*trans*-1,2-diaminocyclobutanes and the (±)-*cis*- and (±)-*trans*-1,2-diaminocyclopropanes were deemed too unstable because of the “push–pull effect” and were not investigated.²⁹

Computational docking experiments were performed using the GOLD 3.1 software package.²⁸ First, InsightII³⁰ was used to draw structures (R = Bn), energy-minimize them and to prepare our homology model of the active site of *PfPFT* for use in GOLD. Novel ligands were assumed to maintain a similar binding mode to that hypothesized for **1a**;^{26,27} the two imidazole rings and the cyanoaniline were loosely constrained to their associated binding pockets for each compound (for full details, see Experimental Methods). Visualization of GOLD low energy docked poses was performed with InsightII. In all figures presented (Figure 2 and Supporting Information Figures 1–8), the binding site of *PfPFT* has been surfaced, in which the enzyme cosubstrate farnesylpyrophosphate (FPP) forms part of that binding surface.

The GOLD docking studies predicted that many of these alternative scaffolds should not be as well tolerated as the parent ethylenediamine scaffold in the active site of *PfPFT* (Figure 2 and Supporting Information Figures 1–8). As Supporting Information Figure 1 illustrates, the 1,3-diaminopropyl scaffold (inhibitor **2a**) is accommodated well in the active site, although the extra methylene appears to require the inhibitor to buckle in order to allow all four N-substituents to reach their predicted subpockets. We anticipated that inhibitors derived from this scaffold may bind *PfPFT* well but not as potently as the parent ethylenediamine-based inhibitors. As expected, docking of the *gem*-dimethylethylenediamine-based inhibitor (Supporting Information Figure 2, inhibitor **3a**) illustrates that all four subpockets can be reasonably accessed by the four N-derivatives in much the same way as the parent ethylenediamine scaffold, suggesting that these compounds may be potent inhibitors of *PfPFT*. While the amide-based scaffolds (Supporting Information Figure 3, inhibitor **4a**) are also predicted to bind well, the constraints we imposed in the GOLD docking experiments have

caused the increase in hydrophilicity of the core scaffold to be ignored, which may lead to an erroneous result due to the hydrophobic environment in which the inhibitor scaffold is predicted to bind. The rigid *cis*-1,2- (Figure 2B inhibitor **6a**), *trans*-1,2- (Supporting Information Figure 4, inhibitor **7a**), and *cis*-1,3-diaminocyclopentyl scaffolds (Supporting Information Figure 5, inhibitor **8a**), and the *cis*-1,4-diaminocyclohexyl (Supporting Information Figure 7, inhibitor **10a**) scaffold do not fit well in the active site because of their constrained structures that prevent simultaneous access by all four N-substituents into the four subpockets. These observations suggest that compounds with these scaffolds may be poor inhibitors of *Pf*PFT. On the other hand, *trans*-1,3-diaminocyclopentyl- (Figure 2C, inhibitor **9a**) and *trans*-1,4-diaminocyclohexyl- (Supporting Information Figure 6, inhibitor **11a**) derivatives appear to be reasonably well accommodated, so we predicted these inhibitors may bind well to *Pf*PFT. However, the increasing scaffold nitrogen–nitrogen distance may prove detrimental with bulkier R groups.

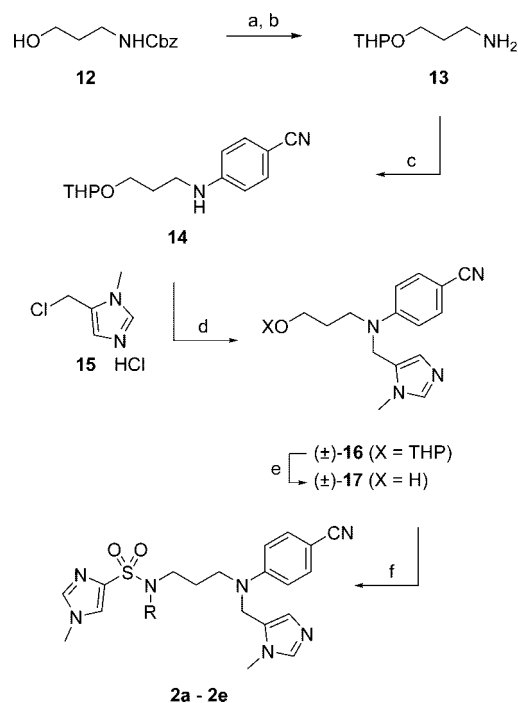
We hypothesized that if a structure with a diamino-based scaffold (whose nitrogens have been functionalized with four previously optimized groups) is loosely constrained to our predicted binding mode and subsequently docks well in the active site homology model, then that structure should bind well experimentally. In turn, this should be reflected by potent enzyme inhibition data. Conversely, structures that are predicted to bind less well should be poorer inhibitors. By testing this hypothesis over a range of different scaffolds that modulate the inhibitors' abilities to simultaneously access all four predicted binding subpockets within the *Pf*PFT active site, we should be able to garner enough information to develop a quantitative structure–activity relationship (QSAR) model and thereby validate both our predicted inhibitor binding mode and the homology model itself. It is our hope that this information will assist in future *Pf*PFT inhibitor design.

Chemistry

1,3-Diaminopropane-Based Inhibitors (2a–e). These inhibitors were prepared as in Scheme 1. *N*-Carbobenzyloxy-3-amino-1-propanol (**12**) was converted to its THP ether derivative (with dihydropyran (DHP) and catalytic pyridinium *p*-toluenesulfonate (PPTS)), after which the Cbz protecting group was removed under standard hydrogenolytic conditions (H₂ and 10% Pd/C) to furnish primary amine **13**. Nucleophilic aromatic substitution of **13** with *p*-fluorobenzonitrile, followed by N-alkylation of secondary aniline **14** with 5-chloromethyl-1-methyl-1*H*-imidazole·HCl (**15**) under optimized conditions gave tertiary aniline **16** in a yield of 81% (or 97% based on recovered starting material (brsm)). Acid-catalyzed methanolysis of the THP protecting group furnished primary alcohol **17**, which was coupled to the secondary sulfonamides **19a–e** (prepared as described in Schemes 2 and 3) under Mitsunobu conditions, employing diisopropyl azodicarboxylate (DIAD)/triphenylphosphine (PPh₃) as the redox system, to give *Pf*PFT inhibitors **2a–e** in excellent yields. Due to the success of the Mitsunobu reaction coupled with its convergent effect on the overall syntheses of these 1,3-diaminopropane-based *Pf*PFTIs, we designed syntheses of the remaining *Pf*PFTIs that also incorporated Mitsunobu as the final step.

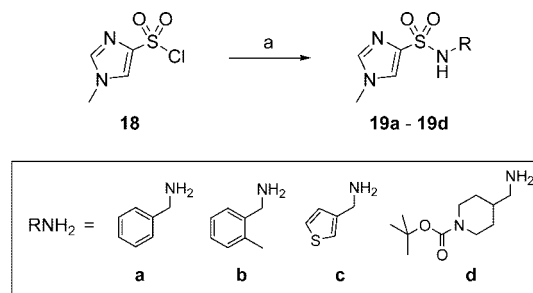
Sulfonamides for Mitsunobu Reactions (19a–e, 21). The secondary sulfonamides **19a–d** required for the Mitsunobu reactions (e.g., step f in Scheme 1) were prepared in simple one-step procedures from 1-methyl-1*H*-imidazole-4-sulfonyl chloride (**18**) and the respective primary amines in yields ranging

Scheme 1^a



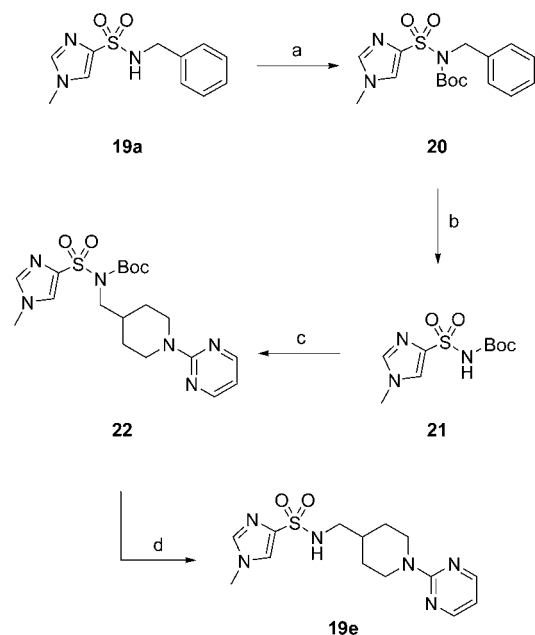
^a (a) DHP, cat. PPTS, CH₂Cl₂, 0 °C → rt, 16 h, 85%; (b) H₂, 10% Pd/C, MeOH, rt, 1 h, 82%; (c) *p*-fluorobenzonitrile, DIPEA, DMSO, 120 °C, 24 h, 87%; (d) (1) NaH, DMF, 0 °C, 30 min; (2) **15**, 0 °C → rt, 3 h, 81% (or 97% brsm); (e) *p*-TsOH·H₂O, MeOH, rt, 1 h, 88%; (f) **19a–e**, DIAD, PPh₃, THF, rt, 1 h, 61–98%.

Scheme 2^a

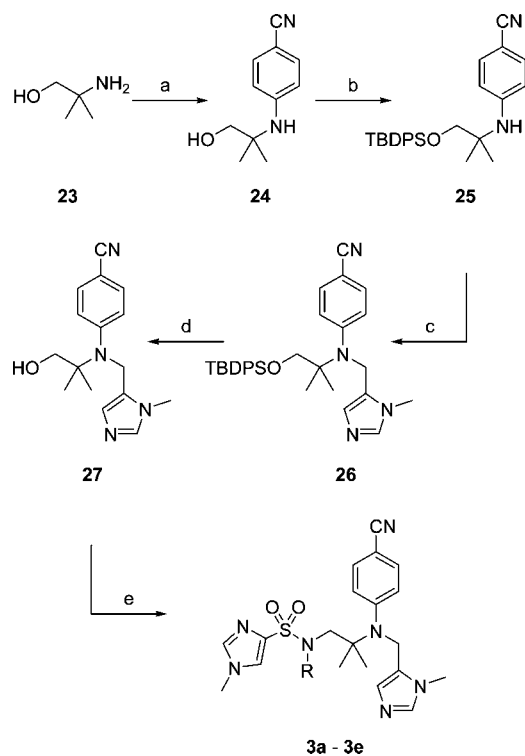


^a (a) RNH₂, DIPEA, CH₃CN, 0 °C → rt, 16 h, 81–93%.

from 81% to 93% (Scheme 2). Due to the unavailability of *N*-(2-pyrimidinyl)-4-aminomethylpiperidine and the need for the more acidic sulfonamide **21** in the synthesis of 3-aminoethanamide derivatives **5a** and **5d** as well as the *trans*-1,2-diaminocyclopentyl derivatives **7a–e**, sulfonamide **19e** was prepared by a different route (Scheme 3). Accordingly, treatment of **19a** with Boc₂O led to the fully derivatized sulfonamide **20** in quantitative yield. Subsequent hydrogenolysis of **20** furnished *N*-tert-butoxycarbonyl-1-methyl-1*H*-imidazole-4-sulfonamide (**21**), whose NH was expected to have a lower p*K*_a than that of simple *N*-alkyl secondary sulfonamides, such as **19a**, whose p*K*_a values are just on the cusp (p*K*_a ≈ 12) of acidic nucleophiles (NuH) allowed in the Mitsunobu reaction. The enhanced acidity of **21** was subsequently found to resolve troublesome Mitsunobu reactions (see sections on the syntheses of **5a,d** and **7a–e**). Additionally, compound **21** was successfully coupled to *N*-(2-pyrimidinyl)-4-hydroxymethylpiperidine, giving **22**, which, after Boc deprotection with TFA, yielded sulfonamide **19e** in an excellent two-step yield of 92%.

Scheme 3^a

^a (a) Boc₂O, cat. DMAP, THF, rt, 16 h, 99%; (b) H₂, 10% Pd/C, EtOH, rt, 16 h, 100%; (c) *N*-(2-pyrimidinyl)-4-hydroxymethylpiperidine, PPh₃, DIAD, THF, rt, 16 h; (d) TFA/CH₂Cl₂, 1:1, rt, 3 h, 92% (two steps).

Scheme 4^a

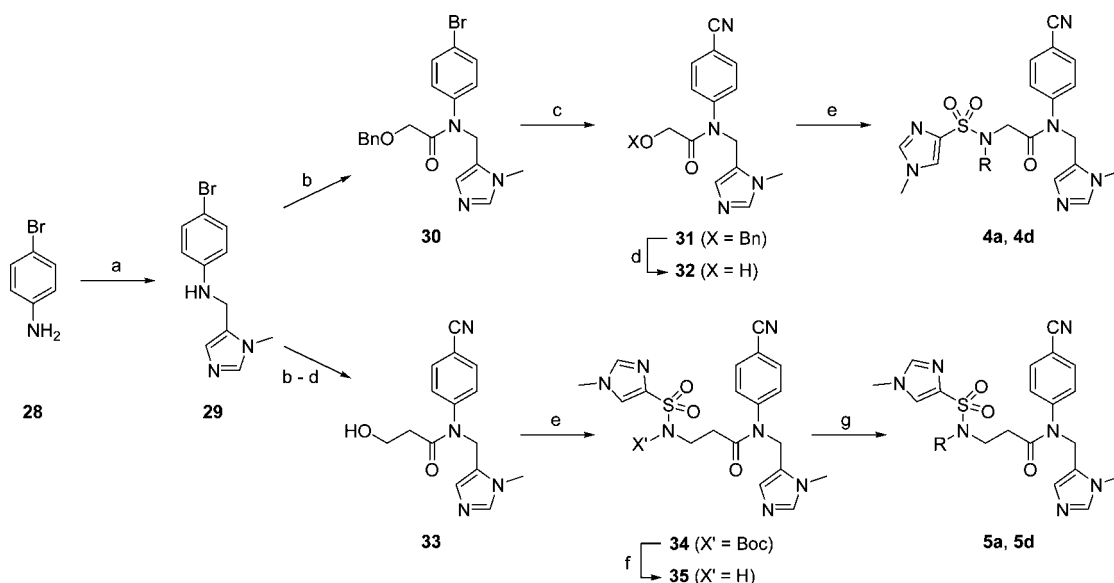
^a (a) *p*-fluorobenzonitrile, DIPEA, DMSO, 180 °C, 48 h, 40%; (b) TBDPSCI, Im, DMF, 45 °C, 18 h, 90%; (c) (1) NaH, DMF, 0 °C, 30 min; (2) **15**, 0 °C → rt, 3 h, 53% (or 82% brsm); (d) TBAF, THF, 0 °C → rt, 2 h, 95%; (e) **19a-e**, DIAD, PPh₃, THF, 45 °C, 18 h, 50–68%.

gem-Dimethylethylenediamine-Based Inhibitors (3a–e). The hindered *gem*-dimethylethylenediamine derivatives **3a–e** were furnished as shown in Scheme 4. Nucleophilic aromatic substitution of 2-amino-2-methylpropan-1-ol (**23**) with *p*-fluorobenzonitrile in a sealed vessel at 180 °C for 48 h afforded **24** in 40% yield. Attempted chemoselective benzylation of the primary hydroxyl of **24** with NaH and BnBr led to a mixture

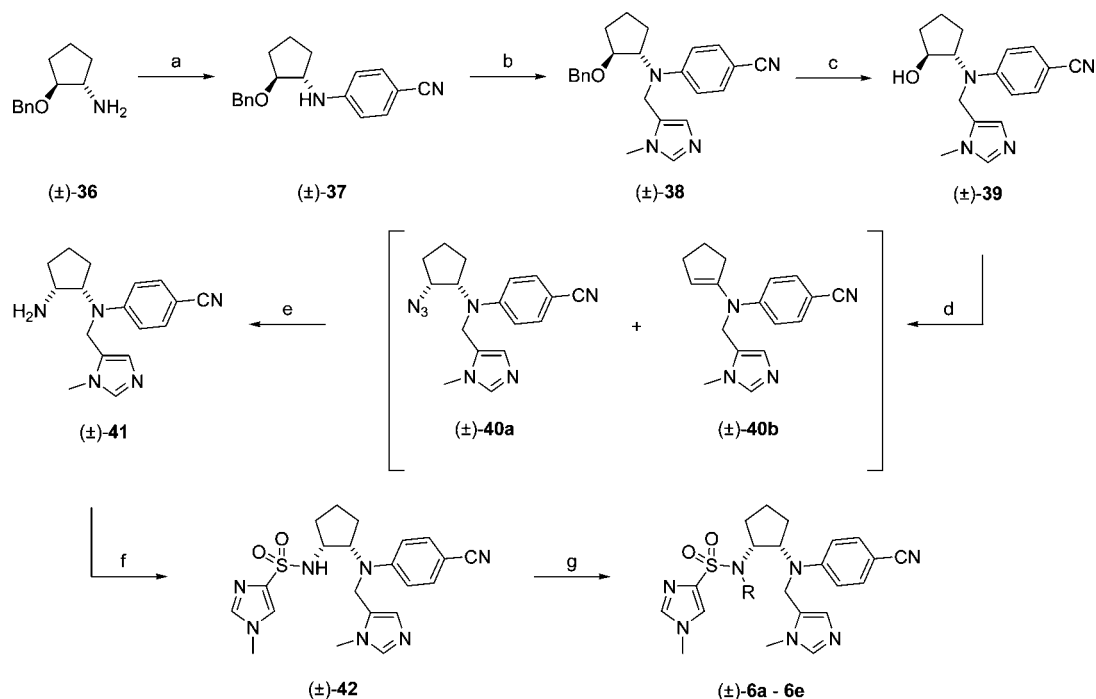
of products. However, alternative protection of the alcohol with *tert*-butyldiphenylsilylchloride (TBDPSCI), employing imidazole (Im) as base and nucleophilic catalyst, gave the desired compound **25** in excellent yield. The zinc-binding imidazole group was next installed by treatment of secondary aniline **25** with NaH at 0 °C followed by addition of 5-chloromethyl-1-methyl-1*H*-imidazole·HCl (**15**) as before to furnish tertiary aniline **26**. Quantitative deprotection of the TBDPS group with tetra-*n*-butylammonium fluoride (TBAF) was observed, and the resultant primary alcohol was condensed with the five sulfonamides **19a–e** under Mitsunobu conditions at 45 °C to afford the final *P/PFTI*s **3a–e** in 50–68% yields.

2-Aminoethanamide-Based Inhibitors (4a, 4d) and 3-Aminopropanamide-Based Inhibitors (5a, 5d). Due to earlier findings that incorporation of an amide bond into the inhibitor scaffold is not tolerated,³¹ we decided to make just two derivatives of each amide-containing scaffold, with a small (**a**, R = Bn) and a large (**d**, R = *N*-Boc-piperidin-4-ylmethyl) R group. The syntheses of these 2-aminoethanamide- (**4a**, **4d**) and 3-aminopropanamide-based *P/PFTI* inhibitors (**5a**, **5d**) are presented in Scheme 5 and are described in full in Supporting Information.

(±)-cis-1,2-Diaminocyclopentane-Based Inhibitors ((±)-6a–e) and (±)-trans-1,2-Diaminocyclopentane-Based Inhibitors ((±)-7a–e). The (±)-*cis*-1,2-diaminocyclopentyl-based inhibitors (±)-**6a–e** were furnished by following the synthetic steps described in Scheme 6. Racemic (±)-*trans*-2-benzyloxycyclopentylamine ((±)-**36**) was arylated with *p*-fluorobenzonitrile, using an excess of the aryl fluoride to compensate for reduced reactivity due to steric hindrance. *N*-Alkylation of the resultant secondary aniline (±)-**37** with **15** as before furnished (±)-**38** in a moderate yield of 56% (or 89% brsm), which was then smoothly debenzylated under optimized conditions (1 atm of H₂, catalyst 10% Pd/C, 0.5% concentrated HCl in EtOH (v/v), 1 h) to furnish secondary alcohol (±)-**39**. The proposed final step in this synthesis, Mitsunobu reaction of (±)-**39** with the secondary sulfonamides **19a–e**, proved unsuccessful, leading to elimination rather than substitution, presumably due to the sterically encumbering tertiary amine and/or the low acidities of the sulfonamides (p*K*_a ≈ 12) that places them at the uppermost limit of allowed nucleophiles for the Mitsunobu reaction. However, even with the more acidic sulfonamide **21** (Scheme 3), we again observed only elimination. Likewise, alternative, more powerful Mitsunobu redox systems such as *N,N,N',N'*-tetramethylazodicarboxamide (TMAD)/tri-*n*-butylphosphine (TBP) and cyanomethyl-tri-*n*-butylphosphorane (CMBP) proved fruitless. We next considered the steric hindrance in the desired transformation and found that Mitsunobu reaction of (±)-**39** with diphenylphosphorylazide (DPPA), which involves the smaller and linear azide ion as the nucleophile, was more successful. These conditions led to a 3:2 inseparable mixture of the azide (substitution) product (±)-**40a**, wherein the usual inversion of stereochemistry had occurred, and the alkene (elimination) product (±)-**40b**. Staudinger reduction of azide (±)-**40a** in the mixture led to the anticipated increase in polarity, enabling facile separation from alkene (±)-**40b** and furnishing primary amine (±)-**41** in a yield of 56% for the two steps. Subsequently, sulfonylation of (±)-**41** afforded secondary sulfonamide (±)-**42** in good yield, which was then alkylated with a series of bromides (or iodides) to give the (±)-*cis*-1,2-diaminocyclopentyl *P/PFTI* inhibitors (±)-**6a–e** in poor to good yields. Importantly, for the two benzylic and thiophen-3-ylmethyl bromides, this reaction had to be performed under dilute (0.01 M) conditions to reduce the facile quaternization

Scheme 5^a

^a (a) (1) 3-Methyl-3H-imidazole-4-carbaldehyde, AcOH, 4 Å molecular sieves, MeOH, rt, 1 h; (2) NaCNBH₃, rt, 16 h, 63%; (b) benzyloxycarbonyl chloride (or 3-benzyloxypropanoyl chloride), pyridine, CH₂Cl₂, rt, 2 h, 87–94%; (c) Zn(CN)₂, 10 mol % Pd(PPh₃)₄, cat. Zn(OAc)₂, cat. Zn dust, DMF, 120 °C, 2 h, 85–89%; (d) H₂, 10% Pd/C, 0.5% conc HCl (v/v), EtOH, rt, 90 min, 84–94%; (e) **19a** or **19d**, PPh₃, DIAD, THF, rt, 1 h, 52% for **4a**, or 20% for **4d**; or **21**, PPh₃, DIAD, THF, rt, 1 h, 56% for **34**; (f) TFA/CH₂Cl₂, 1:1, rt, 3 h, 97%; (g) RBr, Cs₂CO₃, DMF, rt, 16–36 h, 50–96%.

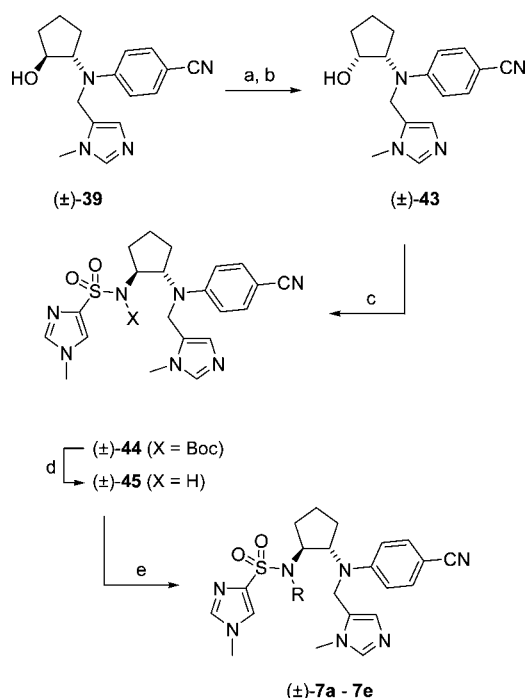
Scheme 6^a

^a (a) *p*-Fluorobenzonitrile, DIPEA, DMSO, 120 °C, 24 h, 87%; (b) (1) NaH, DMF, 0 °C, 30 min; (2) **15**, 0 °C → rt, 3 h, 56% (or 89% brsm); (c) H₂, 10% Pd/C, 0.5% conc HCl, EtOH, rt, 1 h, 87%; (d) PPh₃, DIAD, DPPA, THF, 0 °C → rt, 16 h; (e) (1) PPh₃, THF, rt, 1 h; (2) H₂O, 65 °C, 7 h, 56% (combined yield for steps d and e); (f) **18**, DIPEA, CH₃CN, 0 °C → rt, 16 h, 75%; (g) RBr (or RI), Cs₂CO₃, DMF, rt, 16 h to 7 days, 22–81%.

of the Zn(II)-binding imidazole τ -nitrogen (N^{τ} -alkylation), a side reaction that competed effectively with the desired sulfonamide alkylation because of considerable steric hindrance around the sulfonamide NH.

In order to prepare the corresponding *trans* analogues, (±)-**39** was reacted with *p*-nitrobenzoic acid under Mitsunobu conditions (Scheme 7), which again led to an approximate 3:2 mixture of ester (substitution product) and alkene (elimination product). No attempt at purification was made at this stage, and LiOH·H₂O was added directly to the reaction mixture. After 3 h, the ester hydrolysis

was complete. Purification of the reaction mixture gave the *cis* product (±)-**43** in 39% yield for the two steps, whose inverted stereochemistry was evident from the comparison of ¹H NMR spectra of (±)-**39** and (±)-**43**. Again, the subsequent Mitsunobu reaction with secondary sulfonamide **19a** was unfruitful. However, reaction with the alternative sulfonamide **21** was a success, likely due to a combination of the increased acidity of **21** relative to the other sulfonamides **19a–e** and reduced steric hindrance in the substitution step of the Mitsunobu reaction. Silica gel flash column chromatography furnished (±)-**44** in approximately 90% purity,

Scheme 7^a

^a (a) *p*-Nitrobenzoic acid, PPh₃, DIAD, THF, rt, 16 h; (b) LiOH·H₂O, THF/MeOH/H₂O, 3:1:1, rt, 3 h, 39% (two steps); (c) **21**, PPh₃, DIAD, THF, 45 °C, 16 h; (d) TFA/CH₂Cl₂, 1:1, rt, 3 h, 63% (two steps); (e) RBr, Cs₂CO₃, DMF, rt, 16 h to 7 days, 75–85%.

and subsequent removal of the Boc group with TFA, followed by the usual purification, generated pure secondary sulfonamide (±)-**45** in a yield of 63% for the two steps. Finally, alkylation of sulfonamide (±)-**45** with the five bromides as before gave the final (±)-*trans*-1,2-diaminocyclopentyl PpPFT inhibitors (±)-**7a–e** in good yields.

(±)-*cis*-1,3-Diaminocyclopentane-Based Inhibitors ((±)-**8a–e**) and (±)-*trans*-1,3-Diaminocyclopentane-Based Inhibitors ((±)-**9a–e**). The 1,3-diaminocyclopentyl inhibitors (±)-**8a–e** and (±)-**9a–e** were prepared as shown in Scheme 8. After quantitative *O*-silylation of hepta-1,6-dien-4-ol (**46**) with TB-DPSCl, the cyclopentane scaffold was constructed by treatment with Grubbs's catalyst to give **48**. Subsequent oxidation with *m*-CPBA in CH₂Cl₂ gave *cis* epoxide **49** and *trans* epoxide **50** in an approximate 1:1 ratio, in a combined yield of 84%. Reductive opening of the epoxide ring of **49** with H₂ and a range of catalysts, including 10% Pd/C, Pd(OH)₂, or PtO₂, were all attempted but were very slow even at pressures of up to 70 psi of H₂. Alternative treatment with LiAlH₄ was successful, furnishing racemic (±)-**51** in 93% yield. On the other hand, while executing the reductive opening of the epoxide ring of diastereomeric compound **50**, LiAlH₄ also caused the surprising removal of the TBDPS protecting group to give (±)-*trans*-cyclopentane-1,3-diol ((±)-**56**) in 84% yield. Nucleophilic aromatic substitution test reactions of the primary amino analogue of (±)-**51**, specifically 1-*tert*-butyldiphenylsilyloxy-2-aminocyclopentane, with *p*-fluorobenzonitrile, led to removal of the silicon protecting group, presumably by the action of liberated fluoride ion, and subsequent *O*-arylation. Therefore, single re-silylation of (±)-**56** was not attempted; monobenylation of (±)-**56** under phase transfer conditions was instead effected to give (±)-**57** in excellent yield.

In order to keep the two syntheses, which were already being conducted in tandem, as similar as possible, we executed a two-step protecting group exchange on *O*-TBDPS derivative (±)-

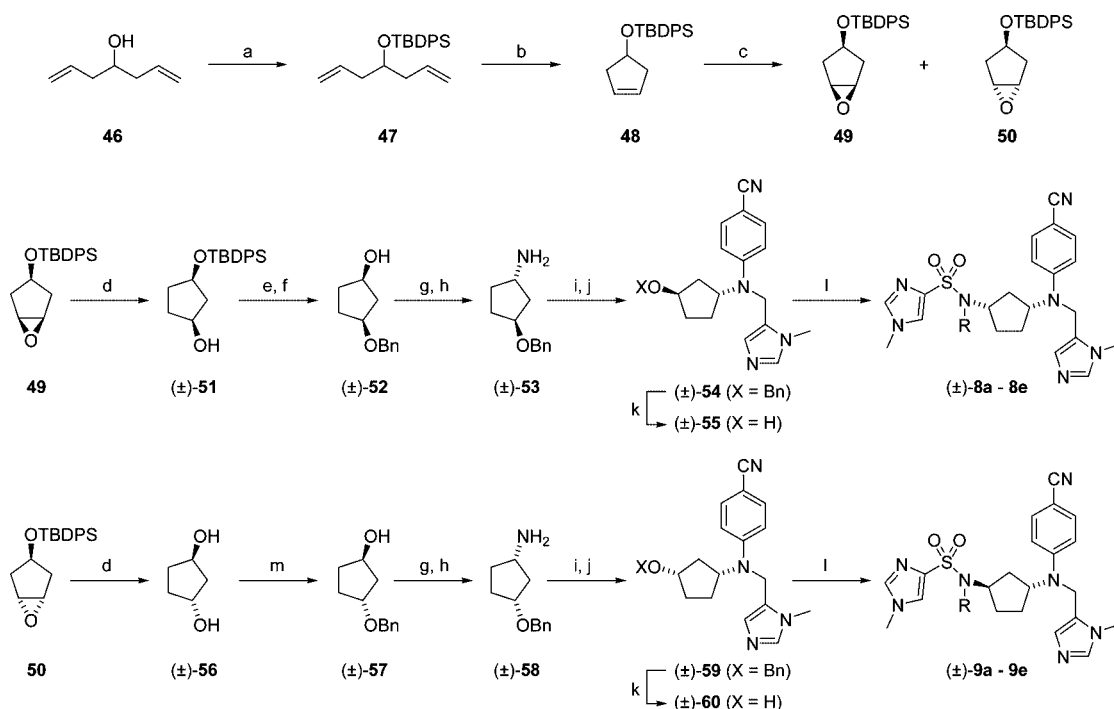
51 to give *O*-benzyl compound (±)-**52** (95%, two steps). Mitsunobu conditions effected conversion of the hydroxyl of (±)-**52** to the inverted azide whose reduction to primary amine (±)-**53** was accomplished with PPh₃ and water (Staudinger reaction). Nucleophilic aromatic substitution of (±)-**53**, followed by *N*-alkylation as before gave tertiary aniline (±)-**54**, which was then subjected to optimized hydrogenolytic cleavage conditions to furnish secondary alcohol (±)-**55** in a yield of 83%. Finally, coupling of (±)-**55** to the series of secondary sulfonamides **19a–d** with PPh₃ and DIAD proceeded in poor to good yields to afford the (±)-*trans*-1,3-diaminocyclopentyl PpPFT inhibitors (±)-**8a–d**. Due to the limited solubility of sulfonamide **19e** and the already low yields for this final Mitsunobu step, compound **8e** had to be prepared in the same manner as that used to prepare the *trans*-1,2-diaminocyclopentane-based inhibitors. Specifically, (±)-**55** was coupled to sulfonamide **21** under standard Mitsunobu conditions, after which the Boc group was removed by TFA, and then the resultant secondary sulfonamide was alkylated with *N*-(2-pyrimidinyl)-4-iodomethylpiperidine, furnishing (±)-**8e**. For the syntheses of the (±)-*trans*-1,3-diaminocyclopentyl PpPFT inhibitors (±)-**9a–e**, the synthetic transformations were identical from (±)-**57**, as depicted in Scheme 8.

(±)-*cis*-1,4-Diaminocyclohexane-Based Inhibitors ((±)-**10a**, (±)-**10d**) and (±)-*trans*-1,4-Diaminocyclohexane-Based Inhibitors ((±)-**11a**, (±)-**11d**). Scheme 9 illustrates the synthetic steps pursued in order to furnish the (±)-*cis*-1,4- ((±)-**10a**, (±)-**10d**) and the (±)-*trans*-1,4-diaminocyclohexyl ((±)-**11a**, (±)-**11d**) PpPFT inhibitors, for which only the R = Bn and R = *N*-Boc-piperidin-4-ylmethyl derivatives were prepared. (±)-*cis*-1,4-Diaminocyclohexane ((±)-**61**) was mono-arylated with *p*-fluorobenzonitrile in 77% yield to give (±)-**62**, which was then sulfonylated with 1-methyl-1*H*-imidazole-4-sulfonyl chloride (**18**) to furnish **63**. Chemoselective alkylation of the sulfonamide NH with benzyl bromide and *N*-Boc-4-bromomethylpiperidine was accomplished without incident, affording (±)-**64a** and (±)-**64d**, respectively. Finally, the secondary anilines were alkylated with **15** to yield the target PpPFT inhibitors (±)-**10a** and (±)-**10d** in moderate yields, where the mass balance was recovered starting material. Starting from (±)-*trans*-1-*tert*-butoxycarbonylamino-4-aminocyclohexane ((±)-**65**), the *trans* isomers (±)-**11a** and (±)-**11d** were furnished in a similar fashion.

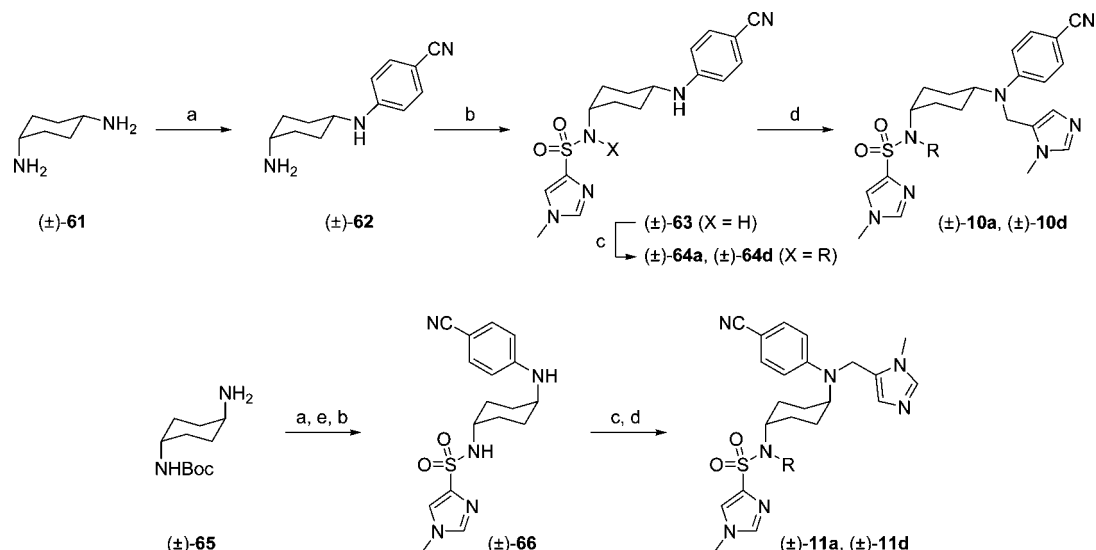
Results and Discussion

Ethylenediamine-Based Inhibitors (1a–e). For comparison with the 10 series of inhibitors in this study, we present a table that includes previously published data on the corresponding ethylenediamine-based inhibitors.^{26,27} Table 1 shows percentage enzyme inhibition of PpPFT by compounds **1a–e** at 50 and 5 nM inhibitor concentration. Also shown are ED₅₀ data, which are the required inhibitor concentration to inhibit 50% of the growth of parasites (two strains of *P. falciparum*: 3D7 and K1) in whole cells (erythrocytes), as determined through the incorporation of tritium-labeled hypoxanthine (see Experimental Methods for details). As indicated in Table 1, all inhibitors exhibited potent inhibition of PpPFT *in vitro* (≥74% inhibition at 5 nM) and proved highly effective antimalarials in whole cells (several ED₅₀ values <100 nM).

1,3-Diaminopropane-Based Inhibitors (2a–e). By comparison of the percentage enzyme inhibition data for the 1,3-diaminopropane-based inhibitors (Table 2) with the corresponding data for the ethylenediamine scaffold derivatives (Table 1), compounds **2a**, **2b**, and **2c** were all much poorer inhibitors of PpPFT. However, with the larger *N*-Boc-piperidin-4-ylmethyl

Scheme 8^a

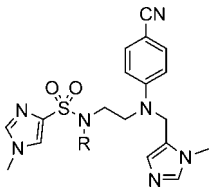
^a (a) TBDPSCl, Im, THF, 45 °C, 16 h, 99%; (b) Grubbs's first generation catalyst, CH₂Cl₂, rt, 3 days, 63%; (c) *m*-CPBA, CH₂Cl₂, 0 °C → rt, 16 h, 43% (**49**), 41% (**50**); (d) LiAlH₄, THF, 0 °C, 2 h, 93% ((±)-**51**) or 84% ((±)-**56**); (e) BnBr, NaH, DMF, 0 °C → rt, 16 h, 98%; (f) TBAF, THF, 0 °C → rt, 3 h, 97%; (g) PPh₃, DIAD, DPPA, THF, rt, 16 h, 88% (from (±)-**52**) or 92% (from (±)-**57**); (h) (1) PPh₃, THF, rt, 1 h; (2) H₂O, 65 °C, 7 h, 94% ((±)-**53**) or 97% ((±)-**58**); (i) *p*-fluorobenzonitrile, DIPEA, DMSO, 120 °C, 2 d, 48 h, 99% (from (±)-**53**) or 94% (from (±)-**58**); (j) (1) NaH, DMF, 0 °C, 30 min; (2) **15**, 0 °C → rt, 3 h, 52% ((±)-**54**) or 47% ((±)-**59**); (k) H₂, 10% Pd/C, 0.5% conc HCl (v/v), EtOH, rt, 1 h, 83% ((±)-**55**) or 85% ((±)-**60**); (l) **19a-e**, PPh₃, DIAD, THF, rt, 16 h, 32–79%; (m) (1) NaH, THF, 0 °C, 1 h; (2) BnBr, TBAI, 0 °C → rt, 16 h, 95%.

Scheme 9^a

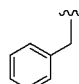
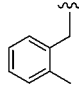
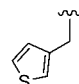
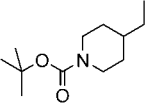
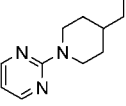
^a (a) *p*-fluorobenzonitrile, DIPEA, DMSO, 120 °C, 48 h, 77% (for (±)-**62**) or 89% (from (±)-**65**); (b) **18**, DIPEA, CH₃CN, rt, 16 h, 76% (for (±)-**63**) or 86% (for (±)-**66**); (c) RBr, Cs₂CO₃, DMF, rt, 16 h to 3 days, 82–99%; (d) (1) NaH, DMF, 0 °C, 30 min; (2) **15**, 0 °C → rt, 12 h, 61–69% (92–95% brsm); (e) TFA/CH₂Cl₂, 1:1, rt, 30 min, 100%.

(**2d**) and *N*-(2-pyrimidinyl)-piperidin-4-ylmethyl derivatives (**2e**), inhibition of the enzyme was almost the same as that for the corresponding ethylenediamine derivatives (e.g., **2d**, 73% inhibition at 5 nM, vs **1d**, 81% inhibition at 5 nM), suggesting that the reduction in activity caused by the additional methylene in the scaffold may have been offset by incorporating a large R group. Indeed, compound **2d** was an especially potent inhibitor of *Pf*PFT, with an IC₅₀ of 1 nM (Table 7). ED₅₀ data reflect the variation in *Pf*PFT inhibitor potency, supporting inhibition of

*Pf*PFT as the target for antimalarial activity, with **2d** proving the most effective antimalarial of this series in whole cells (ED₅₀ = 330 nM (3D7), 190 nM (K1)). A low energy docked conformation of **2a** overlaid with that of **1a** (Supporting Information Figure 1) suggested that the ethylenediamine-based derivative should be a much better fit in the homology model of the *Pf*PFT active site and that **2a** with its extra methylene unit in the scaffold should be too long to bind as well as **1a**, requiring a degree of buckling of the scaffold to enable

Table 1. Enzyme Inhibition and Whole Cell Data for Ethylenediamine-Based Inhibitors **1a–e**^a


The structure shows a central ethylenediamine core where one nitrogen is substituted with an R group and the other with a 4-cyanophenyl group. The R group is further substituted with a 1,2,4-triazole ring via a methylene bridge.

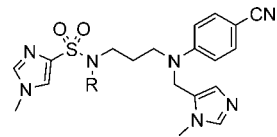
Compound		Inhibition of <i>Pf</i> FTase (%)		ED ₅₀ (nM) ^a	
Number	R	50 nM	5 nM	3D7	K1
1a		98	86	349	375
1b		99	95	93	150
1c		100	91	150	240
1d		96	81	88	54
1e		96	74	130	85

^a ED₅₀ = effective dose of inhibitor required to decrease *P. falciparum* growth (in infected erythrocytes) by 50%.

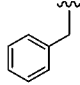
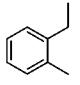
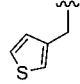
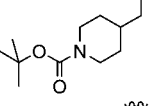
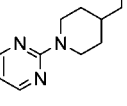
simultaneous access of the four N-appendages into the four subpockets. This prediction appears to have been confirmed experimentally, particularly in the case of the smaller R group derivatives.

gem-Dimethylethylenediamine-Based Inhibitors (3a–e). Discounting thiophene **3c**, the *gem*-dimethylethylenediamine scaffold derivatives (Table 3) were as potent, if not more so, as the corresponding ethylenediamine compounds (e.g., **3a**, 88% inhibition, vs **1a**, 86% inhibition at 5 nM; and **3e**, 93% inhibition, vs **1e**, 74% inhibition at 5 nM). Especially potent whole cell activity, such as ED₅₀ = 160 nM (3D7) and 55 nM (K1) for **3a**, parallels potent enzyme inhibition data in most cases, again supporting *Pf*PFT as the relevant target for antimalarial activity. Indeed, **3a** is one of our most potent, ethylenediamine-inspired antimalarials to date, and the improved whole cell activity relative to **1a** (ED₅₀ = 349 nM (3D7) and 375 nM (K1)) may be a consequence of the increased hydrophobicity of the scaffold, facilitating cellular entry. GOLD docking studies (Supporting Information Figure 2) suggested that these *gem*-dimethylethylenediamine-based inhibitors should be tolerated in the *Pf*PFT active site as well as the parent ethylenediamines, and this has been supported experimentally. The reason for the increased potency of the *gem*-dimethylethylenediamine-based **3e** in vitro may be due to additional hydrophobic contacts between the extra methyls of the inhibitor and the scaffold-binding region of the active site or to improved contacts of the *p*-cyanoaniline as a direct consequence of the Thorpe–Ingold effect³² or to a combination of both effects.

2-Aminoethanamide- and 3-Aminopropanamide-Based Inhibitors (4a,d and 5a,d). All the amide derivatives (**4a,d** and

Table 2. Enzyme Inhibition and Whole Cell Data for 1,3-Diaminopropane-Based Inhibitors **2a–e**^a


The structure shows a 1,3-diaminopropane core where one nitrogen is substituted with an R group and the other with a 4-cyanophenyl group. The R group is further substituted with a 1,2,4-triazole ring via a methylene bridge.

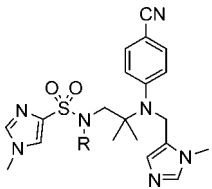
Compound		Inhibition of <i>Pf</i> FTase (%)		ED ₅₀ (nM)	
Number	R	50 nM	5 nM	3D7	K1
2a		71	16	3100	2650
2b		76	24	2900	2900
2c		73	18	2800	2200
2d		94	73	330	190
2e		93	62	1300	ND

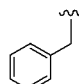
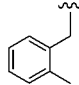
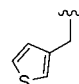
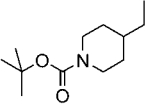
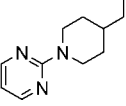
^a ND = not determined because of limited stocks of *Pf*PFT enzyme or *Plasmodium*-infected whole cell cultures.

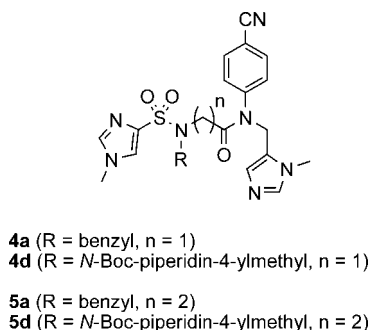
5a,d (Figure 3) showed 0% enzyme inhibition at 50 nM and were not studied further. Even though GOLD docking studies suggested that these derivatives would be reasonably well accommodated in the *Pf*PFT active site (Supporting Information Figure 3), we invoked several constraints that meant the increase in hydrophilicity of the scaffold would be ignored. The scaffold-binding region of the active site is hydrophobic, so it would be expected that a compound with a polar component in the scaffold, such as an amide bond, would be poorly tolerated. In addition, the rigidity incurred upon inclusion of the planar amide bond, which we hoped to offset by the addition of an extra methylene in the scaffold (**4** → **5**), and the amide-induced withdrawal of electrons from the *p*-cyanophenyl group (a moiety that is known to contribute particular potency to our inhibitors²⁷) are two possible further reasons as to why these amide derivatives showed no inhibition of *Pf*PFT at 50 nM.

(±)-cis- and (±)-trans-1,2-Diaminocyclopentane-Based Inhibitors ((±)-6a–e and (±)-7a–e). As Table 4 shows, the (±)-*cis*-1,2-diaminocyclopentyl-based derivatives (±)-**6a–e** performed very poorly indeed, with little or no inhibition of *Pf*PFT at 50 nM inhibitor concentration. Similarly, ED₅₀ values were disappointing; in most cases they were at least an order of magnitude worse than their ethylenediamine-based parent compounds. These results were expected, since docking studies of (±)-**6a** in the homology model of the enzyme active site indicated that the constraint imposed by the *cis* 1,2-cyclic scaffold meant that only one of the two functionalized scaffold amines could project its appendages into its two predicted binding subpockets (Figure 2B).

On the other hand, although the *trans* diastereoisomers (±)-**7a–e** (Table 4) did not perform better than the corresponding ethylenediamine-based inhibitors (Table 1), they were more

Table 3. Enzyme Inhibition and Whole Cell Data for *gem*-Dimethylethylenediamine-Based Inhibitors **3a–e**^a


Compound Number	R	Inhibition of PFTase (%)		ED ₅₀ (nM)	
		50 nM	5 nM	3D7	K1
3a		100	88	160	55
3b		98	91	210	75
3c		70	ND	2450	ND
3d		87	ND	400	250
3e		100	93	180	75

^a ND = not determined.**Figure 3.** 2-Aminoethanamide- (*n* = 1) and 3-aminopropanamide- (*n* = 2) based inhibitors.

active than their *cis* counterparts (\pm)-**6a–e** (Table 4) at both 50 and 5 nM inhibitor concentration; the most potent *trans* compound, (\pm)-**7d**, displayed 41% enzyme inhibition at 5 nM (cf. 81% for **1d** and 3% for **6d**). This improvement in activity in the enzyme assay was also reflected in superior whole cell activity, with (\pm)-**7d** exhibiting an ED₅₀ of 600 nM for K1 strain (cf. ED₅₀ = 1250 nM for (\pm)-**6d** (K1)). These trends in the experimental results (*cis*-1,2-diaminocyclopentane vs *trans*-1,2-diaminocyclopentane vs ethylenediamine) appear to be mirrored in the GOLD docking studies. While the *trans*-1,2-diaminocyclopentyl derivatives were predicted (Supporting Information Figure 4) to be unable to simultaneously access all four subpockets as effectively as the corresponding ethylenediamine-based inhibitors, the *trans* derivatives ((\pm)-**7a–e**) appeared to exhibit better complementarity to the active site than did their more sterically encumbered *cis* counterparts ((\pm)-**6a–e**).

(\pm)-*cis*- and (\pm)-*trans*-1,3-Diaminocyclopentane-Based Inhibitors ((\pm)-**8a–e** and (\pm)-**9a–e**). As Table 5 shows, the (\pm)-*cis*-1,3-diaminocyclopentyl-based derivatives (\pm)-**8a–e** were not very active *PfPFT* inhibitors relative to the ethylenediamine parent compounds **1a–e** (Table 1). Nonetheless, these inhibitors were more potent than the corresponding *cis*-1,2-diaminocyclopentyl derivatives (\pm)-**6a–e** (Table 4) and approximately as potent as the corresponding *trans*-1,2-diaminocyclopentyl-based inhibitors (\pm)-**7a–e** (Table 4). For example, compound (\pm)-**8a** exhibited 40% inhibition at 50 nM inhibitor concentration, compared with 0% for (\pm)-**6a** and 42% for (\pm)-**7a**. *N*-Boc-piperidin-4-ylmethyl compound (\pm)-**8d** was approximately as active as (\pm)-**7d** in terms of inhibition of *PfPFT* ((\pm)-**8d**, 33% inhibition at 5 nM, vs (\pm)-**7d**, 41% inhibition at 5 nM) but even more potent in whole cells with ED₅₀ values of 300 nM (3D7) and 125 nM (K1) for (\pm)-**8d** compared with ED₅₀ values of 2650 nM (3D7) and 600 nM (K1) for (\pm)-**7d**. GOLD docking studies correctly predicted that the *cis*-1,3-diaminocyclopentyl scaffold would not facilitate binding as well as the ethylenediamine scaffold (Supporting Information Figure 5) and also that simultaneous access to the four subpockets would be more reasonable than with the isomeric but more sterically congested *cis*-1,2-diaminocyclopentyls (compare Figure 2B and Supporting Information Figure 5).

As was the case with the 1,2-cyclopentyl derivatives, the *trans*-1,3-diaminocyclopentyl-derived inhibitors (\pm)-**9a–e** were more active (Table 5) than their analogous *cis*-1,3-diaminocyclopentyl diastereomers (\pm)-**8a–e**. Especially noteworthy are compounds (\pm)-**9a** and (\pm)-**9d**, which were approximately as active as the corresponding ethylenediamine inhibitors: **a**, 93% inhibition at 50 nM for (\pm)-**9a** vs 98% for **1a**; **d**, 86% inhibition at 5 nM for (\pm)-**9d** vs 81% for **1d**. These potent enzyme inhibition data are reflected in potent whole cell data, such as ED₅₀ = 80 nM (K1) for (\pm)-**9d**, making (\pm)-**9d** one of our most effective ethylenediamine-inspired antimalarials to date. These experimental findings confirm the docking studies, which suggested that the *trans*-1,3-diaminocyclopentyl scaffold would allow access by all four *N*-substituents to each of the predicted subpockets in a similar manner to the ethylenediamine scaffold and were, therefore, predicted to be good inhibitors of *PfPFT* (Figure 2C).

(\pm)-*cis* and (\pm)-*trans*-1,4-Diaminocyclohexane-Based Inhibitors ((\pm)-**10a**, (\pm)-**10d**, (\pm)-**11a**, and (\pm)-**11d**). For the cyclohexyl scaffold, we made only two derivatives of each diastereoisomer, incorporating either the small benzyl group or the larger *N*-Boc-piperidin-4-ylmethyl group; the percentage enzyme inhibition data and whole cell ED₅₀ data are shown in Table 6. The *cis*-1,4-diaminocyclohexyl derivative (\pm)-**10a** exhibited limited inhibition of *PfPFT* (23% inhibition at 50 nM), while the *trans* isomer (\pm)-**11a** was more active (73% inhibition at 50 nM). Both isomers were less potent than the parent ethylenediamine-based inhibitor **1a**, which was predicted by GOLD docking studies. In the case of (\pm)-**10a**, the *cis* configuration of the scaffold appeared to render it difficult for both the scaffold nitrogens to deliver their appendages into the proposed binding pockets (Supporting Information Figure 6). Conversely, in the case of (\pm)-**11a**, the *trans* configuration was predicted to facilitate simultaneous access to all four subpockets, although the greater interscaffold nitrogen–nitrogen distance appeared to be less optimal than for the parent inhibitor **1a** (Supporting Information Figure 7), possibly accounting for the slightly worse percentage inhibition data. *N*-Boc-piperidin-4-ylmethyl derivatives (\pm)-**10d** and (\pm)-**11d** demonstrated no inhibitory activity against *PfPFT*, which is likely a consequence

Table 4. Enzyme Inhibition and Whole Cell Data for (\pm)-*cis*-1,2-Diaminocyclopentane-Based Inhibitors (\pm)-**6a–e** and for (\pm)-*trans*-1,2-Diaminocyclopentane-Based Inhibitors (\pm)-**7a–e**

Compound		Inhibition of <i>Pf</i> FTase (%)		ED ₅₀ (nM)		Compound		Inhibition of <i>Pf</i> FTase (%)		ED ₅₀ (nM)	
Number	R	50 nM	5 nM	3D7	K1	Number	R	50 nM	5 nM	3D7	K1
6a		0	0	>5000	2400	7a		42	20	3100	2350
6b		17	16	2800	2800	7b		35	12	3000	3200
6c		9	0	>5000	4200	7c		57	11	2700	2700
6d		2	3	3000	1250	7d		82	41	2650	600
6e		0	10	3000	2500	7e		28	12	2600	750

of the large scaffold coupled with the bulky R group rendering these inhibitors too big to access the active site.

Selectivity. Previously reported *Pf*PFT inhibitors have demonstrated poor selectivity for parasitic PFT over mammalian PFT or are highly selective for the mammalian enzyme.^{9,10,18} Although PFT inhibitors have demonstrated limited toxicities to mammalian cells at concentrations required to effect a therapeutic response,¹⁰ the antiproliferative nature of PFT inhibitors may restrict their use by children and pregnant women, two of the main target groups in malaria therapy. Hence, the selective inhibition of parasitic PFT may prove mandatory in order to realize safe and effective antimalarial PFT inhibitors. We previously reported on the selectivity of our ethylenediamine-based inhibitors for *Pf*PFT over rat PFT; IC₅₀ values revealed several inhibitors with greater than 100-fold selectivity for the parasitic PFT.²⁷ The amino acid sequences of rat and human PFT are 95% identical with complete sequence and structural conservation around the active site.³³ While the aim of this research was not to design ever more *Plasmodium*-selective PFT inhibitors, it is worth noting that modification to the inhibitor scaffold has had no detrimental effect on PFT selectivity. Specifically, for a series of the *N*-Boc-piperidin-4-ylmethyl derivatives (selected as representative examples of inhibitors bearing the alternative scaffolds) greater than 100-fold selectivity for parasitic over mammalian PFT was observed (Table 7). In particular, compound **3d** represents one of our most potent (*Pf*PFT IC₅₀ = 1.1 nM) and most selective (136-fold) *Pf*PFT inhibitors.

QSAR Models. Quantitative structure–activity relationship (QSAR) models were generated to help determine the validity of both the proposed binding mode and the *Pf*PFT active site homology model itself. Experimental data selected were the

percentage inhibition of *Pf*PFT at 5 nM inhibitor concentration. Given the often imprecise nature of percentage inhibition data and the unavailability of multiple assay results for any given compound, care was taken to ignore any model that suggested an accuracy of greater than 90% (i.e., r^2 or $q^2 > 0.9$). The corresponding theoretical data for the models were obtained as follows. For the first QSAR model, docked poses of each ligand constrained to our hypothesized binding mode were used for descriptor calculations, and the resultant GOLD-Score values were included as descriptors in the modeling. Nineteen samples were randomly chosen as a training set, leaving nine samples as a test set. Further details can be obtained by consulting the Experimental Methods. As shown in Figure 4, the training set has an r^2 value of 0.86, suggesting there is very good correlation between the observed inhibition and the predicted inhibition of *Pf*PFT at 5 nM inhibitor concentration. Indeed, a test set of the QSAR model was found to have a q^2 value of 0.81, suggesting that this model may hold strong predictive power.

In order to further test our hypothesis regarding the proposed binding mode of these molecules to *Pf*PFT and of the homology model itself, a second QSAR model was prepared. For this model, descriptors were calculated on the basis of molecules that had been energy minimized rather than docked, with the exception of GOLD-Score derived values, which were still included but left unaltered. Also, the training and testing sets were deliberately chosen to be identical to those in the previous model rather than randomly chosen. Other than this, all operations were identical between the two models. The results of this second model are shown in Figure 5. While similar accuracy was achieved for the training set ($r^2 = 0.86$), very little predictive power was seen with the test set ($q^2 = 0.37$), suggesting that this model simply memorized, rather than learned, data from the training set. Also, it suggests that there is

Table 5. Enzyme Inhibition and Whole Cell Data for (±)-*cis*-1,3-Diaminocyclopentane-Based Inhibitors (±)-**8a–e** and for (±)-*trans*-1,3-Diaminocyclopentane-Based Inhibitors (±)-**9a–e**^a

Compound		Inhibition of PfFTase (%)		ED ₅₀ (nM)		Compound		Inhibition of PfFTase (%)		ED ₅₀ (nM)	
Number	R	50 nM	5 nM	3D7	K1	Number	R	50 nM	5 nM	3D7	K1
8a		40	4	700	800	9a		93	65	340	145
8b		24	ND	2400	2600	9b		33	ND	2400	2200
8c		15	ND	2400	2500	9c		56	ND	1500	1200
8d		83	33	300	125	9d		97	86	310	80
8e		6	ND	600	720	9e		38	ND	2600	1500

^a ND = not determined.

information content in the docked poses and thus that these docked poses are reasonable. Taken together, these QSAR models inform us that our hypothesis of the proposed binding mode is sound and that the homology model is a good approximation of the active site of *Pf*PFT.

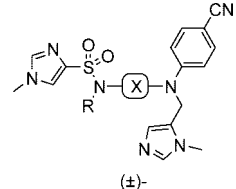
Conclusions

We have synthesized several series of novel antimalarials incorporating a variety of scaffolds based on our previously reported ethylenediamine-derived inhibitors of *Pf*PFT. These antimalarials were designed to allow exploration of the *Pf*PFT active site and therein assess the validity of our predicted inhibitor binding mode and of the active site homology model itself. In turn, it was hoped that this garnered information would, in the near future, facilitate, and thereby accelerate, access to increasingly more-potent *Pf*PFT inhibitors. Low energy docked conformations (GOLD), which were performed by loosely constraining our inhibitors to the docking pose we predicted in our previous publications,^{26,27} suggested which compounds would inhibit *Pf*PFT well and which would not. Broadly speaking, biological evaluation of our compounds agreed with the computational docking studies, and from these data we developed two QSAR models that suggested the predicted binding mode for our inhibitors is reasonable and that the homology model we have used to design inhibitors is a good approximation of the *Pf*PFT active site. In addition, our first QSAR model seems to have considerable predictive power and with suitable biological validation could therefore be used to design new inhibitors. Importantly, as well as proving particularly cytotoxic to cultured parasites (ED₅₀ < 100 nM), some of our novel antimalarial *Pf*PFTIs reported herein are among the

most potent (IC₅₀ ≈ 1 nM) and the most selective for parasitic PFT over mammalian PFT (up to 136-fold) currently reported in the literature.

Considering cost involved and speed and ease of synthesis, we conclude that the parent ethylenediamine-based inhibitors reported previously^{26,27} are our best antimalarials of this series thus far, and given the already high degree of selectivity over the mammalian isoform of PFT, future research should now be directed toward three goals. Inhibitor **1d** is highly potent (IC₅₀ = 1.2 nM), selective for parasitic over mammalian PFT (117-fold), and exhibits very good whole cell activity (ED₅₀ = 88 nM (3D7), 54 nM (K1)). Therefore, we first suggest further work is undertaken on this inhibitor to improve these ED₅₀ values, which may be achieved by substituting the 3-methyl-3*H*-imidazole-4-sulfonyl group with the less basic and more hydrophobic pyridine-2-sulfonyl group,²⁷ for example. Second, efforts should be made toward improving the limited metabolic stability of **1d** reported by us previously.^{26,27} We showed how our inhibitors were quickly oxidized upon incubation with liver microsomes, probably by cytochrome P450, followed by loss of the aniline functionalized zinc-binding imidazole. It is likely that cytochrome P450-mediated inhibitor oxidation is initiated by loss of one electron of the aniline nitrogen lone pair, followed by abstraction of a hydrogen radical from the activated methylene group between the aniline and imidazole, ultimately leading to N-dealkylation of the imidazolymethyl moiety. As described in the manuscript by Seto et al.,³⁴ aniline N-dealkylation can only proceed when the aniline lone pair of electrons is oxidizable and when there is at least one hydrogen on the carbon directly attached to the aniline nitrogen. Thus, improved inhibitor metabolic stability may be achieved by (a)

Table 6. Enzyme Inhibition and Whole Cell Data for (\pm)-*cis*-1,4-Diaminocyclohexane-Based Inhibitors (\pm)-**10a** and (\pm)-**10d** and (\pm)-*trans*-1,4-Diaminocyclohexane-Based Inhibitors (\pm)-**11a** and (\pm)-**11d**



Compound		Inhibition of PfFTase		ED ₅₀ (nM)
Number	X	R	at 50 nM (%)	K1
10a			23	2750
10d			0	650
11a			73	1800
11d			0	1200

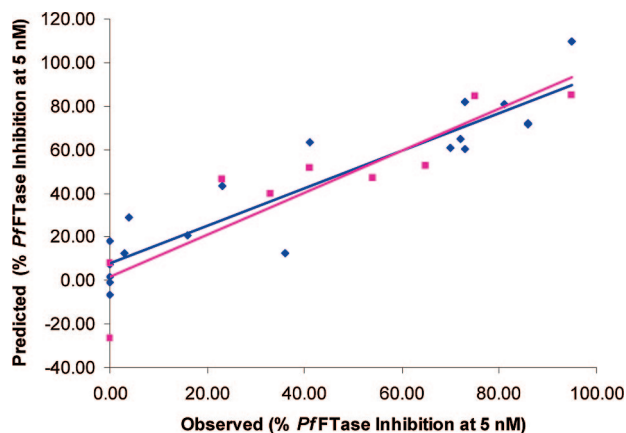


Figure 4. QSAR model in which descriptors were calculated on the basis of docked poses of ligands constrained to our hypothesized binding mode: (blue diamond) training set, $r^2 = 0.86$; (pink square) test set, $q^2 = 0.81$.

reducing electron density on the aniline nitrogen through incorporation of additional electron-withdrawing groups on the cyanophenyl ring and/or (b) replacing the methylene unit between the aniline nitrogen and the zinc-binding imidazole with a *gem*-dimethyl unit. Finally, our third goal should be the investigation of the activities of our antimalarials in drug-resistant strains of *P. falciparum* PFT (such as the Y837C strain¹⁹ that shows resistance to BMS-38891 and the G612A strain²⁰ that shows resistance to BMS-33941). This research is essential not only to evaluate the potencies of our compounds in such strains but also, after preparing similar QSAR models for the mutant active sites as we did for the wild-type, to identify structural modifications that we may undertake to restore inhibitor potency where it may be needed. In this way, new

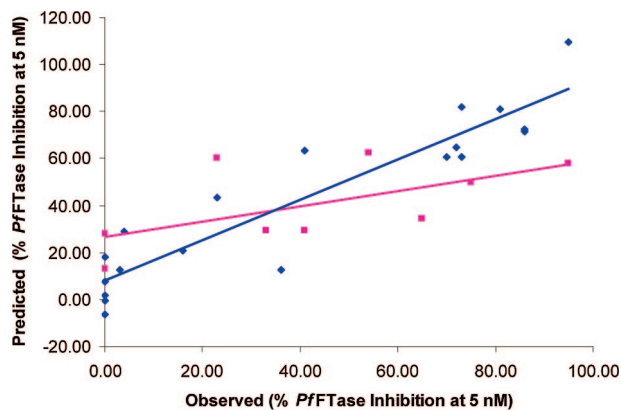
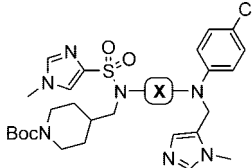


Figure 5. QSAR model in which descriptors were calculated on the basis of ligands that had been energy-minimized: (blue diamond) training set, $r^2 = 0.86$; (pink square) test set, $q^2 = 0.37$.

Table 7. Comparative *P. falciparum* and Rat PFT Inhibition Data for a Series of Inhibitors Where R = *N*-Boc-piperidin-4-ylmethyl



Compound		IC ₅₀ (nM) ^a		Selectivity ^b
Number	X	<i>Plasmodium</i>	rat	
1d		1.2	140	117
2d		1	ND	-
3d		1.1	150	136
6d		350	>1000	>2.9
7d		10	>1000	>100
9d		3.1	ND	-

^a Inhibitor concentration required to decrease *P. falciparum* or rat PFT activity by 50%. ND = not determined. ^b Ratio of rat to *P. falciparum* PFT IC₅₀ values.

antimalarial *Pf*PFTIs that are active against drug-resistant strains of *P. falciparum* may be realized.

Experimental Methods

Ligand Docking Studies. Docking experiments were performed using the GOLD version 3.1²⁸ software package. Ligands were prepared for docking in InsightII.³⁰ Each ligand was drawn as a two-dimensional representation and converted to three dimensions. Ligands were subsequently energy minimized with the cvff force field. The homology model was also prepared for use in InsightII, where each residue was protonated on the basis of calculated pK_a values at a pH of 7.4.

Ligands were constrained in the active site of *Pf*PFT at three points in order to maintain the binding mode hypothesized for lead

compound **1a**. A single atom of each imidazole and the cyanoaniline were chosen and constrained to occupy a region of space within 1 Å of that occupied by the equivalent atoms of docked **1a**. This was performed using the substructure constraint functionality of GOLD. A small spring constant was used as a penalty function such that molecules could dock in alternative conformations, but these would be discouraged. GOLD was allowed to configure the optimal genetic algorithm settings for each ligand.

QSAR Modeling. Descriptors were calculated using the MOE software package.³⁵ RECON TAE and RAD descriptors³⁶ were calculated in addition to the standard assortment of 2D descriptors in MOE. Additional descriptors included energy measurements with the MMFF94x, Amber-99, and OPLS-AA force fields. Feature selection and modeling were performed using the Analyze software package.³⁷ For further details, see Supporting Information.

Chemistry: General Methods. Solvents CH₂Cl₂, THF, CH₃CN, and DMF were dried on an Innovative Technology SPS-400 dry solvent system. Anhydrous MeOH and DMSO were purchased from Sigma-Aldrich and used directly from their Sure-Seal bottles. Molecular sieves were activated by heating to 300 °C under vacuum overnight. All reactions were performed under an atmosphere of dry nitrogen in oven-dried glassware and were monitored for completeness by thin-layer chromatography (TLC) using silica gel (visualized by UV light or developed by treatment with KMnO₄ stain or Hanesian's stain). ¹H and ¹³C NMR spectra were recorded on Bruker AM 400 MHz and Bruker AM 500 MHz spectrometers in either CDCl₃, MeOH-*d*₄ or DMSO-*d*₆. Chemical shifts (δ) are reported in parts per million after calibration to residual isotopic solvent. Coupling constants (*J*) are reported in Hz. Mass spectrometry (MS) was performed using electrospray ionization on either a Varian MAT-CH-5 (HRMS) or a Waters Micromass ZQ (LRMS) instrument. Before biological testing, target molecules (**2a–e**, **3a–e**, **4a**, **4d**, **5a**, **5d**, **6a–e**, **7a–e**, **8a–e**, **9a–e**, **10a**, **10d**, **11a**, **11d**), obtained as glassy films after silica gel flash column chromatographic purification (eluent CH₂Cl₂/MeOH/NH₄OH, 192:7:1), were subjected to further purification by reversed-phase HPLC (rpHPLC). Analysis and purification by rpHPLC were performed using either Phenomenex Luna 5 μm C18 (2) 250 mm × 21 mm column run at 15 mL/min (preparative) or a Microsorb-MV 300 Å C18 250 mm × 4.6 mm column run at 1 mL/min (analytical), using gradient mixtures of (A) water with 0.1% TFA and (B) 10:1 acetonitrile/water with 0.1% TFA. Appropriate product fractions were pooled and lyophilized to dryness, affording the inhibitors as fluffy white powders as their TFA salts. Inhibitor purity was confirmed by analytical rpHPLC using linear gradients from 100% A to 100% B, with changing solvent composition of either (I) 4.5% or (II) 1.5% per minute after an initial 2 min of 100% A. For reporting HPLC data, percentage purity is given in parentheses after the retention time for each condition.

General Procedure A (Mitsunobu Reactions). Reaction of Primary and Secondary Alcohols with Secondary Sulfonamides. To a stirring solution of the alcohol (1 equiv) in THF (0.07 M) (occasionally, sonication and a little warming (40 °C) was required to achieve complete dissolution of the alcohol) was added the secondary sulfonamide (2.5 equiv) and PPh₃ (3 equiv). After the mixture was stirred for 15 min at room temperature, DIAD (2.5 equiv) was added dropwise. For the acyclic, primary alcohols, reactions were typically complete within 1 h; for the less reactive, cyclic secondary alcohols and hindered primary alcohols, mixtures were left stirring overnight (16 h). All solvent was removed in vacuo.

General Procedure B (Sulfonamide Alkylations). Reaction of Secondary Sulfonamides with Benzylic and Alkyl Bromides. To a stirred solution of the secondary sulfonamide (1 equiv) in DMF (0.01 M for benzylic bromide or 0.1 M for alkyl bromide) was added Cs₂CO₃ (3 equiv). After 1 h, at room temperature, the bromide (or iodide) alkylating agent (1.1 equiv) was added dropwise. After 16 h, the reaction mixture was diluted with water and extracted into EtOAc (×3). The EtOAc extractions were combined and washed with 5% NaHCO₃ (×3) and brine, dried (Na₂SO₄), filtered, and concentrated.

General Procedure C (Aniline Alkylation). Reaction of Secondary Anilines with 5-Chloromethyl-1-methyl-1*H*-imidazole·HCl (15**).** The secondary aniline (1 equiv) was dissolved in DMF (0.07 M). Then the mixture was cooled to 0 °C. After 15 min, NaH (3 equiv) was added in one portion. After a further 15 min, 5-chloromethyl-1-methyl-1*H*-imidazole·HCl²⁷ (**15**) (1.1 equiv) was added to the reaction mixture. The mixture was allowed to stir at 0 °C for 2–3 h, when TLC indicated the reaction was complete or had stalled. Upon quenching the reaction with brine (approximately 1 mL), the mixture was diluted with water and extracted with EtOAc (×3). The EtOAc extractions were combined and washed with 5% NaHCO₃ (×3) and brine, dried (Na₂SO₄), filtered, and concentrated.

[*N*-(Benzyl-*N*-3-((4-cyanophenyl)(3-methyl-3*H*-imidazol-4-ylmethyl)amino)propyl]-1-methyl-1*H*-imidazole-4-sulfonamide (2a**).** Primary alcohol **17** was coupled to secondary sulfonamide **19a** on a 0.106 mmol scale via general procedure A. The crude residue was dry-loaded onto silica gel, then flash chromatographed (eluent CH₂Cl₂/MeOH/NH₄OH, 192:7:1) to furnish **2a** (51 mg, 96%): δ_H (400 MHz, MeOH-*d*₄) 1.71 (quin, *J* = 7.0 Hz, 2H, CH₂CH₂CH₂), 3.30–3.36 (obsc m, 4H, CH₂CH₂CH₂), 3.83 (s, 3H, CH₃(Im)), 3.89 (s, 3H, CH₃(Im)), 4.34 (s, 2H, CH₂Ph), 4.62 (s, 2H, CH₂Im), 6.73 (d, *J* = 8.8 Hz, 2H, 2 CH (Ar)), 7.14 (s, 1H, CH (Im)), 7.31–7.43 (m, 5H, 5 CH (Ph)), 7.50 (d, *J* = 8.8 Hz, 2H, 2 CH (Ar)), 7.77 (s, 1H, CH (Im)), 7.84 (s, 1H, CH (Im)), 8.93 (s, 1H, CH (Im)); δ_C (100 MHz, MeOH-*d*₄) 27.4, 34.3, 34.4, 45.8, 48.6, 49.3, 54.7, 99.8, 113.8, 118.8, 121.0, 126.6, 128.9, 129.7, 129.9, 133.1, 134.7, 137.7, 138.7, 139.3, 141.4, 151.8; HRMS (ES+) calcd for [C₂₆H₂₉N₇O₂S + H] 504.2182, found 504.2198; HPLC (I) *t*_R = 15.69 min (100%), (II) *t*_R = 27.81 min (100%).

[*N*-(2-Methylbenzyl)-*N*-3-((4-cyanophenyl)(3-methyl-3*H*-imidazol-4-ylmethyl)amino)propyl]-1-methyl-1*H*-imidazole-4-sulfonamide (2b**).** Primary alcohol **17** was coupled to secondary sulfonamide **19b** on a 0.137 mmol scale via general procedure A. The crude residue was dry-loaded onto silica gel, then flash chromatographed (eluent CH₂Cl₂/MeOH/NH₄OH, 192:7:1) to furnish **2b** (64 mg, 90%): δ_H (400 MHz, MeOH-*d*₄) 1.57 (quin, *J* = 7.3 Hz, 2H, CH₂CH₂CH₂), 2.42 (s, 3H, CH₃Ph), 3.21–3.27 (m, 4H, CH₂CH₂CH₂), 3.85 (s, 3H, CH₃(Im)), 3.88 (s, 3H, CH₃(Im)), 4.33 (s, 2H, CH₂Ph), 4.60 (s, 2H, CH₂Im), 6.70 (d, *J* = 8.8 Hz, 2H, 2 CH (Ar)), 7.11 (s, 1H, CH (Im)), 7.14–7.26 (m, 3H, 3 CH (Ph)), 7.31 (br d, *J* = 7.6 Hz, 1H, CH (Ph)), 7.49 (d, *J* = 8.8 Hz, 2H, 2 CH (Ar)), 7.78 (s, 1H, CH (Im)), 7.86 (s, 1H, CH (Im)), 8.93 (s, 1H, CH (Im)); δ_C (100 MHz, MeOH-*d*₄) 19.5, 27.8, 34.3, 34.4, 45.3, 48.0, 49.2, 53.5, 99.8, 113.8, 118.8, 121.0, 126.7, 127.1, 129.3, 131.2, 131.7, 133.0, 134.7, 135.6, 137.7, 138.7, 138.8, 141.4, 151.7; HRMS (ES+) calcd for [C₂₇H₃₁N₇O₂S + H] 518.2338, found 518.2346; HPLC (I) *t*_R = 15.98 min (100%), (II) *t*_R = 28.75 min (100%).

[*N*-(Thiophen-3-ylmethyl)-*N*-3-((4-cyanophenyl)(3-methyl-3*H*-imidazol-4-ylmethyl)amino)propyl]-1-methyl-1*H*-imidazole-4-sulfonamide (2c**).** Primary alcohol **17** was coupled to secondary sulfonamide **19c** on a 0.16 mmol scale via general procedure A. The crude residue was dry-loaded onto silica gel, then flash chromatographed (eluent CH₂Cl₂/MeOH/NH₄OH, 192:7:1) to give **2c** (80 mg, 98%): δ_H (400 MHz, MeOH-*d*₄) 1.78 (quin, *J* = 7.2 Hz, 2H, CH₂CH₂CH₂), 3.32–3.36 (obsc m, 2H, CH₂CH₂CH₂NSO₂), 3.37–3.41 (m, 2H, CH₂CH₂CH₂NSO₂), 3.83 (s, 3H, CH₃(Im)), 3.91 (s, 3H, CH₃(Im)), 4.36 (s, 2H, CH₂thiophene), 4.68 (s, 2H, CH₂Im), 6.79 (d, *J* = 8.8 Hz, 2H, 2 CH (Ar)), 7.13 (dd, *J* = 5.0, 1.2 Hz, 1H, CH (thiophene)), 7.18 (s, 1H, CH (Im)), 7.32–7.35 (m, 1H, CH (thiophene)), 7.41 (dd, *J* = 5.0, 2.8 Hz, 1H, CH (thiophene)), 7.53 (d, *J* = 8.8 Hz, 2H, 2 CH (Ar)), 7.74 (s, 1H, CH (Im)), 7.83 (s, 1H, CH (Im)), 8.93 (s, 1H, CH (Im)); δ_C (100 MHz, MeOH-*d*₄) 27.3, 34.3, 34.4, 45.4, 48.2, 49.3, 49.4, 99.8, 113.8, 118.9, 121.0, 125.1, 126.5, 127.5, 129.2, 133.1, 134.7, 137.7, 139.4, 139.4, 141.3, 151.8; HRMS (ES+) calcd for [C₂₄H₂₇N₇O₂S₂ + H] 510.1746, found 510.1761; HPLC (I) *t*_R = 15.12 min (100%), (II) *t*_R = 26.20 min (100%).

[*N*-(*N*-*tert*-Butoxycarbonyl)piperidin-4-ylmethyl)-*N*-3-((4-cyanophenyl)(3-methyl-3*H*-imidazol-4-ylmethyl)amino)propyl]-1-methyl-

1H-imidazole-4-sulfonamide (2d). Primary alcohol **17** was coupled to secondary sulfonamide **19d** on a 0.24 mmol scale via general procedure A. The crude residue was dry-loaded onto silica gel, then flash chromatographed (eluent CH₂Cl₂/MeOH/NH₄OH, 192:7:1) to afford **2d** (132 mg, 90%): δ_H (400 MHz, MeOH-*d*₄) 1.07 (qd, *J* = 12.3, 4.0 Hz, 2H, 2 CH (piperidinylmethyl)), 1.49 (s, 9H, C(CH₃)₃), 1.68–1.76 (m, 2H, 2 CH (piperidinylmethyl)), 1.79–1.90 (m, 1H, CH (piperidinylmethyl)), 1.99 (quin, *J* = 7.4 Hz, 2H, CH₂CH₂CH₂), 2.64–2.80 (m, 2H, 2 CH (piperidinylmethyl)), 3.01 (d, *J* = 7.6 Hz, 2H, 2 CH (piperidinylmethyl)), 3.29 (t, *J* = 7.2 Hz, 2H, CH₂CH₂CH₂NSO₂), 3.61 (t, *J* = 7.2 Hz, 2H, CH₂CH₂CH₂NSO₂), 3.81 (s, 3H, CH₃(Im)), 3.95 (s, 3H, CH₃(Im)), 4.03–4.10 (m, 2H, 2 CH (piperidinylmethyl)), 4.87 (s, 2H, CH₂Im), 6.96 (d, *J* = 8.8 Hz, 2H, 2 CH (Ar)), 7.30 (s, 1H, CH (Im)), 7.58 (d, *J* = 8.8 Hz, 2H, 2 CH (Ar)), 7.73 (s, 1H, CH (Im)), 7.79 (s, 1H, CH (Im)), 8.94 (s, 1H, CH (Im)); δ_C (100 MHz, MeOH-*d*₄) 27.9, 28.7, 30.9, 34.2, 34.3, 36.5, 44.7 (br), 45.6, 48.9, 49.0, 56.3, 81.0, 100.0, 114.1, 119.0, 120.9, 126.5, 133.2, 134.8, 137.8, 139.3, 141.3, 151.9, 156.5; HRMS (ES⁺) calcd for [C₃₀H₄₂N₈O₄S + H] 611.3128, found 611.3129; HPLC (I) *t*_R = 12.56 min (100%), (II) *t*_R = 18.92 min (100%).

[N-{N-(2-Pyrimidinyl)-piperidin-4-ylmethyl}-N-3-{(4-cyanophenyl)(3-methyl-3H-imidazol-4-ylmethyl)amino}propyl]-1-methyl-1H-imidazole-4-sulfonamide (2e). Primary alcohol **17** was coupled to secondary sulfonamide **19e** on a 0.106 mmol scale via general procedure A. The crude residue was dry-loaded onto silica gel, then flash chromatographed (eluent CH₂Cl₂/MeOH/NH₄OH, 192:7:1) to yield **2e** (38 mg, 61%): δ_H (400 MHz, MeOH-*d*₄) 1.17 (qd, *J* = 12.2, 4.0 Hz, 2H, 2 CH (piperidinylmethyl)), 1.78–1.86 (m, 2H, 2 CH (piperidinylmethyl)), 1.94–2.04 (m, 3H, CH₂CH₂CH₂, CH (piperidinylmethyl)), 2.90–2.98 (m, 2H, 2 CH (piperidinylmethyl)), 3.04 (d, *J* = 7.6 Hz, 2H, 2 CH (piperidinylmethyl)), 3.26–3.31 (m, 2H, CH₂CH₂CH₂NSO₂), 3.59–3.66 (m, 2H, CH₂CH₂CH₂NSO₂), 3.81 (s, 3H, CH₃(Im)), 3.96 (s, 3H, CH₃(Im)), 4.64–4.71 (m, 2H, 2 CH (piperidinylmethyl)), 4.88 (s, 2H, CH₂Im), 6.66 (t, *J* = 5.1 Hz, 1H, CH (pyrimidine)), 6.97 (d, *J* = 9.2 Hz, 2H, 2 CH (Ar)), 7.31 (s, 1H, CH (Im)), 7.59 (d, *J* = 9.2 Hz, 2H, 2 CH (Ar)), 7.73 (s, 1H, CH (Im)), 7.80 (s, 1H, CH (Im)), 8.38 (d, *J* = 5.1 Hz, 2H, 2 CH (pyrimidine)), 8.95 (s, 1H, CH (Im)); δ_C (100 MHz, MeOH-*d*₄) 27.9, 30.9, 34.2, 34.3, 36.6, 45.2, 45.6, 49.1, 49.3, 56.3, 100.1, 110.6, 114.1, 119.0, 120.9, 126.5, 133.2, 134.8, 137.8, 139.3, 141.3, 151.9, 158.7, 160.7; HRMS (ES⁺) calcd for [C₂₉H₃₁N₁₀O₂S + H] 589.2822, found 589.2831; HPLC (I) *t*_R = 13.00 min (100%), (II) *t*_R = 20.28 min (99.69%).

[N-Benzyl-N-{(4-cyanophenyl)(3-methyl-3H-imidazol-4-ylmethyl)amino}-2,2-dimethylethyl]-1-methyl-1H-imidazole-4-sulfonamide (3a). The synthesis was as per general procedure A with alcohol **27** on a 0.037 mmol scale and secondary sulfonamide **19a**. The mixture was heated to 45 °C for 18 h, reduced, and then dry-loaded onto silica gel and purified by flash column chromatography (eluent CH₂Cl₂/MeOH/NH₄OH, 192:7:1) to give **3a** (12 mg, 65%): δ_H (400 MHz, CDCl₃) 1.40 (s, 6H, C(CH₃)₂), 3.46 (s, 3H, CH₃(Im)), 3.72 (s, 3H, CH₃(Im)), 3.87 (s, 2H, CH₂C(CH₃)₂), 4.47 (s, 2H, CH₂Ph), 4.70 (s, 2H, CH₂Im), 6.58 (s, 1H, CH(Im)), 6.60 (d, *J* = 8.3 Hz, 2H, 2 CH (Ar)), 7.27–7.38 (m, 7H, 2 CH (Im), 5 CH (Ph)), 7.45 (d, *J* = 8.3 Hz, 2H, 2 CH (Ar)), 7.47 (s, 1H, CH (Im)); δ_C (125 MHz, CDCl₃) 26.9, 31.8, 33.9, 47.1, 50.8, 59.3, 65.6, 99.3, 113.7, 120.0, 123.5, 126.7, 127.4, 127.7, 128.6, 129.0, 133.2, 138.4, 138.6, 139.4, 143.1, 151.6; HRMS (ES⁺) calcd for [C₂₈H₃₁N₆O₂S + H] 518.2343, found 518.2338; HPLC (I) *t*_R = 12.25 min (99.66%), (II) *t*_R = 17.75 min (99.34%).

[N-(2-Methylbenzyl)-N-{(4-cyanophenyl)(3-methyl-3H-imidazol-4-ylmethyl)amino}-2,2-dimethylethyl]-1-methyl-1H-imidazole-4-sulfonamide (3b). The synthesis was as per general procedure A with alcohol **27** on a 0.035 mmol scale and secondary sulfonamide **19b**. The mixture was heated to 45 °C for 18 h, then reduced, and dry-loaded onto silica gel and purified by flash column chromatography (eluent CH₂Cl₂/MeOH/NH₄OH, 192:7:1) to give **3b** (11 mg, 60%): δ_H (400 MHz, CDCl₃) 1.40 (s, 6H, C(CH₃)₂), 2.23 (s, 3H, CH₃Ph), 3.51 (s, 3H, CH₃(Im)), 3.70 (s, 3H, CH₃(Im)), 4.02 (s, 2H, CH₂C(CH₃)₂), 4.56 (s, 2H, CH₂Ph), 4.62 (s, 2H, CH₂Im),

6.65 (s, 1H, CH (Im)), 6.72 (d, *J* = 9.0 Hz, 2H, 2 CH (Ar)), 7.10–7.39 (m, 6H, 2 CH (Im), 4 CH (Ar)), 7.45 (s, 1H, CH (Im)), 7.60 (d, *J* = 9.0 Hz, 2H, 2 CH (Ar)); δ_C (125 MHz, CDCl₃) 18.9, 26.5, 31.6, 33.6, 47.0, 47.3, 58.9, 65.2, 99.2, 113.6, 119.7, 123.6, 125.8, 126.5, 126.6, 127.0, 128.8, 130.0, 133.0, 133.6, 136.8, 138.2, 138.7, 142.5, 151.4; HRMS (ES⁺) calcd for [C₂₈H₃₃N₇O₂S + H] 532.2416, found 532.2452; HPLC (I) *t*_R = 12.80 min (95.01%), (II) *t*_R = 19.70 min (95.06%).

[N-(Thiophen-3-ylmethyl)-N-{(4-cyanophenyl)(3-methyl-3H-imidazol-4-ylmethyl)amino}-2,2-dimethylethyl]-1-methyl-1H-imidazole-4-sulfonamide (3c). The synthesis was as per general procedure A with alcohol **27** on a 0.088 mmol scale and secondary sulfonamide **19c**. The mixture was heated to 45 °C for 18 h, reduced, and then dry-loaded onto silica gel and purified by flash column chromatography (eluent CH₂Cl₂/MeOH/NH₄OH, 192:7:1) to give **3c** (25 mg, 55%): δ_H (400 MHz, CDCl₃) 1.45 (s, 6H, C(CH₃)₂), 3.48 (s, 3H, CH₃(Im)), 3.72 (s, 3H, CH₃(Im)), 3.82 (s, 2H, CH₂C(CH₃)₂), 4.46 (s, 2H, CH₂thiophene), 4.67 (s, 2H, CH₂Im), 6.61 (d, *J* = 8.5 Hz, 2H, Ar), 6.64 (s, 1H, CH (Im)), 7.22–7.37 (m, 7H, 2 CH (Im), 2 CH (Ar), 3 CH (thiophene)), 7.45 (s, 1H, CH (Im)); δ_C (125 MHz, CDCl₃) 26.9, 31.8, 33.9, 46.0, 46.9, 59.2, 65.3, 99.3, 113.7, 120.0, 122.9, 123.4, 126.0, 126.8, 128.1, 128.8, 133.2, 138.4, 138.5, 140.7, 143.2, 151.6; HRMS (ES⁺) calcd for [C₂₅H₂₉N₇O₂S₂ + H] 524.1904, found 524.1902; HPLC (I) *t*_R = 12.56 min (100%), (II) *t*_R = 18.70 min (100%).

[N-(*N*-tert-Butoxycarbonylpiperidin-4-ylmethyl)-N-{(4-cyanophenyl)(3-methyl-3H-imidazol-4-ylmethyl)amino}-2,2-dimethylethyl]-1-methyl-1H-imidazole-4-sulfonamide (3d). The synthesis was as per general procedure A with alcohol **27** on a 0.217 mmol scale and secondary sulfonamide **19d**. The mixture was heated to 45 °C for 18 h, reduced, and then dry-loaded onto silica gel and purified by flash column chromatography (eluent CH₂Cl₂/MeOH/NH₄OH, 192:7:1) to give **3d** (68 mg, 50%): δ_H (400 MHz, CDCl₃) 1.10 (qd, *J* = 12.3, 4.0 Hz, 2H, 2 CH (piperidinylmethyl)), 1.39 (s, 6H, C(CH₃)₂), 1.44 (s, 9H, C(CH₃)₃), 1.67–1.79 (m, 3H, 3 CH (piperidinylmethyl)), 2.58–2.67 (m, 2H, 2 CH (piperidinylmethyl)), 3.28–3.36 (m, 2H, 2 CH (piperidinylmethyl)), 3.53 (s, 3H, CH₃(Im)), 3.72 (s, 3H, CH₃(Im)), 3.85 (s, 2H, CH₂(CH₃)₂), 4.05–4.15 (m, 2H, 2 CH (piperidinylmethyl)), 4.66 (s, 2H, CH₂Im), 6.70 (s, 1H, CH (Im)), 6.92 (d, *J* = 9.0 Hz, 2H, 2 CH (Ar)), 7.35 (s, 1H, CH (Im)), 7.39 (s, 1H CH (Im)), 7.41 (s, 1H CH (Im)), 7.45 (d, *J* = 9.0 Hz, 2H, 2 CH (Ar)); δ_C (125 MHz, CDCl₃) 14.4, 27.3, 28.7, 29.9, 30.4, 32.1, 34.2, 38.3, 47.1, 52.5, 58.1, 64.8, 79.6, 100.0, 114.1, 120.1, 123.4, 129.4, 133.7, 138.5, 144.0, 152.1, 155.0, 171.4; HRMS (ES⁺) calcd for [C₃₁H₄₄N₈O₄S + H] 625.2765, found 625.2720; HPLC (I) *t*_R = 13.61 min (100%), (II) *t*_R = 21.80 (100%).

[N-{N-(2-Pyrimidinyl)-piperidin-4-ylmethyl}-N-{(4-cyanophenyl)(3-methyl-3H-imidazol-4-ylmethyl)amino}-2,2-dimethylethyl]-1-methyl-1H-imidazole-4-sulfonamide (3e). The synthesis was as per general procedure A with alcohol **27** on a 0.037 mmol scale and secondary sulfonamide **19e**. The mixture was heated to 45 °C for 18 h, then dry-loaded onto silica gel and purified by flash column chromatography (eluent CH₂Cl₂/MeOH/NH₄OH, 92:7:1) to give **3e** (15 mg, 68% yield): δ_H (500 MHz, CDCl₃) 1.17 (qd, *J* = 12.2, 4.0 Hz, 2H, 2 CH (piperidinylmethyl)), 1.41 (s, 6H, C(CH₃)₂), 1.81–2.02 (m, 3H, 3 CH (piperidinylmethyl)), 2.79 (m, 2H, 2 CH (piperidinylmethyl)), 3.33 (d, *J* = 7.0 Hz, 2H, 2 CH (piperidinylmethyl)), 3.54 (s, 3H, CH₃(Im)), 3.71 (s, 3H, CH₃(Im)), 3.87 (m, 2H, CH₂C(CH₃)₂), 4.68 (s, 2H, CH₂Im), 4.73–4.79 (m, 2H, 2 CH (piperidinylmethyl)), 6.42 (t, *J* = 4.9 Hz, 1H, CH (pyrimidine)), 6.69 (s, 1H, CH (Im)), 6.91 (d, *J* = 9.0 Hz, 2H, 2 CH (Ar)), 7.35 (s, 1H, CH (Im)), 7.39 (s, 1H, CH (Im)), 7.42 (s, 1H, CH (Im)), 7.44 (d, *J* = 9.0 Hz, 2H, 2 CH (Ar)), 8.27 (d, *J* = 4.9 Hz, 2H, 2 CH (pyrimidine)); δ_C (125 MHz, CDCl₃) 27.4, 30.3, 32.1, 34.2, 38.6, 44.2, 47.1, 52.6, 58.3, 64.8, 99.9, 109.6, 114.1, 120.2, 123.5, 129.1, 133.7, 138.5, 139.0, 143.9, 152.1, 157.9, 161.8, 162.7; HRMS (ES⁺) calcd for [C₃₀H₃₈N₁₀O₂S + H] 603.2969, found 603.2978; HPLC (I) *t*_R = 13.62 min (100%), (II) *t*_R = 19.16 min (100%).

2-[Benzyl(1-methyl-1H-imidazole-4-sulfonylamino)-N-(4-cyanophenyl)-N-(3-methyl-3H-imidazol-4-ylmethyl)acetamide (4a).

Compound **32** was coupled to secondary sulfonamide **19a** as per general procedure A on a 0.164 mmol scale. After workup, the crude residue was purified by silica gel flash column chromatography (eluent CH₂Cl₂/MeOH/NH₄OH, 192:7:1) to furnish **4a** (43 mg, 52%): δ_{H} (500 MHz, CDCl₃) 3.60 (s, 3H, CH₃(Im)), 3.70 (s, 2H, CH₂CO), 3.76 (s, 3H, CH₃(Im)), 4.60 (s, 2H, CH₂Ph), 4.85 (s, 2H, CH₂Im), 6.59 (br s, 1H, CH (Im)), 6.95 (d, $J = 8.5$ Hz, 2H, 2 CH (Ar)), 7.19–7.24 (m, 2H, 2 CH (Ph)), 7.27–7.31 (m, 3H, 3 CH (Ph)), 7.43 (br s, 1H, CH (Im)), 7.45 (s, 1H, CH (Im)), 7.46 (s, 1H, CH (Im)), 7.58 (d, $J = 8.5$ Hz, 2H, 2 CH (Ar)); δ_{C} (125 MHz, CDCl₃) 31.7, 33.9, 41.5, 47.6, 51.6, 112.6, 117.6, 123.9, 126.1, 127.9, 128.5, 128.6, 129.3, 130.4, 133.6, 135.2, 138.9, 139.1, 140.1, 143.6, 167.1; HRMS (ES⁺) calcd for [C₂₅H₂₅N₇O₃S + H] 504.1818, found 504.1830; HPLC (I) $t_{\text{R}} = 11.48$ min (100%), (II) $t_{\text{R}} = 15.67$ min (100%).

2-[(*N*-tert-Butoxycarbonylpiperidin-4-ylmethyl)(1-methyl-1*H*-imidazole-4-sulfonyl)amino]-*N*-(4-cyanophenyl)-*N*-(3-methyl-3*H*-imidazol-4-ylmethyl)acetamide (4d**).** Compound **32** was coupled to secondary sulfonamide **19d** as per general procedure A on a 0.164 mmol scale. After workup, the crude residue was purified by silica gel flash column chromatography (eluent CH₂Cl₂/MeOH/NH₄OH, 192:7:1) to furnish **4b** (20 mg, 20%): δ_{H} (500 MHz, CDCl₃) 0.99 (m, 2H, 2 CH (piperidinylmethyl)), 1.44 (s, 9H, C(CH₃)₃), 1.59–1.75 (m, 3H, 3 CH (piperidinylmethyl)), 2.54–2.68 (m, 2H, 2 CH (piperidinylmethyl)), 3.07–3.19 (m, 2H, 2 CH (piperidinylmethyl)), 3.61 (s, 3H, CH₃(Im)), 3.71 (s, 3H, CH₃(Im)), 3.73–3.81 (m, 2H, CH₂CO), 3.95–4.08 (m, 2H, CHCH₂N (piperidinylmethyl)), 4.81–4.94 (m, 2H, CH₂Im), 6.59 (s, 1H, CH (Im)), 7.22 (d, $J = 8.5$ Hz, 2H, 2 CH (Ar)), 7.33 (app s, 2H, 2 CH (Im)), 7.43 (s, 1H, CH (Im)), 7.69 (d, $J = 8.5$ Hz, 2H, 2 CH (Ar)); δ_{C} (125 MHz, CDCl₃) 28.4, 29.6, 31.9, 34.0, 35.3, 41.7, 43.5 (br), 50.2, 55.1, 79.5, 112.8, 117.6, 123.6, 126.1, 129.7, 130.4, 133.9, 138.8, 139.1, 140.0, 143.8, 154.6, 167.5; HRMS (ES⁺) calcd for [C₂₉H₃₈N₈O₅S + H] 611.2764, found 611.2769; HPLC (I) $t_{\text{R}} = 12.44$ min (99.53%), (II) $t_{\text{R}} = 17.97$ min (98.67%).

3-[Benzyl-(1-methyl-1*H*-imidazole-4-sulfonyl)amino]-*N*-(4-cyanophenyl)-*N*-(3-methyl-3*H*-imidazol-4-ylmethyl)propanamide (5a**).** **5a** was prepared as per general procedure B with **35** and benzyl bromide on a 0.0845 mmol scale. The crude residue was purified by silica gel flash column chromatography (eluent CH₂Cl₂/MeOH/NH₄OH, 192:7:1) to give **5a** (42 mg, 96%): δ_{H} (500 MHz, CDCl₃) 2.12 (m, 2H, CH₂CH₂CO), 3.47 (t, $J = 7.3$ Hz, 2H, CH₂CH₂CO), 3.53 (s, 3H, CH₃(Im)), 3.72 (s, 3H, CH₃(Im)), 4.31 (s, 2H, CH₂Ph), 4.78 (s, 2H, CH₂Im), 6.53 (s, 1H, CH (Im)), 6.68 (d, $J = 8.3$ Hz, 2H, 2 CH (Ar)), 7.19–7.25 (m, 5H, 5 CH (Ph)), 7.37 (s, 1H, CH (Im)), 7.38 (br s, 1H, CH (Im)), 7.41 (s, 1H, CH (Im)), 7.58 (d, $J = 8.3$ Hz, 2H, 2 CH (Ar)); δ_{C} (125 MHz, CDCl₃) 31.7, 34.9, 35.2, 40.9, 45.3, 53.8, 112.3, 117.7, 124.2, 126.5, 127.7, 128.3, 128.4, 129.3, 129.7, 130.2, 133.6, 136.8, 138.9, 139.7, 144.5, 169.7; HRMS (ES⁺) calcd for [C₂₆H₂₇N₇O₃S + H] 518.1974, found 518.1994; HPLC (I) $t_{\text{R}} = 11.82$ min (98.91%), (II) $t_{\text{R}} = 16.38$ min (99.01%).

3-[(*N*-tert-Butoxycarbonylpiperidin-4-ylmethyl)(1-methyl-1*H*-imidazole-4-sulfonyl)amino]-*N*-(4-cyanophenyl)-*N*-(3-methyl-3*H*-imidazol-4-ylmethyl)propanamide (5d**).** **5d** was prepared as per general procedure B with **35** and *N*-tert-butoxycarbonylpiperidin-4-ylmethyl bromide (1.5 equiv) in DMF (0.1 M) on a 0.0986 mmol scale. After the mixture was stirred at room temperature for 36 h, byproduct began to form. So the reaction mixture was worked up and then the crude residue was purified by silica gel flash column chromatography (eluent CH₂Cl₂/MeOH/NH₄OH, 192:7:1) to give **5d** (30 mg, 50% (73% brsm)): δ_{H} (500 MHz, CDCl₃) 1.03 (qd, $J = 12.2$, 4.0 Hz, 2H, 2 CH (piperidinylmethyl)), 1.43 (s, 9H, C(CH₃)₃), 1.59 (br app d, $J = 12.2$ Hz, 2H, 2 CH (piperidinylmethyl)), 1.77 (m, 1H, CH (piperidinylmethyl)), 2.46 (m, 2H, CH₂CH₂CO), 2.63 (m, 2H, 2 CH (piperidinylmethyl)), 2.92 (m, 2H, 2 CH (piperidinylmethyl)), 3.50 (m, 2H, 2 CH (piperidinylmethyl)), 3.59 (s, 3H, CH₃(Im)), 3.71 (s, 3H, CH₃(Im)), 4.05 (m, 2H, CHCH₂N (piperidinylmethyl)), 4.90 (s, 2H, CH₂Im), 6.61 (s, 1H, CH (Im)), 7.13 (d, $J = 8.0$ Hz, 2H, 2 CH (Ar)), 7.32 (s, 1H, CH (Im)), 7.33 (s, 1H, CH (Im)), 7.42 (s, 1H, CH (Im)), 7.68 (d, $J = 8.3$ Hz, 2H, 2 CH (Ar)); δ_{C} (125 MHz, CDCl₃) 28.4, 29.7,

31.8, 33.9, 34.9, 35.1, 41.2, 43.4 (br), 46.0, 55.3, 79.4, 112.5, 117.7, 124.2, 126.5, 129.5, 130.3, 133.7, 138.7, 139.0, 139.5, 144.6, 154.7, 170.0; HRMS (ES⁺) calcd for [C₃₀H₄₀N₈O₅S + H] 625.2921, found 625.2923; HPLC (I) $t_{\text{R}} = 12.74$ min (98.83%), (II) $t_{\text{R}} = 19.28$ min (99.47%).

(±)-[*N*-Benzyl-*N*-{*cis*-2-[(4-cyanophenyl)(3-methyl-3*H*-imidazol-4-ylmethyl)amino]cyclopentyl}-1-methyl-1*H*-imidazole-4-sulfonamide (**6a**)]. The synthesis was as per general procedure B with **42** and benzyl bromide on a 0.0273 mmol scale. The crude residue was purified by silica gel flash column chromatography (eluent CH₂Cl₂/MeOH/NH₄OH, 192:7:1) to afford **6a** (8 mg, 55%): δ_{H} (400 MHz, CDCl₃) 1.37–1.50 (m, 1H, CH (cyclopentyl)), 1.84–1.96 (m, 2H, 2 CH (cyclopentyl)), 2.04–2.19 (m, 2H, 2 CH (cyclopentyl)), 2.49–2.56 (m, 1H, CH (cyclopentyl)), 3.55 (s, 3H, CH₃(Im)), 3.67 (s, 3H, CH₃(Im)), 3.88 (d, $J = 16.4$ Hz, 1H, CH₂Ph), 4.14 (m, 1H, CHN (cyclopentyl)), 4.20 (d, $J = 18.0$ Hz, 1H, CH₂Im), 4.25 (m, 1H, CHN (cyclopentyl)), 4.52 (d, $J = 16.4$ Hz, 1H, CH₂Ph), 4.75 (d, $J = 18.0$ Hz, 1H, CH₂Im), 6.52 (s, 1H, CH (Im)), 6.68 (d, $J = 9.2$ Hz, 2H, 2 CH (Ar)), 6.97–7.01 (m, 2H, 2 CH (Ph)), 7.15–7.20 (m, 3H, 3 CH (Ph)), 7.25 (s, 1H, CH (Im)), 7.37 (s, 1H, CH (Im)), 7.43 (d, $J = 9.2$ Hz, 2H, 2 CH (Ar)), 7.47 (s, 1H, CH (Im)); δ_{C} (125 MHz, CDCl₃) 21.1, 28.4, 28.6, 31.6, 33.9, 41.6, 52.3, 61.2, 61.8, 98.8, 113.2, 120.3, 124.7, 127.0, 127.4, 127.9, 128.3, 128.4, 133.2, 136.7, 137.8, 138.9, 140.6, 151.4; HRMS (ES⁺) calcd for [C₂₈H₃₁N₇O₂S + H] 530.2338, found 530.2350; HPLC (I) $t_{\text{R}} = 12.73$ min (100%), (II) $t_{\text{R}} = 18.89$ min (99.35%).

(±)-[*N*-(2-Methylbenzyl)-*N*-{*cis*-2-[(4-cyanophenyl)(3-methyl-3*H*-imidazol-4-ylmethyl)amino]cyclopentyl}-1-methyl-1*H*-imidazole-4-sulfonamide (**6b**)]. The synthesis was as per general procedure B with **42** and 2-methylbenzyl bromide on a 0.116 mmol scale. The crude residue was purified by silica gel flash column chromatography (eluent CH₂Cl₂/MeOH/NH₄OH, 192:7:1) to afford **6b** (14 mg, 22%): δ_{H} (500 MHz, CDCl₃) 1.38–1.48 (m, 1H, CH (cyclopentyl)), 1.86–1.99 (m, 5H, CH₂Ph, 2 CH (cyclopentyl)), 2.14–2.26 (m, 2H, 2 CH (cyclopentyl)), 2.67–2.76 (m, 1H, CH (cyclopentyl)), 3.59 (s, 3H, CH₃(Im)), 3.62 (s, 3H, CH₃(Im)), 4.05 (d, $J = 17.5$ Hz, 1H, CH₂Ph), 4.09–4.15 (m, 1H, CHN (cyclopentyl)), 4.26 (m, 1H, CHN (cyclopentyl)), 4.31 (d, $J = 18.0$ Hz, 1H, CH₂Im), 4.42 (d, $J = 17.5$ Hz, 1H, CH₂Ph), 4.90 (d, $J = 18.0$ Hz, 1H, CH₂Im), 6.55 (s, 1H, CH (Im)), 6.69 (d, $J = 9.0$ Hz, 2H, 2 CH (Ar)), 6.95–7.01 (m, 3H, 3 CH (Ph)), 7.07 (td, $J = 7.3$, 1.5 Hz, 1H, CH (Ph)), 7.16 (s, 1H, CH (Im)), 7.25 (s, 1H, CH (Im)), 7.43 (d, $J = 9.0$ Hz, 2H, 2 CH (Ar)), 7.45 (s, 1H, CH (Im)); δ_{C} (125 MHz, CDCl₃) 18.8, 21.2, 28.6, 28.7, 31.6, 33.8, 41.7, 50.6, 61.5, 62.2, 98.8, 112.9, 120.3, 124.5, 125.5, 126.9, 127.1, 127.3, 128.4, 130.2, 133.4, 134.2, 135.7, 137.8, 138.7, 140.8, 151.5; HRMS (ES⁺) calcd for [C₂₉H₃₃N₇O₂S + H] 544.2495, found 544.2509; HPLC (I) $t_{\text{R}} = 12.77$ min (100%), (II) $t_{\text{R}} = 19.02$ min (100%).

(±)-[*N*-(Thiophen-3-ylmethyl)-*N*-{*cis*-2-[(4-cyanophenyl)(3-methyl-3*H*-imidazol-4-ylmethyl)amino]cyclopentyl}-1-methyl-1*H*-imidazole-4-sulfonamide (**6c**)]. The synthesis was as per general procedure B with **42** and thiophen-3-ylmethyl bromide (prepared by employing a standard bromination procedure of thiophen-3-ylmethanol with PPh₃Br₂; the bromide darkened on standing at room temperature, but ¹H NMR of the material after 1 month suggested no decomposition had occurred) on a 0.121 mmol scale. The crude residue was purified by silica gel flash column chromatography (eluent CH₂Cl₂/MeOH/NH₄OH, 192:7:1) to afford **6c** (35 mg, 54%): δ_{H} (500 MHz, CDCl₃) 1.43–1.53 (m, 1H, CH (cyclopentyl)), 1.85–1.96 (m, 2H, 2 CH (cyclopentyl)), 2.04–2.13 (m, 2H, 2 CH (cyclopentyl)), 2.41–2.50 (m, 1H, CH (cyclopentyl)), 3.57 (s, 3H, CH₃(Im)), 3.66 (s, 3H, CH₃(Im)), 3.96 (d, $J = 16.5$ Hz, 1H, CH₂thiophene), 4.18 (m, 1H, CHN (cyclopentyl)), 4.27–4.34 (m, 2H, CH₂Im, CHN (cyclopentyl)), 4.43 (d, $J = 16.5$ Hz, 1H, CH₂thiophene), 4.74 (d, $J = 18.0$ Hz, 1H, CH₂Im), 6.53 (s, 1H, CH (Im)), 6.70 (dd, $J = 5.0$, 1.5 Hz, 1H, CH (thiophene)), 6.72 (d, $J = 9.0$ Hz, 2H, 2 CH (Ar)), 6.90–6.93 (m, 1H, CH (thiophene)), 7.11–7.13 (dd, $J = 5.0$, 2.8 Hz, 1H, CH (thiophene)), 7.22 (s, 1H, CH (Im)), 7.39 (s, 1H, CH (Im)), 7.43 (d, $J = 9.0$ Hz, 2H, 2 CH (Ar)), 7.44 (s, 1H, CH (Im)); δ_{C} (125 MHz, CDCl₃) 21.0, 28.2, 28.3, 31.5, 33.9, 41.8, 47.4, 60.7, 61.8, 98.8, 113.2, 120.4, 123.0,

124.5, 125.7, 127.5, 127.7, 128.2, 133.2, 137.9, 138.0, 138.8, 140.8, 151.5; HRMS (ES+) calcd for [C₂₆H₂₉N₇O₂S₂ + H] 536.1902, found 536.1915; HPLC (I) *t_R* = 11.08 min (100%), (II) *t_R* = 18.85 min (98.38%).

(±)-[*N*-(*N*-*tert*-Butoxycarbonylpiperidin-4-ylmethyl)-*N*-{*cis*-2-[(4-cyanophenyl)(3-methyl-3*H*-imidazol-4-ylmethyl)amino]cyclopentyl}]-1-methyl-1*H*-imidazole-4-sulfonamide (**6d**). The synthesis was as per general procedure B with **42** and *N*-*tert*-butoxycarbonylpiperidin-4-ylmethyl iodide (prepared by Finkelstein transformation on *N*-*tert*-butoxycarbonylpiperidin-4-ylmethyl bromide with sodium iodide in acetone) (1.5 equiv) on a 0.116 mmol scale in DMF (0.1 M), and the mixture was stirred for 7 days at room temperature. After the usual workup, the crude residue was purified by silica gel flash column chromatography (eluent CH₂Cl₂/MeOH/NH₄OH, 192:7:1) to yield **6d** (60 mg, 81%): δ_H (500 MHz, CDCl₃) 0.62–0.72 (m, 1H, CH (piperidinylmethyl)), 0.81–0.89 (m, 1H, CH (piperidinylmethyl)), 1.24–1.31 (m, 2H, 2 CH (piperidinylmethyl)), 1.41 (s, 9H, C(CH₃)₃), 1.42–1.61 (m, 3H, 2 CH (piperidinylmethyl), CH (cyclopentyl)), 1.85–1.95 (m, 2H, 2 CH (cyclopentyl)), 2.06–2.23 (m, 2H, 2 CH (cyclopentyl)), 2.25–2.35 (m, 1H, CH (piperidinylmethyl)), 2.38–2.49 (m, 1H, CH (cyclopentyl)), 2.73–2.81 (m, 1H, CH (piperidinylmethyl)), 2.86–2.99 (m, 1H, CH (piperidinylmethyl)), 3.64 (s, 3H, CH₃(Im)), 3.73 (s, 3H, CH₃(Im)), 3.81–3.97 (m, 2H, CHCH₂N (piperidinylmethyl)), 4.13 (m, 1H, CHN (cyclopentyl)), 4.24 (m, 1H, CHN (cyclopentyl)), 4.57 (d, *J* = 18.0 Hz, 1H, CH₂Im), 5.06 (br d, *J* = 18.0 Hz, 1H, CH₂Im), 6.56 (s, 1H, CH (Im)), 6.81 (d, *J* = 9.0 Hz, 2H, 2 CH (Ar)), 7.38 (s, 1H, CH (Im)), 7.41–7.46 (m, 4H, 2 CH (Im), 2 CH (Ar)); δ_C (125 MHz, CDCl₃) 20.9, 28.0, 28.2, 28.4, 29.9, 31.6, 34.0, 35.1, 42.3, 43.4 (br), 55.9, 61.8, 62.1, 79.4, 99.1, 113.3, 120.1, 124.1, 127.5, 128.0, 133.3, 138.0, 138.8, 141.4, 151.5, 154.6; HRMS (ES+) calcd for [C₃₂H₄₄N₈O₄S + H] 637.3284, found 637.3288; HPLC (I) *t_R* = 13.28 min (100%), (II) *t_R* = 20.60 min (100%).

(±)-[*N*-(*N*-2-Pyrimidinyl)-piperidin-4-ylmethyl]-*N*-{*cis*-2-[(4-cyanophenyl)(3-methyl-3*H*-imidazol-4-ylmethyl)amino]cyclopentyl}]-1-methyl-1*H*-imidazole-4-sulfonamide (**6e**). The synthesis was as per general procedure B with **42** and *N*-(2-pyrimidinyl)-piperidin-4-ylmethyl iodide (prepared by the reaction of PPh₃Br₂ on *N*-(2-pyrimidinyl)-piperidin-4-ylmethanol to give *N*-(2-pyrimidinyl)-piperidin-4-ylmethyl bromide, followed by Finkelstein halide exchange with NaI) (1.5 equiv) on a 0.118 mmol scale in DMF (0.1 M), and the mixture was stirred for 7 days at room temperature. The crude residue was purified by silica gel flash column chromatography (eluent CH₂Cl₂/MeOH/NH₄OH, 192:7:1) to furnish **6e** (57 mg, 79%): δ_H (500 MHz, CDCl₃) 0.76 (qd, *J* = 12.5, 4.0 Hz, 1H, CH (piperidinylmethyl)), 0.94 (qd, *J* = 12.5, 4.0 Hz, 1H, CH (piperidinylmethyl)), 1.35–1.41 (m, 1H, 1 CH (cyclopentyl)), 1.48–1.57 (m, 2H, 2 CH (piperidinylmethyl)), 1.68–1.77 (m, 1H, CH (piperidinylmethyl)), 1.87–1.97 (m, 2H, 2 CH (cyclopentyl)), 2.09–2.20 (m, 2H, 2 CH (cyclopentyl)), 2.39 (td, *J* = 12.5, 2.5 Hz, 1H, CH (piperidinylmethyl)), 2.44–2.52 (m, 2H, CH (cyclopentyl), CH (piperidinylmethyl)), 2.80 (dd, *J* = 14.5, 7.0 Hz, 1H, CH (piperidinylmethyl)), 2.97 (dd, *J* = 14.5, 7.5 Hz, 1H, CH (piperidinylmethyl)), 3.66 (s, 3H, CH₃(Im)), 3.73 (s, 3H, CH₃(Im)), 4.17 (m, 1H, CHN (cyclopentyl)), 4.26 (m, 1H, CHN (cyclopentyl)), 4.53–4.63 (m, 3H, CH₂Im, CHCH₂N (piperidinylmethyl)), 5.02 (br d, *J* = 17.5 Hz, 1H, CH₂Im), 6.42 (t, *J* = 4.9 Hz, 1H, CH (pyrimidine), 6.59 (s, 1H, CH (Im)), 6.82 (d, *J* = 9.5 Hz, 2H, 2 CH (Ar)), 7.38 (s, 1H, CH (Im)), 7.44–7.47 (m, 3H, CH (Im), 2 CH (Ar)), 7.49 (s, 1H, CH (Im)), 8.25 (d, *J* = 4.9 Hz, 2H, 2 CH (pyrimidine)); δ_C (125 MHz, CDCl₃) 21.0, 28.1, 28.4, 29.8, 31.7, 34.0, 35.4, 42.3, 43.5, 55.7, 61.9, 62.7, 99.2, 109.4, 113.3, 120.1, 124.0, 127.0, 128.2, 133.4, 137.9, 138.7, 141.6, 151.5, 157.7, 161.4; HRMS (ES+) calcd for [C₃₁H₃₈N₁₀O₂S + H] 615.2978, found 615.2999; HPLC (I) *t_R* = 13.12 min (99.94%), (II) *t_R* = 19.98 min (99.39%).

(±)-[*N*-Benzyl-*N*-{*trans*-2-[(4-cyanophenyl)(3-methyl-3*H*-imidazol-4-ylmethyl)amino]cyclopentyl}]-1-methyl-1*H*-imidazole-4-sulfonamide (**7a**). The synthesis was as per general procedure B with **45** and benzyl bromide on a 0.0228 mmol scale. The crude residue was purified by silica gel flash column chromatography (eluent

CH₂Cl₂/MeOH/NH₄OH, 192:7:1) to afford **7a** (10 mg, 85%): δ_H (400 MHz, CDCl₃) 1.19–1.29 (m, 1H, CH (cyclopentyl)), 1.54–1.64 (m, 2H, 2 CH (cyclopentyl)), 1.65–1.79 (m, 2H, 2 CH (cyclopentyl)), 1.83–1.91 (m, 1H, CH (cyclopentyl)), 3.60 (s, 3H, CH₃(Im)), 3.73 (s, 3H, CH₃(Im)), 3.87 (m, 1H, CHN (cyclopentyl)), 4.04 (d, *J* = 16.4 Hz, 1H, CH₂Ph), 4.41 (d, *J* = 17.8 Hz, 1H, CH₂Im), 4.61–4.72 (m, 2H, CH₂Ph, CHN (cyclopentyl)), 4.80 (d, *J* = 17.8 Hz, 1H, CH₂Im), 6.33 (d, *J* = 8.8 Hz, 2H, 2 CH (Ar)), 6.60 (s, 1H, CH (Im)), 6.94–7.02 (m, 3H, 3 CH (Ph)), 7.20–7.25 (m, 4H, 2 CH (Ph), 2 CH (Ar)), 7.39 (s, 1H, CH (Im)), 7.47 (s, 1H, CH (Im)), 7.45 (s, 1H, CH (Im)); δ_C (125 MHz, CDCl₃) 19.3, 24.1, 26.2, 32.1, 34.0, 39.6, 48.1, 60.0, 61.1, 98.6, 113.1, 120.3, 124.2, 127.0, 127.3 (2), 128.2, 128.6, 133.0, 137.1, 137.9, 139.0, 140.2, 151.2; HRMS (ES+) calcd for [C₂₈H₃₁N₇O₂S + H] 530.2338, found 530.2353; HPLC (I) *t_R* = 12.98 min (98.35%), (II) *t_R* = 19.76 min (98.05%).

(±)-[*N*-(2-Methylbenzyl)-*N*-{*trans*-2-[(4-cyanophenyl)(3-methyl-3*H*-imidazol-4-ylmethyl)amino]cyclopentyl}]-1-methyl-1*H*-imidazole-4-sulfonamide (**7b**). The synthesis was as per general procedure B with **45** and 2-methylbenzyl bromide on a 0.082 mmol scale. The crude residue was purified by silica gel flash column chromatography (eluent CH₂Cl₂/MeOH/NH₄OH, 192:7:1) to afford **7b** (37 mg, 83%): δ_H (500 MHz, CDCl₃) 1.20–1.29 (m, 1H, CH (cyclopentyl)), 1.55–1.66 (m, 2H, 2 CH (cyclopentyl)), 1.76–1.89 (m, 3H, 3 CH (cyclopentyl)), 2.21 (s, 3H, CH₃Ph), 3.58 (s, 3H, CH₃(Im)), 3.76 (s, 3H, CH₃(Im)), 3.90 (m, 1H, CHN (cyclopentyl)), 4.23 (d, *J* = 16.0 Hz, 1H, CH₂Ph), 4.35 (d, *J* = 18.0 Hz, 1H, CH₂Im), 4.57 (d, *J* = 16.0 Hz, 1H, CH₂Ph), 4.62 (m, 1H, CHN (cyclopentyl)), 4.75 (d, *J* = 18.0 Hz, 1H, CH₂Im), 6.40 (d, *J* = 9.0 Hz, 2H, 2 CH (Ar)), 6.61 (s, 1H, CH (Im)), 6.83–6.97 (m, 3H, 3 CH (Ph)), 7.25–7.30 (m, 3H, 2 CH (Ar), CH (Ph)), 7.41 (s, 1H, CH (Im)), 7.43 (s, 1H, CH (Im)), 7.50 (s, 1H, CH (Im)); δ_C (125 MHz, CDCl₃) 19.2, 19.6, 24.2, 26.4, 31.9, 34.0, 39.5, 46.3, 59.1, 61.2, 98.6, 113.2, 120.4, 124.3, 125.7, 127.3, 128.0, 128.3, 128.4, 130.4, 133.1, 134.6, 135.5, 138.2, 139.0, 140.4, 151.4; HRMS (ES+) calcd for [C₂₉H₃₃N₇O₂S + H] 544.2495, found 544.2501; HPLC (I) *t_R* = 12.91 min (100%), (II) *t_R* = 19.69 min (99.61%).

(±)-[*N*-(Thiophen-3-ylmethyl)-*N*-{*trans*-2-[(4-cyanophenyl)(3-methyl-3*H*-imidazol-4-ylmethyl)amino]cyclopentyl}]-1-methyl-1*H*-imidazole-4-sulfonamide (**7c**). The synthesis was as per general procedure B with **45** and thiophen-3-ylmethyl bromide on a 0.0888 mmol scale. The crude residue was purified by silica gel flash column chromatography (eluent CH₂Cl₂/MeOH/NH₄OH, 192:7:1) to afford **7c** (36 mg, 75%): δ_H (500 MHz, CDCl₃) 1.27–1.35 (m, 1H, CH (cyclopentyl)), 1.57–1.69 (m, 3H, 3 CH (cyclopentyl)), 1.75–1.82 (m, 1H, CH (cyclopentyl)), 1.88–1.95 (m, 1H, CH (cyclopentyl)), 3.56 (s, 3H, CH₃(Im)), 3.71 (s, 3H, CH₃(Im)), 4.02 (m, 1H, CHN (cyclopentyl)), 4.14 (d, *J* = 16.0 Hz, 1H, CH₂thiophene), 4.44 (d, *J* = 18.0 Hz, 1H, CH₂Im), 4.55 (d, *J* = 16.0 Hz, 1H, CH₂thiophene), 4.63 (m, 1H, CHN (cyclopentyl)), 4.76 (d, *J* = 18.0 Hz, 1H, CH₂Im), 6.57 (d, *J* = 9.0 Hz, 2H, 2 CH (Ar)), 6.60 (s, 1H, CH (Im)), 6.92 (dd, *J* = 5.3, 1.5 Hz, 1H, CH (thiophene)), 6.97 (dd, *J* = 5.3, 3.0 Hz, 1H, CH (thiophene)), 7.00–7.02 (m, 1H, CH (thiophene)), 7.30 (d, *J* = 9.0 Hz, 2H, 2 CH (Ar)), 7.34 (s, 1H, CH (Im)), 7.41 (s, 1H, CH (Im)), 7.44 (s, 1H, CH (Im)); δ_C (125 MHz, CDCl₃) 19.4, 24.7, 26.3, 31.8, 33.9, 39.8, 43.5, 60.0, 61.3, 98.8, 113.3, 120.3, 122.4, 124.1, 126.0, 127.2, 128.0, 128.2, 133.1, 138.2, 138.5, 138.9, 140.4, 151.4; HRMS (ES+) calcd for [C₂₆H₂₉N₇O₂S₂ + H] 536.1902, found 536.1912; HPLC (I) *t_R* = 12.93 min (100%), (II) *t_R* = 19.55 min (100%).

(±)-[*N*-(*N*-*tert*-Butoxycarbonylpiperidin-4-ylmethyl)-*N*-{*trans*-2-[(4-cyanophenyl)(3-methyl-3*H*-imidazol-4-ylmethyl)amino]cyclopentyl}]-1-methyl-1*H*-imidazole-4-sulfonamide (**7d**). The synthesis was as per general procedure B with **45** and *N*-*tert*-butoxycarbonylpiperidin-4-ylmethyl bromide (1.5 equiv) on a 0.0774 mmol scale in DMF (0.1 M), and the mixture was stirred for 7 days at room temperature. The crude residue was purified by silica gel flash column chromatography (eluent CH₂Cl₂/MeOH/NH₄OH, 192:7:1) to afford **7d** (41 mg, 83%): δ_H (500 MHz, CDCl₃) 1.00–1.09 (m, 1H, CH (piperidinylmethyl)), 1.24–1.35 (m, 2H, CH (cyclopentyl), CH (piperidinylmethyl)), 1.37–1.46 (m, 1H, C(CH₃)₃, and 2 CH

(piperidinylmethyl), 1.51–1.65 (m, 5H, 3 CH (cyclopentyl), 2 CH (piperidinylmethyl)), 2.00–2.08 (m, 2H, 2 CH (cyclopentyl)), 2.17–2.26 (m, 1H, CH (piperidinylmethyl)), 2.68–2.80 (m, 1H, CH (piperidinylmethyl)), 3.23 (dd, $J = 15.0, 9.0$ Hz, 1H, CH (piperidinylmethyl)), 3.65 (s, 3H, CH₃(Im)), 3.75 (s, 3H, CH₃(Im)), 3.89–4.00 (m, 3H, CHCH₂N (piperidinylmethyl), CHN (cyclopentyl)), 4.63 (m, 1H, CHN (cyclopentyl)), 4.72 (d, $J = 18.0$ Hz, 1H, CH₂Im), 5.06 (d, $J = 18.0$ Hz, 1H, CH₂Im), 6.71 (s, 1H, CH (Im)), 6.78 (d, $J = 9.0$ Hz, 2H, 2 CH (Ar)), 7.42 (s, 1H, CH (Im)), 7.46 (s, 1H, CH (Im)), 7.48 (d, $J = 9.0$ Hz, 2H, 2 CH (Ar)), 7.60 (s, 1H, CH (Im)); δ_C (125 MHz, CDCl₃) 18.5, 23.0, 25.8, 28.4, 30.2, 32.0, 34.0, 36.8, 39.5, 43.7 (br), 49.6, 60.0, 61.5, 79.3, 99.5, 113.1, 119.9, 124.1, 127.7, 128.2, 133.6, 138.2, 139.0, 140.1, 151.6, 154.5; HRMS (ES+) calcd for [C₃₂H₄₄N₈O₄S + H] 637.3284, found 637.3292; HPLC (I) $t_R = 13.45$ min (100%), (II) $t_R = 21.09$ min (100%).

(±)-[N-{N-(2-Pyrimidinyl)-piperidin-4-ylmethyl}-N-{*trans*-2-(4-cyanophenyl)(3-methyl-3H-imidazol-4-ylmethyl)amino]cyclopentyl]-1-methyl-1H-imidazole-4-sulfonamide (**7e**). The synthesis was as per general procedure B with **45** and *N*-(2-pyrimidinyl)-piperidin-4-ylmethyl bromide (1.5 equiv) on a 0.0799 mmol scale in DMF (0.1 M), and the mixture was stirred for 7 days at room temperature. The crude residue was purified by silica gel flash column chromatography (eluent CH₂Cl₂/MeOH/NH₄OH, 192:7:1) to afford **7e** (38 mg, 78%): δ_H (500 MHz, CDCl₃) 0.88 (qd, $J = 12.2, 4.0$ Hz, 1H, CH (piperidinylmethyl)), 1.01 (qd, $J = 12.3, 4.0$ Hz, 1H, CH (piperidinylmethyl)), 1.25–1.34 (m, 1H, 1 CH (cyclopentyl)), 1.38–1.48 (m, 2H, 2 CH (piperidinylmethyl)), 1.52–1.78 (m, 4H, 3 CH (cyclopentyl), CH (piperidinylmethyl)), 1.98–2.09 (m, 2H, 2 CH (cyclopentyl)), 2.28 (br t, $J = 12.0$, 1H, CH (piperidinylmethyl)), 2.40 (br t, $J = 12.0$ Hz, 1H, CH (piperidinylmethyl)), 2.74 (dd, $J = 14.8, 6.0$ Hz, 1H, CH (piperidinylmethyl)), 3.24 (dd, $J = 14.8, 8.5$ Hz, 1H, CH (piperidinylmethyl)), 3.61 (s, 3H, CH₃(Im)), 3.74 (s, 3H, CH₃(Im)), 3.97 (m, 1H, CHN (cyclopentyl)), 4.47–4.54 (m, 2H, CHCH₂N (piperidinylmethyl)), 4.63 (m, 1H, CHN (cyclopentyl)), 4.73 (d, $J = 17.5$ Hz, 1H, CH₂Im), 5.05 (d, $J = 17.5$ Hz, 1H, CH₂Im), 6.41 (t, $J = 4.9$ Hz, 1H, CH (pyrimidine)), 6.59 (s, 1H, CH (Im)), 6.78 (d, $J = 8.5$ Hz, 2H, 2 CH (Ar)), 7.41 (s, 1H, CH (Im)), 7.43–7.49 (m, 4H, 2 CH (Im), 2 CH (Ar)), 8.25 (d, $J = 4.9$ Hz, 2H, 2 CH (pyrimidine)); δ_C (125 MHz, CDCl₃) 18.6, 23.1, 25.8, 29.9, 31.8, 33.9, 37.0, 39.5, 43.5, 49.7, 60.1, 61.6, 99.4, 109.3, 113.2, 119.9, 124.1, 128.2, 128.4, 133.6, 138.4, 138.9, 140.1, 151.8, 157.6, 161.3; HRMS (ES+) calcd for [C₃₁H₃₈N₁₀O₂S + H] 615.2978, found 615.2990; HPLC (I) $t_R = 12.91$ min (99.70%), (II) $t_R = 19.32$ min (99.65%).

(±)-[N-Benzyl-N-{*cis*-3-(4-cyanophenyl)(3-methyl-3H-imidazol-4-ylmethyl)amino]cyclopentyl]-1-methyl-1H-imidazole-4-sulfonamide (**8a**). The synthesis was as per general procedure A with alcohol **55** and sulfonamide **19a** on a 0.102 mmol scale. The crude residue was purified by silica gel flash column chromatography (eluent CH₂Cl₂/MeOH/NH₄OH, 192:7:1) to furnish **8a** (38 mg, 71%): δ_H (500 MHz, CDCl₃) 1.45–1.55 (m, 1H, CH (cyclopentyl)), 1.62–1.86 (m, 4H, 4 CH (cyclopentyl)), 1.92–1.98 (m, 1H, CH (cyclopentyl)), 3.42 (s, 3H, CH₃(Im)), 3.65 (s, 3H, CH₃(Im)), 4.02–4.17 (m, 4H, CH₂Ph, 2 CHN (cyclopentyl)), 4.30 (d, $J = 16.5$ Hz, 1H, CH₂Im), 4.41 (d, $J = 16.5$ Hz, 1H, CH₂Im), 6.52–6.58 (m, 3H, 2 CH (Ar), CH (Im)), 7.14–7.27 (m, 6H, 5 CH (Ph), CH (Im)), 7.30 (d, $J = 8.5$ Hz, 2H, 2 CH (Ar)), 7.33 (s, 1H, CH (Im)), 7.39 (s, 1H, CH (Im)); δ_C (125 MHz, CDCl₃) 26.8, 28.0, 31.5, 33.6, 33.9, 41.6, 49.5, 56.4, 57.3, 99.2, 113.5, 120.0, 123.8, 127.1, 127.2, 127.3, 128.0, 128.4, 133.3, 138.2, 138.4, 138.9, 140.7, 151.9; HRMS (ES+) calcd for [C₂₈H₃₁N₇O₂S + H] 530.2338, found 530.2357; HPLC (I) $t_R = 12.28$ min (100%), (II) $t_R = 18.26$ min (100%).

(±)-[N-(2-Methylbenzyl)-N-{*cis*-3-(4-cyanophenyl)(3-methyl-3H-imidazol-4-ylmethyl)amino]cyclopentyl]-1-methyl-1H-imidazole-4-sulfonamide (**8b**). The synthesis was as per general procedure A with alcohol **55** and sulfonamide **19b** on a 0.102 mmol scale. The crude residue was purified by silica gel flash column chromatography (eluent CH₂Cl₂/MeOH/NH₄OH, 192:7:1) to yield **8b** (36 mg, 65%): δ_H (500 MHz, CDCl₃) 1.51–1.58 (m, 1H, CH (cyclo-

pentyl)), 1.66–1.75 (m, 1H, CH (cyclopentyl)), 1.75–1.93 (m, 3H, 3 CH (cyclopentyl)), 2.03–2.08 (m, 1H, CH (cyclopentyl)), 2.26 (s, 3H, CH₃Ph), 3.46 (s, 3H, CH₃(Im)), 3.73 (s, 3H, CH₃(Im)), 4.13 (m, 1H, CHN (cyclopentyl)), 4.17–4.24 (m, 3H, CH₂Ph, CHN (cyclopentyl)), 4.34 (d, $J = 16.5$ Hz, 1H, CH₂Im), 4.46 (d, $J = 16.5$ Hz, 1H, CH₂Im), 6.60–6.64 (m, 3H, CH (Im), 2 CH (Ar)), 7.08–7.11 (m, 1H, CH (Ph)), 7.13–7.17 (m, 2H, 2 CH (Ph)), 7.28 (s, 1H, CH (Im)), 7.36–7.40 (m, 3H, 2 CH (Ar), CH (Im)), 7.41–7.44 (m, 1H, CH (Ph)), 7.45 (s, 1H, CH (Im)); δ_C (125 MHz, CDCl₃) 19.2, 26.9, 27.8, 31.5, 33.5, 34.0, 41.7, 47.4, 56.4, 57.2, 99.3, 113.5, 120.1, 123.9, 126.0, 127.2, 127.7, 128.0, 128.1, 130.2, 133.4, 135.2, 135.8, 138.3, 138.9, 140.7, 151.9; HRMS (ES+) calcd for [C₂₉H₃₃N₇O₂S + H] 544.2495, found 544.2495; HPLC (I) $t_R = 12.41$ min (98.55%), (II) $t_R = 17.99$ min (98.89%).

(±)-[N-(Thiophen-3-ylmethyl)-N-{*cis*-3-(4-cyanophenyl)(3-methyl-3H-imidazol-4-ylmethyl)amino]cyclopentyl]-1-methyl-1H-imidazole-4-sulfonamide (**8c**). The synthesis was as per general procedure A with alcohol **55** and sulfonamide **19c** on a 0.102 mmol scale. The crude residue was purified by silica gel flash column chromatography (eluent CH₂Cl₂/MeOH/NH₄OH, 192:7:1) to afford **8c** (43 mg, 79%): δ_H (500 MHz, CDCl₃) 1.53–1.62 (m, 1H, CH (cyclopentyl)), 1.74–1.86 (m, 3H, 3 CH (cyclopentyl)), 1.87–1.93 (m, 1H, CH (cyclopentyl)), 2.01–2.06 (m, 1H, CH (cyclopentyl)), 3.54 (s, 3H, CH₃(Im)), 3.71 (s, 3H, CH₃(Im)), 4.11–4.19 (m, 2H, 2 CHN (cyclopentyl)), 4.25 (AB quartet, $J = 17.8$ Hz, 2H, CH₂Ph), 4.37 (d, $J = 16.4$ Hz, 1H, CH₂Im), 4.45 (d, $J = 16.4$ Hz, 1H, CH₂Im), 6.61–6.61 (m, 3H, 2 CH (Ar), CH (Im)), 7.04 (dd, $J = 5.0, 1.2$ Hz, 1H, CH (thiophene)), 7.05–7.07 (m, 1H, CH (thiophene)), 7.22 (dd, $J = 5.0, 3.0$ Hz, 1H, CH (thiophene)), 7.25 (s, 1H, CH (Im)), 7.38 (d, $J = 9.0$ Hz, 2H, 2 CH (Ar)), 7.41 (s, 1H, CH (Im)), 7.42 (s, 1H, CH (Im)); δ_C (125 MHz, CDCl₃) 26.9, 28.1, 31.5, 33.6, 33.9, 41.8, 45.2, 56.5, 57.2, 99.3, 113.5, 120.0, 122.0, 123.7, 126.0, 127.2, 127.4, 128.1, 133.4, 138.3, 138.8, 139.7, 141.0, 152.0; HRMS (ES+) calcd for [C₂₆H₂₉N₇O₂S₂ + H] 536.1902, found 536.1910; HPLC (I) $t_R = 12.09$ min (100%), (II) $t_R = 17.62$ min (100%).

(±)-[N-(*N*-tert-Butoxycarbonylpiperidin-4-ylmethyl)-N-{*cis*-3-(4-cyanophenyl)(3-methyl-3H-imidazol-4-ylmethyl)amino]cyclopentyl]-1-methyl-1H-imidazole-4-sulfonamide (**8d**). The synthesis was as per general procedure A with alcohol **55** and sulfonamide **19d** on a 0.102 mmol scale. The crude residue was purified by silica gel flash column chromatography (eluent CH₂Cl₂/MeOH/NH₄OH, 192:7:1) to furnish **8d** (40 mg, 62%): δ_H (500 MHz, CDCl₃) 0.92–0.98 (m, 1H, CH (piperidinylmethyl)), 1.04 (qd, $J = 12.5, 4.0$ Hz, 1 H, CH (piperidinylmethyl)), 1.45 (s, 9H, C(CH₃)₃), 1.65–1.77 (m, 3H, 2 CH (piperidinylmethyl), CH (cyclopentyl)), 1.79–1.91 (m, 4H, 3 CH (cyclopentyl), CH (piperidinylmethyl)), 1.94–2.06 (m, 2H, 2 CH (cyclopentyl)), 2.58–2.69 (m, 2H, 2 CH (piperidinylmethyl)), 2.87–2.98 (m, 1H, CH (piperidinylmethyl)), 2.99–3.10 (m, 1H, CH (piperidinylmethyl)), 3.62 (s, 3H, CH₃(Im)), 3.72 (s, 3H, CH₃(Im)), 3.98 (m, 1H, CHN (cyclopentyl)), 4.03–4.14 (m, 2H, CHCH₂N (piperidinylmethyl)), 4.18 (m, 1H, CHN (cyclopentyl)), 4.42 (AB quartet, $J = 17.5$ Hz, 2H, CH₂Im), 6.67 (s, 1H, CH (Im)), 6.69 (d, $J = 9.0$ Hz, 2H, 2 CH (Ar)), 7.20 (s, 1H, CH (Im)), 7.39 (s, 1H, CH (Im)), 7.41 (d, $J = 9.0$ Hz, 2 CH (Ar)), 7.44 (s, 1H, CH (Im)); δ_C (125 MHz, CDCl₃) 26.9, 28.2, 28.4, 29.9, 31.6, 33.5, 33.9, 36.7, 41.9, 43.6 (br), 52.5, 56.3, 58.3, 79.3, 99.4, 113.6, 120.0, 123.7, 128.1, 128.3, 133.4, 138.3, 138.7, 140.7, 152.0, 154.7; HRMS (ES+) calcd for [C₃₂H₄₄N₈O₄S + H] 637.3284, found 637.3283; HPLC (I) $t_R = 12.89$ min (99.52%), (II) $t_R = 20.14$ min (99.30%).

(±)-[N-{N-(2-Pyrimidinyl)-piperidin-4-ylmethyl}-N-{*cis*-3-(4-cyanophenyl)(3-methyl-3H-imidazol-4-ylmethyl)amino]cyclopentyl]-1-methyl-1H-imidazole-4-sulfonamide (**8e**). The synthesis was as per general procedure A with alcohol **55** (0.203 mmol, 1 equiv) and sulfonamide **21** (1.5 equiv), with 2 equiv of PPh₃ and 1.5 equiv of DIAD. The crude residue was purified by silica gel flash column chromatography (eluent CH₂Cl₂/MeOH/NH₄OH, 192:7:1) to furnish (±)-[*N*-tert-butoxycarbonyl-N-{*cis*-3-(4-cyanophenyl)(3-methyl-3H-imidazol-4-ylmethyl)amino]cyclopentyl]-1-methyl-1H-imidazole-4-sulfonamide as a white powder (108 mg, 99%): δ_H (500

MHz, CDCl₃) 1.37 (s, 9H, C(CH₃)₃), 1.90–1.96 (m, 1H, CH (cyclopentyl)), 1.98–2.06 (m, 1H, CH (cyclopentyl)), 2.09–2.17 (m, 1H, CH (cyclopentyl)), 2.25–2.41 (m, 3H, 3 CH (cyclopentyl)), 3.66 (s, 3H, CH₃(Im)), 3.76 (s, 3H, CH₃(Im)), 4.28 (m, 1H, CHN (cyclopentyl)), 4.50 (AB quartet, *J* = 17.5 Hz, 2H, CH₂Im), 4.95 (m, 1H, CHN (cyclopentyl)), 6.72–6.79 (m, 3H, CH (Im) 2 CH (Ar)), 7.41–7.50 (m, 4H, 2 CH (Im), 2 CH (Ar)), 7.59 (s, 1H, CH (Im)); δ_C (125 MHz, CDCl₃) 27.5, 27.7, 28.1, 31.3, 32.7, 33.9, 41.1, 56.1, 57.5, 83.8, 98.5, 113.1, 120.1, 124.9, 127.6, 128.3, 133.2, 138.0, 138.4, 140.0, 150.6, 152.0; HRMS (ES⁺) calcd for [C₂₆H₃₃N₇O₄S + H] 540.2393, found 540.2391. The material (108 mg, 0.201 mmol) was redissolved in a 1:1 mixture of CH₂Cl₂/TFA (7 mL). After the mixture was stirred for 3 h at room temperature, TLC indicated the reaction was complete, and so all solvent was removed in vacuo. The residue was dry-loaded onto silica gel and purified by flash column chromatography (eluent CH₂Cl₂/MeOH/NH₄OH, 92:7:1) to give (±)-[*N*-{*cis*-3-[(4-cyanophenyl)(3-methyl-3*H*-imidazol-4-ylmethyl)amino]cyclopentyl}]-1-methyl-1*H*-imidazole-4-sulfonamide as a glassy film (88 mg, 96%): δ_H (500 MHz, MeOH-*d*₄) 1.55–1.61 (m, 1H, CH (cyclopentyl)), 1.64–1.72 (m, 2H, 2 CH (cyclopentyl)), 1.81–1.89 (m, 1H, CH (cyclopentyl)), 1.93–1.99 (m, 1H, CH (cyclopentyl)), 2.08–2.13 (m, 1H, CH (cyclopentyl)), 3.56 (m, 1H, CHNH₂O₂), 3.69 (s, 3H, CH₃(Im)), 3.75 (s, 3H, CH₃(Im)), 4.26 (m, 1H, CHN (cyclopentyl)), 4.46 (AB quartet, *J* = 18.0 Hz, 2H, CH₂Im), 6.57 (s, 1H, CH (Im)), 6.68 (d, *J* = 9.3 Hz, 2H, 2 CH (Ar)), 7.41 (d, *J* = 9.3 Hz, 2H, 2 CH (Ar)), 7.47 (s, 1H, CH (Im)), 7.50 (s, 1H, CH (Im)), 7.52 (s, 1H, CH (Im)); δ_C (125 MHz, CDCl₃) 26.3, 30.3, 30.5, 32.9, 35.7, 40.6, 51.7, 56.8, 97.5, 112.7, 119.5, 123.9, 125.7, 128.5, 132.7, 137.5, 138.9, 139.2, 151.7; HRMS (ES⁺) calcd for [C₂₁H₂₅N₇O₂S + H] 440.1869, found 440.1881. Finally, (±)-[*N*-{*cis*-3-[(4-cyanophenyl)(3-methyl-3*H*-imidazol-4-ylmethyl)amino]cyclopentyl}]-1-methyl-1*H*-imidazole-4-sulfonamide (0.096 mmol) and *N*-(2-pyrimidinyl)-4-iodomethylpiperidine (1.5 equiv) were reacted together as per general procedure B in DMF (0.1 M), and the mixture was stirred for 3 days at room temperature. After the usual workup, the crude residue was purified by silica gel flash column chromatography (eluent CH₂Cl₂/MeOH/NH₄OH, 92:7:1) to yield the title compound **8e** (50 mg, 85%): δ_H (500 MHz, CDCl₃) 1.04 (qd, *J* = 12.3, 4.0 Hz, 1H, CH (piperidinylmethyl)), 1.11 (qd, *J* = 12.3, 4.0 Hz, 1H, CH (piperidinylmethyl)), 1.65–1.72 (m, 1H, 1 CH (cyclopentyl)), 1.78–2.09 (m, 8H, 5 CH (cyclopentyl), 3 CH (piperidinylmethyl)), 2.77–2.85 (m, 2H, 2 CH (piperidinylmethyl)), 2.95 (dd, *J* = 14.5, 7.0 Hz, 1H, CH (piperidinylmethyl)), 3.07 (dd, *J* = 14.5, 7.5 Hz, 1H, CH (piperidinylmethyl)), 3.59 (s, 3H, CH₃(Im)), 3.72 (s, 3H, CH₃(Im)), 4.04 (m, 1H, CHN (cyclopentyl)), 4.18 (m, 1H, CHN (cyclopentyl)), 4.43 (AB quartet, *J* = 17.5 Hz, 2H, CH₂Im), 4.73–4.80 (m, 2H, CHCH₂N (piperidinylmethyl)), 6.44 (t, *J* = 4.8 Hz, 1H, CH (pyrimidine)), 6.67 (s, 1H, CH (Im)), 6.69 (d, *J* = 9.0 Hz, 2H, 2 CH (Ar)), 7.20 (s, 1H, CH (Im)), 7.39 (s, 1H, CH (Im)), 7.40–7.44 (m, 3H, CH (Im), 2 CH (Ar)) 8.28 (d, *J* = 4.8 Hz, 2H, 2 CH (pyrimidine)); δ_C (125 MHz, CDCl₃) 26.9, 28.3, 29.9, 31.6, 33.5, 33.9, 37.1, 41.9, 43.7, 52.6, 56.3, 58.3, 99.6, 109.4, 113.6, 120.0, 123.7, 128.2, 128.3, 133.5, 138.4, 138.7, 140.9, 152.1, 157.7, 161.5; HRMS (ES⁺) calcd for [C₃₁H₃₈N₁₀O₂S + H] 615.2978, found 615.3008; HPLC (I) *t*_R = 12.56 min (99.21%), (II) *t*_R = 19.15 min (99.37%).

(±)-[*N*-Benzyl-*N*-{*trans*-3-[(4-cyanophenyl)(3-methyl-3*H*-imidazol-4-ylmethyl)amino]cyclopentyl}]-1-methyl-1*H*-imidazole-4-sulfonamide (**9a**). The synthesis was as per general procedure A with alcohol **60** and sulfonamide **19a** on a 0.102 mmol scale. The crude residue was purified by silica gel flash column chromatography (eluent CH₂Cl₂/MeOH/NH₄OH, 92:7:1) to furnish **9a** (29 mg, 54%): δ_H (500 MHz, CDCl₃) 1.31–1.39 (m, 1H, CH (cyclopentyl)), 1.46–1.54 (m, 1H, CH (cyclopentyl)), 1.69–1.76 (m, 1H, CH (cyclopentyl)), 1.76–1.84 (m, 2H, 2 CH (cyclopentyl)), 1.91–1.97 (m, 1H, CH (cyclopentyl)), 3.56 (s, 3H, CH₃(Im)), 3.63 (s, 3H, CH₃(Im)), 4.14 (m, 1H, CHN (cyclopentyl)), 4.24 (s, 2H, CH₂Ph), 4.26 (d, *J* = 16.8 Hz, 1H, CH₂Im), 4.43 (d, *J* = 16.8 Hz, 1H, CH₂Im), 4.49 (m, 1H, CHN (cyclopentyl)), 6.48 (d, *J* = 9.0 Hz, 2H, 2 CH (Ar)), 6.54 (s, 1H, CH (Im)), 7.20–7.23 (m, 2H, CH (Ph), CH (Im)), 7.25–7.31 (m, 5H, 2 CH (Ar), 2 CH (Ph), CH (Im)), 7.32–7.36 (m, 2H, CH (Im), CH (Ph)), 7.38 (s, 1H, CH

(Im)); δ_C (125 MHz, CDCl₃) 29.0, 29.1, 30.9, 31.6, 33.9, 41.7, 48.1, 56.9, 57.9, 99.1, 113.3, 120.1, 123.7, 127.1, 127.3, 127.9, 128.2, 128.5, 133.3, 138.2, 138.3, 138.9, 140.5, 151.8; HRMS (ES⁺) calcd for [C₂₈H₃₁N₇O₂S + H] 530.2338, found 530.2349; HPLC (I) *t*_R = 12.21 min (100%), (II) *t*_R = 18.09 min (99.84%).

(±)-[*N*-{2-Methylbenzyl}-*N*-{*trans*-3-[(4-cyanophenyl)(3-methyl-3*H*-imidazol-4-ylmethyl)amino]cyclopentyl}]-1-methyl-1*H*-imidazole-4-sulfonamide (**9b**). The synthesis was as per general procedure A with alcohol **60** and sulfonamide **19b** on a 0.136 mmol scale. The crude residue was purified by silica gel flash column chromatography (eluent CH₂Cl₂/MeOH/NH₄OH, 92:7:1) to give **9b** (36 mg, 49%): δ_H (500 MHz, CDCl₃) 1.37–1.53 (m, 2H, 2 CH (cyclopentyl)), 1.78–1.85 (m, 1H, CH (cyclopentyl)), 1.86–1.92 (m, 2H, 2 CH (cyclopentyl)), 1.97–2.02 (m, 1H, CH (cyclopentyl)), 2.32 (s, 3H, CH₃Ph), 3.63 (s, 3H, CH₃(Im)), 3.69 (s, 3H, CH₃(Im)), 4.17 (m, 1H, CHN (cyclopentyl)), 4.27–4.31 (m, 3H, CH₂Ph, CH₂Im), 4.44 (d, *J* = 16.5 Hz, 1H, CH₂Im), 4.58 (m, 1H, CHN (cyclopentyl)), 6.53 (d, *J* = 9.0 Hz, 2H, 2 CH (Ar)), 6.61 (s, 1H, CH (Im)), 7.12–7.15 (m, 1H, CH (Ph)), 7.16–7.22 (m, 2H, 2 CH (Ph)), 7.28 (s, 1H, CH (Im)), 7.34–7.37 (m, 3H, 2 CH (Ar), CH (Im)), 7.44 (s, 1H, CH (Im)), 7.48–7.51 (m, 1H, CH (Ph)); δ_C (125 MHz, CDCl₃) 19.3, 28.9, 29.0, 31.5, 31.6, 33.9, 41.8, 45.9, 57.0, 57.9, 99.2, 113.3, 120.1, 123.8, 126.1, 127.1, 127.4, 128.0, 128.2, 130.1, 133.4, 134.9, 135.8, 138.3, 138.9, 140.4, 151.8; HRMS (ES⁺) calcd for [C₂₉H₃₃N₇O₂S + H] 544.2495, found 544.2503; HPLC (I) *t*_R = 12.34 min (98.09%), (II) *t*_R = 18.02 min (98.07%).

(±)-[*N*-{Thiophen-3-ylmethyl}-*N*-{*trans*-3-[(4-cyanophenyl)(3-methyl-3*H*-imidazol-4-ylmethyl)amino]cyclopentyl}]-1-methyl-1*H*-imidazole-4-sulfonamide (**9c**). The synthesis was as per general procedure A with alcohol **60** and sulfonamide **19c** on a 0.136 mmol scale. The crude residue was purified by silica gel flash column chromatography (eluent CH₂Cl₂/MeOH/NH₄OH, 92:7:1) to furnish **9c** (47 mg, 65%): δ_H (500 MHz, CDCl₃) 1.40–1.48 (m, 1H, CH (cyclopentyl)), 1.58–1.67 (m, 1H, CH (cyclopentyl)), 1.77–1.83 (m, 1H, CH (cyclopentyl)), 1.86–1.92 (m, 2H, 2 CH (cyclopentyl)), 2.00–2.06 (m, 1H, CH (cyclopentyl)), 3.62 (s, 3H, CH₃(Im)), 3.68 (s, 3H, CH₃(Im)), 4.25 (m, 1H, CHN (cyclopentyl)), 4.31 (s, 2H, CH₂thiophene), 4.32 (d, *J* = 16.5 Hz, 1H, CH₂Im), 4.46 (d, *J* = 16.5 Hz, 1H, CH₂Im), 4.52 (m, 1H, CHN (cyclopentyl)), 6.58 (d, *J* = 9.1 Hz, 2H, 2 CH (Ar)), 6.61 (s, 1H, CH (Im)), 7.09 (dd, *J* = 5.0, 1.2 Hz, 1H, CH (thiophene)), 7.12–7.14 (m, 1H, CH (thiophene)), 7.26 (s, 1H, CH (Im)), 7.28 (dd, *J* = 5.0, 3.0 Hz, 1H, CH (thiophene)), 7.35 (s, 1H, CH (Im)), 7.37 (d, *J* = 9.1 Hz, 2H, 2 CH (Ar)), 7.43 (s, 1H, CH (Im)); δ_C (125 MHz, CDCl₃) 29.0, 29.1, 31.6, 31.8, 33.9, 41.8, 43.9, 57.0, 57.9, 99.2, 113.3, 120.1, 122.1, 123.7, 126.0, 127.2, 128.0, 128.1, 133.4, 138.3, 138.8, 139.6, 140.6, 151.8; HRMS (ES⁺) calcd for [C₂₆H₂₉N₇O₂S₂ + H] 536.1902, found 536.1911; HPLC (I) *t*_R = 12.05 min (98.16%), (II) *t*_R = 17.43 min (98.44%).

(±)-[*N*-{*N*-tert-Butoxycarbonylpiperidin-4-ylmethyl}-*N*-{*trans*-3-[(4-cyanophenyl)(3-methyl-3*H*-imidazol-4-ylmethyl)amino]cyclopentyl}]-1-methyl-1*H*-imidazole-4-sulfonamide (**9d**). The synthesis was as per general procedure A with alcohol **60** and sulfonamide **19d** on a 0.136 mmol scale. The crude residue was purified by silica gel flash column chromatography (eluent CH₂Cl₂/MeOH/NH₄OH, 92:7:1) to afford **9d** (27 mg, 32%): δ_H (500 MHz, CDCl₃) 1.00–1.13 (m, 2H, 2 CH (piperidinylmethyl)), 1.40–1.52 (s, 11H, C(CH₃)₃, CH (piperidinylmethyl), CH (cyclopentyl)), 1.56–1.65 (m, 1H, CH (cyclopentyl)), 1.70–1.84 (m, 3H, 2 CH (piperidinylmethyl), CH (cyclopentyl)), 1.87–2.01 (m, 2H, 2 CH (cyclopentyl)), 2.12–2.19 (m, 1H, CH (cyclopentyl)), 2.61–2.75 (m, 3H, 3 CH (piperidinylmethyl)), 3.02–3.11 (m, 1H, CH (piperidinylmethyl)), 3.67 (s, 3H, CH₃(Im)), 3.68 (s, 3H, CH₃(Im)), 4.04–4.19 (m, 2H, CHCH₂N (piperidinylmethyl)), 4.31–4.37 (m, 3H, CH₂Im, CHN (cyclopentyl)), 4.42 (m, 1H, CHN (cyclopentyl)), 6.62 (s, 1H, CH (Im)), 6.66 (d, *J* = 9.3 Hz, 2H, 2 CH (Ar)), 7.24 (s, 1H, CH (Im)), 7.25 (s, 1H, CH (Im)), 7.41 (d, *J* = 9.3 Hz, 2H, 2 CH (Ar)), 7.47 (s, 1H, CH (Im)); δ_C (125 MHz, CDCl₃) 28.4, 29.0, 29.8, 30.2, 31.4, 33.9, 34.1, 36.9, 41.1, 43.7 (br), 49.9, 56.2, 58.7, 79.7, 100.7, 113.2, 118.6, 119.5, 124.7, 132.4, 133.8, 136.0, 138.1, 139.2, 150.9,

154.9; HRMS (ES+) calcd for [C₃₂H₄₄N₈O₄S + H] 637.3284, found 637.3293; HPLC (I) *t*_R = 12.97 min (98.72%), (II) *t*_R = 20.52 min (99.01%).

(±)-[*N*-{*N*-(2-Pyrimidinyl)-piperidin-4-ylmethyl}-*N*-(*trans*-3-[(4-cyanophenyl)(3-methyl-3*H*-imidazol-4-ylmethyl)amino]cyclopentyl)]-1-methyl-1*H*-imidazole-4-sulfonamide (**9e**). The synthesis was as per general procedure A with alcohol **60** (0.203 mmol, 1 equiv) and sulfonamide **21** (1.5 equiv), with 2 equiv of PPh₃ and 1.5 equiv of DIAD. The crude residue was purified by silica gel flash column chromatography (eluent CH₂Cl₂/MeOH/NH₄OH, 192:7:1) to furnish (±)-[*N*-*tert*-butoxycarbonyl-*N*-{2-*trans*-[(4-cyanophenyl)(3-methyl-3*H*-imidazol-4-ylmethyl)amino]cyclopentyl}]-1-methyl-1*H*-imidazole-4-sulfonamide as a white powder (90 mg, 83%): δ_H (500 MHz, CDCl₃) 1.42 (s, 9H, C(CH₃)₃), 1.51–1.61 (m, 1H, CH (cyclopentyl)), 1.92–1.99 (m, 1H, CH (cyclopentyl)), 2.09–2.18 (m, 2H, 2 CH (cyclopentyl)), 2.20–2.28 (m, 1H, CH (cyclopentyl)), 2.43–2.49 (m, 1H, 1 CH (cyclopentyl)), 3.65 (s, 3H, CH₃(Im)), 3.76 (s, 3H, CH₃(Im)), 4.38 (AB quartet, *J* = 17.0 Hz, 2H, CH₂Im), 4.72 (m, 1H, CHN (cyclopentyl)), 5.03 (m, 1H, CHN (cyclopentyl)), 6.72–6.77 (m, 3H, CH (Im), 2 CH (Ar)), 7.41 (d, *J* = 9.0 Hz, 2H, 2 CH (Ar)), 7.45 (s, 1H, CH (Im)), 7.51 (s, 1H, CH (Im)), 7.52 (s, 1H, CH (Im)); δ_C (125 MHz, CDCl₃) 28.1, 30.0, 30.8, 31.6, 32.2, 34.0, 41.4, 56.4, 57.7, 84.3, 98.8, 113.3, 120.2, 125.0, 127.6, 128.0, 133.3, 138.5, 139.1, 140.1, 150.5, 152.2; HRMS (ES+) calcd for [C₂₆H₃₃N₇O₄S + H] 540.2393, found 540.2396. The material (85 mg, 0.158 mmol) was redissolved in a 1:1 mixture of CH₂Cl₂/TFA (5 mL). After the mixture was stirred for 3 h at room temperature, TLC indicated the reaction was complete, and so all solvent was removed in vacuo. The residue was dry-loaded onto silica gel and purified by flash column chromatography (eluent CH₂Cl₂/MeOH/NH₄OH, 92:7:1) to give (±)-[*N*-{2-*trans*-[(4-cyanophenyl)(3-methyl-3*H*-imidazol-4-ylmethyl)amino]cyclopentyl}]-1-methyl-1*H*-imidazole-4-sulfonamide as a glassy film (68 mg, 99%): δ_H (500 MHz, CDCl₃) 1.39–1.47 (m, 1H, CH (cyclopentyl)), 1.57–1.70 (m, 2H, 2 CH (cyclopentyl)), 1.90–2.06 (m, 3H, 3 CH (cyclopentyl)), 3.58 (s, 3H, CH₃(Im)), 3.68 (s, 3H, CH₃(Im)), 3.78 (m, 1H, CHNHSO₂), 4.27 (s, 2H, CH₂Im), 4.40 (m, 1H, CHN (cyclopentyl)), 6.56 (s, 1H, CH (Im)), 6.61 (d, *J* = 9.0 Hz, 2H, 2 CH (Ar)), 7.20 (s, 1H, CH (Im)), 7.28 (d, *J* = 9.0 Hz, 2H, 2 CH (Ar)), 7.40 (s, 1H, CH (Im)), 7.43 (s, 1H, CH (Im)), 7.47 (s, 1H, CH (Im)); δ_C (125 MHz, CDCl₃) 27.9, 31.6, 32.7, 34.0, 35.7, 42.6, 53.0, 57.2, 98.6, 113.4, 120.2, 123.9, 127.6, 128.2, 133.2, 138.3, 139.0, 140.5, 151.9; HRMS (ES+) calcd for [C₂₁H₂₅N₇O₂S + H] 440.1869, found 440.1882. Finally, (±)-[*N*-{*trans*-3-[(4-cyanophenyl)(3-methyl-3*H*-imidazol-4-ylmethyl)amino]cyclopentyl}]-1-methyl-1*H*-imidazole-4-sulfonamide (0.095 mmol) and *N*-(2-pyrimidinyl)-piperidin-4-ylmethyl iodide (1.5 equiv) were reacted together as per general procedure B in DMF (0.1 M), and the mixture was stirred for 3 days at room temperature. After the usual workup, the crude residue was purified by silica gel flash column chromatography (eluent CH₂Cl₂/MeOH/NH₄OH, 92:7:1) to yield the title compound **9e** (49 mg, 85%): δ_H (500 MHz, CDCl₃) 1.08–1.19 (m, 2H, 2 CH (piperidinylmethyl)), 1.41–1.51 (m, 1H, 1 CH (cyclopentyl)), 1.57–1.65 (m, 1H, CH (cyclopentyl)), 1.69–1.93 (m, 3H, 2 CH (piperidinylmethyl), CH (cyclopentyl)), 1.97–2.02 (m, 1H, CH (cyclopentyl)), 2.04–2.15 (m, 2H, 2 CH (cyclopentyl)), 2.74 (dd, *J* = 14.8, 8.1 Hz, 1H, CH (piperidinylmethyl)), 2.80–2.87 (m, 2H, 2 CH (piperidinylmethyl)), 2.97 (dd, *J* = 14.5, 7.5 Hz, 1H, CH (piperidinylmethyl)), 3.08 (dd, *J* = 14.8, 6.8 Hz, 1H, CH (piperidinylmethyl)), 3.67 (s, 3H, CH₃), 3.68 (s, 3H, CH₃), 4.29–4.39 (m, 3H, CHN (cyclopentyl), CH₂Im), 4.45 (m, 1H, CHN (cyclopentyl)), 4.76–4.81 (m, 2H, CHCH₂N (piperidinylmethyl)), 6.43 (t, *J* = 4.8 Hz, 1H, CH (pyrimidine)), 6.60 (s, 1H, CH (Im)), 6.65 (d, *J* = 9.0 Hz, 2H, 2 CH (Ar)), 7.26 (m, 2H, 2 CH (Im)), 7.38 (d, *J* = 8.9 Hz, 2H, 2 CH (Ar)), 7.41 (s, 1H, CH (Im)), 8.28 (d, *J* = 4.8 Hz, 2H, 2 CH (pyrimidine)); δ_C (125 MHz, CDCl₃) 26.6, 29.5, 29.9, 31.0, 31.7, 33.9, 37.4, 41.8, 43.8, 50.4, 57.7, 58.6, 99.2, 109.4, 113.3, 120.0, 123.8, 127.8, 128.3, 133.1, 138.4, 138.8, 139.8, 151.7, 157.8, 161.5; HRMS (ES+) calcd for [C₃₁H₃₈N₁₀O₂S + H] 615.2978, found 615.2959; HPLC (I) *t*_R = 12.59 min (100%), (II) *t*_R = 19.17 min (100%).

(±)-[*N*-Benzyl-*N*-{*cis*-4-[(4-cyanophenyl)(3-methyl-3*H*-imidazol-4-ylmethyl)amino]cyclohexyl}]-1-methyl-1*H*-imidazole-4-sulfonamide (**10a**). The synthesis was as per general procedure C with **64a** on a 0.149 mmol scale. After workup, the crude residue was dry-loaded onto silica gel, then purified by flash column chromatography (eluent CH₂Cl₂/MeOH/NH₄OH, 192:7:1) to afford **10a** (52 mg, 65% (or 92% brsm)): δ_H (400 MHz, CDCl₃) 1.55–1.67 (m, 8H, 2 NCH₂CH₂N), 3.35 (s, 3H, CH₃(Im)), 3.65 (m, 1H, CHN (cyclohexyl)), 3.73 (s, 3H, CH₃(Im)), 3.77 (m, 1H, CHN (cyclopentyl)), 4.17 (s, 2H, CH₂Ph), 4.43 (s, 2H, CH₂Im), 6.58 (s, 1H, CH (Im)), 6.67 (d, *J* = 9.0 Hz, 2H, CH (Ar)), 7.23–7.44 (m, 10H, CH (Im), 5 CH (Ph), 2 CH (Ar), 2 CH (Im)); δ_C (125 MHz, CDCl₃) 27.0, 27.2, 31.1, 33.7, 42.3, 48.9, 52.1, 56.3, 94.9, 97.5, 101.0, 116.5, 119.5, 123.6, 126.9, 127.2, 128.0, 128.3, 132.9, 138.6, 138.7, 140.9, 151.6; HPLC (I) *t*_R = 12.59 min (96.06%), (II) *t*_R = 18.98 min (95.85%); HRMS (ES+) calcd for [C₂₉H₃₃N₇O₂S + H] 544.2507, found 544.2495.

(±)-[*N*-(*N*-*tert*-Butoxycarbonylpiperidin-4-ylmethyl)-*N*-{*cis*-4-[(4-cyanophenyl)(3-methyl-3*H*-imidazol-4-ylmethyl)amino]cyclohexyl}]-1-methyl-1*H*-imidazole-4-sulfonamide (**10d**). The synthesis was as per general procedure C with **64d** on a 0.108 mmol scale. After workup, the crude residue was dry-loaded onto silica gel, then purified by flash column chromatography (eluent CH₂Cl₂/MeOH/NH₄OH, 192:7:1) to furnish **10d** (48 mg, 69% (or 94% brsm)): δ_H (400 MHz, CDCl₃) 0.94–1.03 (m, 2H, 2 CH (piperidinylmethyl)), 1.46 (s, 9H, C(CH₃)₃), 1.56–1.85 (m, 9H, 2 NCH₂CH₂N (cyclohexyl), CH (piperidinylmethyl)), 2.00–2.10 (m, 2H, 2 CH (piperidinylmethyl)), 2.58–2.70 (m, 2H, 2 CH (piperidinylmethyl)), 2.87–3.01 (m, 2H, 2 CH (piperidinylmethyl)), 3.49 (s, 3H, CH₃Im), 3.63 (m, 1H, CHN (cyclohexyl)), 3.72 (s, 3H, CH₃(Im)), 3.81 (m, 1 H, CHN (cyclohexyl)), 4.03–4.16 (m, 2H, 2 CH (piperidinylmethyl)), 4.48 (s, 2H, CH₂Im), 6.66 (s, 1H, CH (Im)), 6.78 (d, *J* = 9.0 Hz, 2H, 2 CH (Ar)), 7.32 (s, 1H, CH (Im)), 7.37 (s, 1H, CH (Im)), 7.39 (s, 1H, CH (Im)), 7.45 (d, *J* = 9.0 Hz, 2H, CH(Ar)); δ_C (125 MHz, CDCl₃) 27.9, 28.2, 28.7, 29.7, 30.3, 31.7, 34.2, 36.9, 43.6, 51.3, 52.1, 58.3, 79.6, 101.9, 117.5, 119.9, 124.0, 127.8, 129.0, 133.5, 138.6, 139.0, 141.5, 152.4, 155.0; HRMS (ES+) calcd for [C₃₃H₄₆N₈O₄S + H] 651.3420, found 651.3455; HPLC (I) *t*_R = 13.42 min (100%), (II) *t*_R = 21.42 min (100%).

(±)-[*N*-Benzyl-*N*-{*trans*-4-[(4-cyanophenyl)(3-methyl-3*H*-imidazol-4-ylmethyl)amino]cyclohexyl}]-1-methyl-1*H*-imidazole-4-sulfonamide (**11a**). Compound **66** was benzylated on the sulfonamide NH as per general procedure B on a 0.139 mmol scale with benzyl bromide. The sample was purified by silica gel flash column chromatography (eluent CH₂Cl₂/MeOH/NH₄OH, 292:7:1 1:2) to furnish (±)-[*N*-benzyl-*N*-{*trans*-4-(4-cyanophenylamino)cyclohexyl}]-1-methyl-1*H*-imidazole-4-sulfonamide as a colorless film (61 mg, 98%): δ_H (500 MHz, CDCl₃) 1.17 (qd, *J* = 12.5, 3.0 Hz, 2H, 2 CH (cyclohexyl)), 1.41 (qd, *J* = 12.5, 3.0 Hz, 2H, 2 CH (cyclohexyl)), 1.76–1.82 (m, 2H, 2 CH (cyclohexyl)), 1.96–2.02 (m, 2H, 2 CH (cyclohexyl)), 3.02 (tt, *J* = 11.0, 3.5 Hz, 1H, CHNSO₂), 3.69 (s, 3H, CH₃(Im)), 3.91 (tt, *J* = 12.5 Hz, 3.5 Hz, 1H, CHNHAr), 4.43 (s, 2H, CH₂Ph), 6.42 (d, *J* = 8.0 Hz, 2H, 2 CH (Ar)), 7.21–7.32 (m, 5H, 5 CH (Ph)), 7.33 (s, 1H, CH (Im)), 7.39 (d, *J* = 8.0 Hz, 2H, 2 CH (Ar)), 7.44 (s, 1H, CH (Im)); δ_C (125 MHz, CDCl₃) 30.0, 32.2, 33.9, 47.8, 50.6, 57.7, 98.3, 112.4, 120.4, 123.8, 127.2, 127.5, 128.3, 133.5, 138.8, 138.9, 141.2, 150.2; HRMS (ES+) calcd for [C₂₄H₂₇N₅O₂S + H] 450.1964, found 450.1972. The secondary aniline NH was then alkylated with imidazole **15** as per general procedure C on a 0.107 mmol scale, but the mixture was allowed to stir for 12 h, with the temperature gradually warming from 0 °C to room temperature, after which time the reaction appeared to have stalled. After usual workup, the crude residue was purified by silica gel flash column chromatography (eluent CH₂Cl₂/MeOH/NH₄OH, 192:7:1) to give the title compound **11a** (38 mg, 65% (or 97% brsm)): δ_H (500 MHz, CDCl₃) 1.41–1.53 (m, 4H, 4 CH (cyclohexyl)), 1.80–1.86 (m, 4H, 4 CH (cyclohexyl)), 3.55 (m, 1H, CHNSO₂), 3.61 (s, 3H, CH₃(Im)), 3.71 (s, 3H, CH₃(Im)), 3.95 (m, 1H, CHNAr), 4.29 (s, 2H, CH₂Im), 4.42 (s, 2H, CH₂Ph), 6.59 (d, *J* = 9.5 Hz, 2H, 2 CH (Ar)), 6.62 (br s, 1H, CH (Im)), 7.24–7.44 (m, 10H, 5 CH (Ph), 2 CH (Ar), 3 CH

(Im)); δ_C (125 MHz, $CDCl_3$) 29.1, 30.4, 31.6, 33.9, 40.7, 47.6, 56.3, 57.5, 98.9, 112.9, 120.1, 123.7, 127.3, 127.4, 128.1, 127.9, 128.3, 133.4, 138.2, 138.6, 138.8, 141.2, 151.2; HRMS (ES+) calcd for $[C_{29}H_{33}N_7O_2S + H]$ 544.2495, found 544.2502; HPLC (I) t_R = 11.97 (100%), (II) t_R = 17.04 (99.37%).

(±)-[*N*-(*N*-*tert*-Butoxycarbonylpiperidin-4-ylmethyl)-*N*-(*trans*-4-(4-cyanophenyl)(3-methyl-3*H*-imidazol-4-ylmethyl)amino)cyclohexyl]-1-methyl-1*H*-imidazole-4-sulfonamide (**11d**). Compound **66** was alkylated on the sulfonamide NH as per general procedure B on a 0.139 mmol scale and with *N*-*tert*-butoxycarbonyl-4-bromomethylpiperidine in DMF (0.1 M). After 4 days, the reaction was worked up, then purified by silica gel flash column chromatography (eluent $CH_2Cl_2/MeOH/NH_4OH$, 292:7:1) to furnish the (±)-[*N*-(*N*-*tert*-butoxycarbonylpiperidin-4-ylmethyl)-*N*-(4-(*trans*-cyanophenylamino)cyclohexyl)]-1-methyl-1*H*-imidazole-4-sulfonamide as a colorless film (77 mg, 100%): δ_H (500 MHz, $CDCl_3$) 1.07 (qd, J = 12.3, 4.3 Hz, 2H, 2 CH (piperidinylmethyl)), 1.25 (qd, J = 12.3, 3.0 Hz, 2H, 2 CH (cyclohexyl)), 1.44 (s, 9H, C(CH₃)₃), 1.56 (qd, J = 12.2, 3.0 Hz, 2H, 2 CH (cyclohexyl)), 1.72–1.79 (m, 2H, 2 CH (cyclohexyl)), 1.81–1.92 (m, 3H, 3 CH (piperidinylmethyl)), 2.07–2.13 (m, 2H, 2 CH (cyclohexyl)), 2.61–2.71 (m, 2H, 2 CH (piperidinylmethyl)), 3.01–3.08 (m, 2H, 2 CH (piperidinylmethyl)), 3.18 (tt, J = 11.5, 3.5 Hz, 1H, CHNSO₂), 3.73 (s, 3H, CH₃(Im)), 3.77 (qd, J = 12.0, 3.5 Hz, 1H, CHNH), 4.06–4.15 (m, 2H, 2 CH (piperidinylmethyl)), 6.50 (d, J = 8.8 Hz, 2H, 2 CH (Ar)), 7.36 (d, J = 8.8 Hz, 2H, 2 CH (Ar)), 7.39 (s, 1H, CH (Im)), 7.44 (s, 1H, CH (Im)); δ_C (125 MHz, $CDCl_3$) 28.4, 30.0, 30.2, 32.2, 33.9, 36.9, 43.4 (br), 50.2, 50.7, 57.7, 78.6, 98.3, 112.4, 120.4, 123.6, 134.6, 139.8, 141.0, 150.2, 154.7; HRMS (ES+) calcd for $[C_{28}H_{40}N_6O_4S + H]$ 557.2910, found 557.2931. The secondary aniline NH was then alkylated with imidazole **15** as per general procedure C on a 0.0937 mmol scale, but the mixture was allowed to stir for 12 h, with the temperature gradually warming from 0 °C to room temperature. After usual workup, the crude residue was purified by silica gel flash column chromatography (eluent $CH_2Cl_2/MeOH/NH_4OH$, 192:7:1) to furnish the target molecule **11d** (37 mg, 61% (or 95% brsm)): δ_H (500 MHz, $CDCl_3$) 1.07 (qd, J = 12.3, 4.3 Hz, 2H, 2 CH (piperidinylmethyl)), 1.44 (s, 9H, C(CH₃)₃), 1.51–1.61 (m, 4H, 4 CH (cyclohexyl)), 1.72–1.80 (m, 2H, 2 CH (cyclohexyl)), 1.82–1.95 (m, 5H, 3 CH (piperidinylmethyl), 2 CH (cyclohexyl)), 2.60–2.71 (m, 2H, 2 CH (piperidinylmethyl)), 2.97–3.03 (m, 2H, 2 CH (piperidinylmethyl)), 3.63 (s, 3H, CH₃(Im)), 3.68 (m, 1H, CHNSO₂), 3.72 (s, 3H, CH₃(Im)), 3.80 (m, 1H, CHNAr), 4.05–4.17 (m, 2H, 2 CH (piperidinylmethyl)), 4.36 (s, 2H, CH₂Im), 6.63–6.69 (m, 3H, 2 CH (Ar), CH (Im)), 7.37 (s, 1H, Im), 7.40 (d, J = 9.0 Hz, 2H, 2 CH (Ar)), 7.42 (s, 1H, CH (Im)), 7.45 (br s, 1H, CH (Im)); δ_C (125 MHz, $CDCl_3$) 28.2, 29.1, 30.0, 30.5 (br), 31.8, 33.9, 36.8, 40.8, 43.4 (br), 50.0, 56.4, 57.5, 79.5, 99.1, 113.0, 120.1, 123.5, 127.9, 128.2, 133.5, 138.3, 138.9, 140.9, 151.2, 154.7; HRMS (ES+) calcd for $[C_{33}H_{46}N_8O_4S + H]$ 651.3441, found 651.3446; HPLC (I) t_R = 13.18 (100%), (II) t_R = 20.66 (99.92%).

Biological Assays. Plasmodium Strains. The *P. falciparum* strains used in this study were 3D7 (The Netherlands, [airport-associated malaria], chloroquine-sensitive) provided by Dr. Pradipsinh Rathod from the University of Washington and K1 (Thailand, chloroquine-resistant, pyrimethamine-resistant) obtained from the MR4 Unit of the American Type Culture Collection (ATCC, Manassas, VA).

***P. falciparum* Culture.** Strains of *P. falciparum* were sustained in vitro on the basis of experimental techniques as described by Trager and Jensen.³⁸ Cultures were maintained in RPMI-1640 (Sigma, St. Louis, MO) with 2 mM L-glutamine, 25 mM HEPES, 33 mM NaHCO₃, 20 µg/mL gentamicin sulfate, and 20% (v/v) heat-inactivated human plasma type A+ (RP-20P). Type A+ erythrocytes were obtained from laboratory donors, washed three times with RPMI, resuspended in 50% RPMI, and stored at 4 °C. Parasites were grown in 10 mL of a 2% hematocrit/RP-20P (v/v) in 50 mL flasks under a 5% CO₂, 5% O₂, and 90% N₂ atmosphere.

***P. falciparum* ED₅₀ Determination.** An amount of 1 µL of *P. falciparum* PFT inhibitor (*Pf*PFTI) dissolved in DMSO was added to each well of a 96-well plate followed by the addition of 200 µL of *P. falciparum* culture at parasitemia and hematocrit of 0.5%.

Plates were flushed with 5% CO₂, 5% O₂, and 90% N₂ and then incubated at 37 °C for 48 h. [³H]Hypoxanthine (0.3 µCi, 20 Ci/mmol, American Radiolabeled Chemicals) in 30 µL of RP-20P was added to cultures and incubated for an additional 24 h. Cells were harvested onto filter mats by a Multiharvester (Skatron, Sunnyvale, CA), and the radioactivity incorporated into the parasites was counted on a β-scintillation counter. The background level detected with uninfected erythrocytes was subtracted from the data. The ³H-incorporation into infected RBCs with 1 µL of DMSO vehicle alone represents 100% malaria growth. ED₅₀ values were determined by linear regression analysis of the plots of ³H-hypoxanthine incorporation versus concentration of compound.

PPFT and Rat PFT IC₅₀ Determination. The PFT assay used to determine the IC₅₀ values (inhibitor concentration that causes 50% enzyme inhibition) of the compounds is based on a PFT [³H] scintillation proximity assay (SPA) (TRKQ7010 Amersham Biosciences Corp., Piscataway, NJ). Assays were carried out in assay buffer (pH 7.5, 50 mM HEPES, 30 mM MgCl₂, 20 mM KCl, 5 mM DTT, 0.01% Triton X-100), 1 µM human lamin-B carboxy-terminus sequence peptide (biotin-YRASNRSICAIM), and 1 µCi [³H]farnesylpyrophosphate (Amersham specific activity 15–20 Ci/mM) in a total volume of 50 µL which included 1 µL of *Pf*PFT inhibitor solution in DMSO and 5 µL of partially purified *Pf*PFT.¹⁷ Assays in the absence of *Pf*PFT inhibitor and *Pf*PFT were included as positive and negative controls, respectively. Reaction mixtures were incubated at 37 °C for 60 min and terminated by addition of 70 µL of assay STOP solution and 5 µL of SPA beads. The assay mixture was incubated at room temperature for 30 min. The assay was counted on a plate Chameleon 425-104 multilabel counter (Hidex Oy Turku, Finland). IC₅₀ values were calculated using linear regression analysis of the plots of the amount of radioprenylation versus the concentration of compound. For ratPFT IC₅₀ determination, 0.01 µM human lamin-B carboxy-terminus sequence peptide (biotin-YRASNRSICAIM) was used. The assay was incubated at 37 °C for 15 min; otherwise, experimental conditions were the same as for *Pf*PFT IC₅₀ determination.

Acknowledgment. Financial support for this work was provided by the Medicines for Malaria Venture (MMV) and the National Institutes of Health (Grants CA67771 and A154384). We thank David Floyd, Lou Lombardo, and David Williams from Bristol-Myers Squibb for helpful suggestions.

Supporting Information Available: GOLD low energy docked pictures of compounds **2a–5a**, **7a**, **8a**, **10a**, and **11a**, experimental procedures and full characterizations of compounds **14–64d**, and HPLC traces of two independent conditions for all target molecules (**2a–9e**, **10a**, **10d**, **11a**, **11d**). This material is available free of charge via the Internet at <http://pubs.acs.org>.

References

- (1) Sachs, J.; Malaney, P. The economic and social burden of malaria. *Nature* **2002**, *415*, 680–685.
- (2) www.mmv.org.
- (3) Snow, R. W.; Trape, J. F.; Marsh, K. The past, present and future of childhood malaria mortality in Africa. *Trends Parasitol.* **2001**, *17*, 593–597.
- (4) Olliaro, P. L.; Bloland, P. B. Clinical and public health implications of antimalarial drug resistance. *Antimalar. Chemother.* **2001**, 65–83.
- (5) Wiesner, J.; Ortmann, R.; Jomaa, H.; Schlitzer, M. New antimalarial drugs. *Angew. Chem., Int. Ed.* **2003**, *42*, 5274–5293.
- (6) May, J.; Meyer, C. G. Chemoresistance in falciparum malaria. *Trends Parasitol.* **2003**, *19*, 432–435.
- (7) Ridley, R. G. Medical need, scientific opportunity and the drive for antimalarial drugs. *Nature* **2002**, *415*, 686–693.
- (8) Greenwood, B.; Mutabingwa, T. Malaria in 2002. *Nature* **2002**, *415*, 670–672.
- (9) Chakrabarti, D.; Azam, T.; DeVecchio, C.; Qiu, L.; Park, Y.-I.; Allen, C. M. Protein prenyl transferase activities of *Plasmodium falciparum*. *Mol. Biochem. Parasitol.* **1998**, *94*, 175–184.
- (10) (a) Nallan, L.; Bauer, K. D.; Bendale, P.; Rivas, K.; Yokoyama, K.; Hornéy, C. P.; Pendyala, P. R.; Floyd, D.; Lombardo, L. J.; Williams,

- D. F.; Hamilton, A.; Sebt, S.; Windsor, W. T.; Weber, P. C.; Buckner, F. S.; Chakrabarti, D.; Gelb, M. H.; van Voorhis, W. C. Protein farnesyltransferase inhibitors exhibit potent antimalarial activity. *J. Med. Chem.* **2005**, *48*, 3704–3713. (b) Bendale, P.; Olepu, S.; Suryadevara, P. K.; Bulbule, V.; Rivas, K.; Nallan, L.; Smart, B.; Yokoyama, K.; Ankala, S.; Pendyala, P. R.; Floyd, D.; Lombardo, L. J.; Williams, D. K.; Buckner, F. S.; Chakrabarti, D.; Verlinde, C. L. M. J.; van Voorhis, W. C.; Gel, M. H. Second generation tetrahydroquinoline-based protein farnesyltransferase inhibitors as antimalarials. *J. Med. Chem.* **2007**, *50*, 4585–4605.
- (11) Clough, N.; Wilson, R. J. M. Antibiotics and plasmodial plastid organelle. *Antimalar. Chemother.* **2001**, 265–286.
- (12) Loyevsky, M.; Gordeuk, V. R. Iron chelators. *Antimalar. Chemother.* **2001**, 307–324.
- (13) Gelb, M. H.; van Voorhis, W. C.; Buckner, F. S.; Yokoyama, K.; Eastman, R.; Carpenter, E. P.; Panethymitaki, C.; Brown, K. A.; Smith, D. F. Protein farnesyl and *N*-myristoyl transferases: piggy-back medicinal chemistry targets for the development of antitrypanosomatid and antimalarial therapeutics. *Mol. Biochem. Parasitol.* **2003**, *126*, 155–163.
- (14) (a) Wiesner, J.; Kettler, K.; Sakowski, J.; Ortmann, R.; Katzin, A. M.; Kimura, E. A.; Silber, K.; Klebe, G.; Jomaa, H.; Schlitzer, M. Farnesyltransferase inhibitors inhibit the growth of malaria parasites in vitro and in vivo. *Angew. Chem., Int. Ed.* **2004**, *43*, 251–254. (b) Schlitzer, M. Structure based design of benzophenone-based non-thiol farnesyltransferase inhibitors. *Curr. Pharm. Des.* **2002**, *8*, 1713–1722.
- (15) Sebt, S. M.; Hamilton, A. D. Farnesyltransferase and geranylgeranyltransferase-I inhibitors and cancer therapy: lessons from mechanism and bench-to-bedside translational studies. *Oncogene* **2000**, *19*, 6584–6593.
- (16) Bell, I. M. Inhibitors of farnesyltransferase: a rational approach to cancer chemotherapy. *J. Med. Chem.* **2004**, *47*, 1870–1878.
- (17) Strickland, C. L.; Windsor, W. T.; Syto, R.; Wang, L.; Bond, R.; Wu, Z.; Schwartz, J.; Le, H. V.; Beese, L. S.; Weber, P. C. Crystal structure of farnesyl protein transferase complexed with a CaaX peptide and farnesyl diphosphate analog. *Biochemistry* **1998**, *37*, 16601–16611.
- (18) Chakrabarti, D.; Da Silva, T.; Barger, J.; Paquette, S.; Patel, H.; Patterson, S.; Allen, C. M. Protein farnesyltransferase and protein prenylation in *Plasmodium falciparum*. *J. Biol. Chem.* **2002**, *277*, 42066–42073.
- (19) Eastman, R. T.; White, J.; Hucce, O.; Bauer, K.; Yokoyama, K.; Nallan, L.; Chakrabarti, D.; Verlinde, C. L.; Gelb, M. H.; Rathod, P. K.; van Voorhis, W. C. Resistance to a protein farnesyltransferase inhibitor in *Plasmodium falciparum*. *J. Biol. Chem.* **2005**, *280*, 13554–13559.
- (20) Eastman, R. T.; White, J.; Hucce, O.; Yokoyama, K.; Verlinde, C. L. M. J.; Hast, M. A.; Beese, L. S.; Gelb, M. H.; Rathod, P. K.; van Voorhis, W. C. Resistance mutations at the lipid substrate binding site of *Plasmodium falciparum* protein farnesyltransferase. *Mol. Biochem. Parasitol.* **2007**, *152*, 66–71.
- (21) Ohkanda, J.; Lockman, J. W.; Yokoyama, K.; Gelb, M. H.; Croft, S. L.; Kendrick, H.; Harrell, M. I.; Feagin, J. E.; Blaskovich, M. A.; Sebt, S. M.; Hamilton, A. D. Peptidomimetic inhibitors of protein farnesyltransferase show potent antimalarial activity. *Bioorg. Med. Chem. Lett.* **2001**, *11*, 761–764.
- (22) Ohkanda, J.; Knowles, D. B.; Blaskovich, M. A.; Sebt, S. M.; Hamilton, A. D. Inhibitors of protein farnesyltransferase as novel anticancer agents. *Curr. Top. Med. Chem.* **2002**, *2*, 303–323.
- (23) Carrico, D.; Ohkanda, J.; Kendrick, H.; Yokoyama, K.; Blaskovich, M. A.; Bucher, C. J.; Buckner, F. S.; van Voorhis, W. C.; Chakrabarti, D.; Croft, S. L.; Gelb, M. H.; Sebt, S. M.; Hamilton, A. D. In vitro and in vivo antimalarial activity of peptidomimetic protein farnesyltransferase inhibitors with improved membrane permeability. *Bioorg. Med. Chem.* **2004**, *12*, 6517–6526.
- (24) van Voorhis, W. C.; Rivas, K. L.; Bendale, P.; Nallan, L.; Horney, C.; Barrett, L. K.; Bauer, K. D.; Smart, B. P.; Ankala, S.; Hucce, O.; Verlinde, C. L. M. J.; Chakrabarti, D.; Strickland, C.; Yokoyama, K.; Buckner, F. S.; Hamilton, A. D.; Williams, D. K.; Lombardo, L. J.; Floyd, D.; Gelb, M. H. Efficacy, pharmacokinetics, and metabolism of tetrahydroquinoline inhibitors of *Plasmodium falciparum* protein farnesyltransferase. *Antimicrob. Agents Chemother.* **2007**, *51*, 3659–3671.
- (25) www.plasmodb.org.
- (26) Glenn, M. P.; Chang, S.-Y.; Hucce, O.; Verlinde, C. L.; Rivas, K.; Hornéy, C.; Yokoyama, K.; Buckner, F. S.; Pendyala, P. R.; Chakrabarti, D.; Gelb, M.; van Voorhis, W. C.; Sebt, S. M.; Hamilton, A. D. Structurally simple farnesyltransferase inhibitors arrest the growth of malaria parasites. *Angew. Chem., Int. Ed.* **2005**, *44*, 4903–4906.
- (27) Glenn, M. P.; Chang, S.-Y.; Hornéy, C.; Rivas, K.; Yokoyama, K.; Pusateri, E. E.; Fletcher, S.; Cummings, C. G.; Buckner, F. S.; Pendyala, P. R.; Chakrabarti, D.; Sebt, S. M.; Gelb, M.; van Voorhis, W. C.; Hamilton, A. D. Structurally simple, potent *Plasmodium* selective farnesyltransferase inhibitors that arrest the growth of malaria parasites. *J. Med. Chem.* **2006**, *49*, 5710–5727.
- (28) Jones, G.; Willett, P.; Glen, R. C.; Leach, A. R.; Taylor, R. Development and validation of a genetic algorithm for flexible docking. *J. Mol. Biol.* **1997**, *267*, 727–748.
- (29) Reissig, H. U.; Zimmer, R. Donor–acceptor-substituted cyclopropane derivatives and their application in organic synthesis. *Chem. Rev.* **2003**, *103*, 1151–1196.
- (30) *InsightII*; Accelrys Inc.: San Diego, CA, 2000; <http://www.accelrys.com>.
- (31) Unpublished results.
- (32) Thorpe–Ingold effect, or the “gem-dialkyl effect”: replacement of a C–CH₂–C group with a C–CR₂–C group causes a compression of the C–C–C bond angle at the now-quarternary carbon.
- (33) Long, S. B.; Hancock, P. J.; Kral, A. M.; Hellinga, H. W.; Beese, L. S. The crystal structure of human protein farnesyltransferase reveals the basis for inhibition by CaaX tetrapeptides and their mimetics. *Proc. Natl. Acad. Sci. U.S.A.* **2001**, *98*, 12948–12953.
- (34) Seto, Y.; Guengerich, F. P. Partitioning between *N*-dealkylation and *N*-oxygenation in the oxidation of *N,N*-dialkylarylamines catalyzed by cytochrome P450 2B1. *J. Biol. Chem.* **1993**, *268*, 9986–9997.
- (35) *Molecular Operating Environment*, version 2007.11; Chemical Computing Group: Montreal, Quebec, Canada, 2007.
- (36) Sukumar, N.; Breneman, C. M. QTAIM in Drug Discovery and Protein Modeling. In *The Quantum Theory of Atoms in Molecules: From Solid State to DNA and Drug Design*; Matta, C. F., Boyd, R. J., Eds.; Wiley-VCH: Weinheim, Germany, 2007.
- (37) Embrechts, M. J. *KernelPLS(Analyze)*, version 6.36; Rensselaer Polytechnic Institute: Troy, NY, 2001.
- (38) Trager, W.; Jensen, J. B. Human malaria parasites in continuous culture. *Science* **1976**, *193*, 673–675.

JM800113P